

**INVESTIGATION AND REVIEW OF STRUCTURAL ADHESIVES FOR STEEL
BRIDGE REPAIR AND “STEEL GROUTING”**

A Thesis

Presented to

the faculty of the School of Engineering and Applied Science at

University of Virginia

In partial fulfillment

of the requirements for the degree

Master of Science

by

Joshua M. Starr

May 2024

APPROVAL SHEET

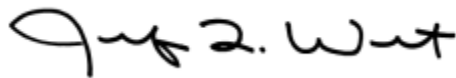
This thesis
is submitted in partial fulfillment of the requirements
for the degree of
Master of Science
Author: Joshua M. Starr



This thesis has been read and approved by the examining committee:

Advisor: Dr. Osman E. Ozbulut
Committee Member: Dr. Jose P. Gomez
Committee Member: Dr. Devin K. Harris
Committee Member: Jason T. Provines

Accepted for the School of Engineering and Applied Science:



Jennifer L. West, School of Engineering and Applied Science

May 2024

ABSTRACT

Traditional methods of repairing steel bridges often involve welding or mechanical fastening, processes that can be time-consuming, expensive, and disruptive to traffic flow. In response to these challenges, the utilization of structural adhesives has emerged as a promising alternative for steel bridge repair. Structural adhesives can exhibit fluid or injectable properties, which are ideal for filling small gaps or cracks in steel bridge applications with minimal surface preparation required during application. Alternatively, they may demonstrate viscous or putty-like behavior, suitable for packing into more significant gaps. Structural adhesives offer advantages such as enhanced durability, corrosion resistance, and ease of application by providing high-strength bonding solutions. This approach presents a promising avenue for effectively addressing gap-related issues in steel bridges. However, uncertainties persist regarding the compressibility of adhesives at different thicknesses under sustained compressive and environmental loads, as well as the slip coefficient of adhesives applied to fill gaps on faying surfaces. Furthermore, despite the wide range of structural adhesives used across various industries, there is limited information on the selection of adhesives for steel bridge repair applications.

This study comprehensively explores structural adhesives selected for gap filling in steel bridges, "steel grouting," to prevent crevice corrosion and enhance loading conditions. The study incorporates bulk materials testing of selected structural adhesives and structural testing of steel connections. It evaluates various material properties, including compressive strength and creep behavior under sustained compressive conditions and temperatures in environmental cure conditions. Compressive creep tests are conducted to quantify the compressibility of structural

adhesives while considering environmental factors. Slip tests are performed to determine the slip coefficient of adhesives in slip-critical bolted connections, and tensile creep tests are carried out to assess the slip performance of adhesives under sustained tensile and environmental loading with different steel surfaces. Additionally, the project includes a literature review focusing on structural adhesive selection and an analysis of previous testing methodologies and industrial usage. The findings of this study contribute valuable insights into structural adhesive behavior and performance through meticulous experimentation, literature review, and analysis, informing future selection and application techniques in steel bridge maintenance and repair.

DEDICATION

To my father and grandfather, your love, guidance, and sacrifices have shaped my academic journey.

ACKNOWLEDGMENTS

I extend my deepest gratitude to those who have made my journey towards obtaining my master's degree possible. Firstly, I am immensely thankful to my advisor, Dr. Ozman Ozbulut, whose invaluable insights and guidance have been instrumental in shaping my work and steering my research endeavors. I am indebted to Dr. Jose Gomez for his exceptional teaching and for igniting my passion for my master's program. His unwavering support and encouragement have been pivotal in my academic journey. My heartfelt appreciation goes to Jason Provines for his dedicated supervision and support throughout this project. Whether it was staying a late evening before Christmas Eve at the lab or meeting during his parental leave, Jason's mentorship has been indispensable to me. Lastly, I express my gratitude to the Department of Civil and Environmental Engineering for their support and to all the esteemed professors whose expertise and dedication have enriched my academic experience. This achievement would not have been possible without these individuals and institutions' guidance, encouragement, and support.

NOMENCLATURE

HP	Structural adhesive, Sikadur-31 Hi-Mod Gel
HFL	Structural adhesive, Sikadur-32 Hi-Mod
MP	Structural adhesive, MM1018 P
MFL	Structural adhesive, MM1018 FL
CP	Structural adhesive, K-009
CFL	Structural adhesive, K-082
ε	Strain
σ	Stress
J	Creep compliance
k_s	Surface Factor or Slip Coefficient
ϕ	Creep coefficient
θ_c	contact angle
t	time since the start of the test in hours
m	Mill scale
lbs	Pounds force
kip	Kilo-pounds force
ksi	Kilo-pounds force per square inch

Investigation and Review of Structural Adhesives
for Steel Bridge Repair and "Steel Grouting"

psi	pounds force per square inch
N	Newtons force
kN	Kilonewtons force
MPa	Megapascals
GPa	Gigapascals
hr	Hours
t	Time in hours
in	inches
ft	feet
mm	millimeters
cm	centimeters
°F	degrees Fahrenheit
°C	degrees Celsius
ASTM	American Society for Testing and Materials
RCSC	The Research Council on Structural Connections
VDOT	Virginia Department of Transportation
A	Cross-sectional area of load path for sample
P	creep load requirement

Π	Pi (3.14152365)
D	diameter of the sample
d	depth of the sample
k_s	compressive slip surface coefficient
P_s	slip load
T	clamping load
R	tensile creep load
CTE	Coefficient of Thermal Expansion
STD	standard deviation
H	humidity
UV	ultraviolet light

TABLE OF CONTENTS

DEDICATION.....	5
ACKNOWLEDGMENTS	6
NOMENCLATURE	7
TABLE OF CONTENTS	10
LIST OF TABLES.....	12
LIST OF EQUATIONS.....	14
LIST OF FIGURES	15
1 INTRODUCTION	20
2 LITERATURE REVIEW	26
2.1 Introduction.....	26
2.2 Applications of Adhesives	27
2.2.1 Aerospace.....	27
2.2.2 Navy	30
2.2.3 Transportation Infrastructure	32
2.3 Behavior and Standards for Structural Adhesives	36
2.3.1 Surface Preparation.....	36
2.3.2 Curing and Environment.....	41
2.3.3 Material Properties.....	47
2.4 Safety and Hazards	52
3 SELECTION OF ADHESIVE MATERIAL	56
3.1 Selection of Adhesive Class.....	56
3.2 Selection of Properties	58
3.3 Selection of Initial Materials.....	61
4 EXPERIMENTAL PROCEDURE AND METHODOLOGY	63
4.1 Experimental Procedures	63
4.1.1 Compressive Strength	63
4.1.2 Compressive Creep	66
4.1.3 Short-Term Compressive Slip.....	71

4.1.4	Long-Term Tensile Creep	76
5	EXPERIMENTAL RESULTS AND DISCUSSIONS	82
5.1	Testing Results.....	82
5.1.1	Compression Test Results.....	82
5.1.2	Compression Creep Test Results	95
5.1.3	Slip Test Results	101
5.1.4	Long-Term Tensile Creep Results	106
5.2	Discussions on Test Results.....	110
6	CONCLUSION AND RECOMMENDATIONS	114
	APPENDIX.....	119
	REFERENCES	133

LIST OF TABLES

Table 1. Comparison of the advantages and disadvantages of polymers for structural applications	29
Table 2. Surface preparation methods for adhesive application on steel (Zhang & Huang, 2021).	39
Table 3. Key chemical safety concerns (NIOSH, 2020)	53
Table 4. Typical classes of adhesives (Banea & Silva, 2009)	58
Table 5. Initial adhesive selection.	62
Table 6. Compressive test matrix	64
Table 7. Compression creep exposure periods	71
Table 8. Test matrix for short-term compression slip testing	71
Table 9. Test matrix for tension creep testing	77
Table 10. Average compressive strength for each cure condition summary table	94
Table 11 Average compressive strength for all conditions summary table	95
Table 12. Specimen summary of creep coefficient and compliance.	100
Table 13. Average summary of creep coefficient and compliance	101
Table 14. Summary table of slip testing	105
Table 15. Tensile creep summary	109

Table 16. Comparison of various properties of studied structural adhesives. 112

LIST OF EQUATIONS

Equation 1. Load requirement for designed compression stress for creep (ASTM C1181)..	70
Equation 2. Compressive slip coefficient	75
Equation 3. Tensile creep vertical load.....	81
Equation 4. Creep compliance	96
Equation 5. Creep coefficient	97

LIST OF FIGURES

Figure 1. An example of a gap repair between a flange on a bridge (Provines, 2022).	21
Figure 2. An example of a gap repair between a beam end and a concrete abutment (Provines, 2022).	21
Figure 3. Images of steel connection injected with epoxy (Makevičius et al., 2021)	22
Figure 4. Steel girder expansion joint corrosion illustration	23
Figure 5. Richmond girder spot repair visit (taken by Joshua Starr).....	24
Figure 6. Drawing of steel grouting examples.....	25
Figure 7. Materials on modern planes (Mouritz, 2012).....	28
Figure 8. Depiction of the U.S.S. Independence corroding from dissimilar metals (Specker, 2023).	31
Figure 9. Concrete crack epoxy injection repair (Ainge, 2012)	33
Figure 10. Injection bolt, double lap joint (Gresnigt, 2000).....	34
Figure 11. New Avançon bridge, Bex, Switzerland; with the installation of the semi-integral bridge comprising GFRP deck bonded onto steel, longitudinal girders, and supported by cross beams. (Keller et al., 2013).....	35
Figure 12. GFRP- Balso sandwich deck joint. (Keller et al., 2013).....	35
Figure 13. Voids in adhesives: The top image shows adhesives with no insulation when curing, while the bottom image used insulation. (Park et al., 2010).....	38

Figure 14. Resin precoating metal substrate before adhesion (Wang et al., 2016)	40
Figure 15. Illustration of wettability (Perm Inc., 2016).....	41
Figure 16. Shear strength development over time at different temperatures. (Loctite, 2022.)	43
Figure 17. Graph of the effect of testing temperatures on compressive mechanical properties of epoxy resin: (a) Representative load-deflection curves. (b) Compressive strength and ultimate compressive load. (Jahani Y, et al, 2022)	44
Figure 18. Epoxy samples aged in seawater (Rudawska, 2020).....	45
Figure 19. Compressive strength of two different structural adhesives: Epoxies aged in different moisture conditions for three months. TW is tap water, while REF is reference seawater with 2xRED being double the salinity content of reference. (Rudawska, 2020).....	46
Figure 20. Tensile creep test with details of setup (Emara et al., 2017).....	48
Figure 21. Single lap joint shear test; (a) the boundary conditions, (b) the loading, and (c) the joint failure. (Ozel, 2014).....	48
Figure 22. Tensile creep test for injection bolted connection (Gresnigt, 2000)	49
Figure 23. Possible failure modes in bonded joints (Sullivan & Peterman, 2024).....	51
Figure 24. PPE for long-duration interaction with uncured structural adhesives.....	55
Figure 25. Compression silicone molds and water jet cutting.....	64
Figure 26. MTS compression test setup and laser setup.....	65

Figure 27. Drawing of ASTM C1181 creep test specimen	67
Figure 28. Compression creep mold pictures	68
Figure 29. Compression creep assembled rig with cured adhesive specimen	68
Figure 30. Example of creep test setup (ASTM C1181)	69
Figure 31. Compression slip test specimens.....	72
Figure 32. Picture of compression slip test assembly	73
Figure 33. Definition of slip loading (Province & Abebe, 2020)	74
Figure 34. Sketch of slip molds (Joshua Starr).....	76
Figure 35. Sketch of tension creep test specimens (Jason Provines).....	77
Figure 36. Tensile slip plate specimen	78
Figure 37. Tensile slip plate clamping.....	79
Figure 38. Tensile slip plate rig assembly	80
Figure 39. Bar graphs of the compressive ultimate strength of HFL (Sikadure-32 Hi-Mod) and HP (Sikadure-31 Hi-Mod Gel) based on different curing and testing temperatures. Bar graphs compare cure conditions to the advertised strength from the provider.....	83
Figure 40. Bar graphs of CFL (K-082) and CP (K-009) compressive ultimate strength based on different curing and testing temperatures. Bar graphs compare cure conditions to the advertised strength from the provider.	84

Figure 41. Bar graphs of the compressive ultimate strength of MFL (MM1018 FL) and MP (MM1018 P) based on different curing and testing temperatures. Bar graphs compare cure conditions to the advertised strength from the provider.	85
Figure 42. Averaged compressive ultimate and compressive yield strength bar graphs of all adhesives	88
Figure 43. Averaged compressive ultimate peak strain and bar graphs of all adhesives. Peak strain is the strain at max stress.....	90
Figure 44. Comparison of compression peak strain for Sikadur-31 Hi-Mod Gel (HP) and Sikadur-32 (HFL) at three different temperatures under a range of low to high-temperature conditions while maintaining humidity at 50%.	91
Figure 45. Comparison of compression peak strain for Copps K-082 (CFL) and K-009 (CP) at three different temperatures under a range of low to high-temperature conditions while maintaining humidity at 50%.	92
Figure 46. Comparison of the compression peak strain for Diamant MM1018 FL (MFL) and Diamant MM1018 P (MP) at three different temperatures under a range of low to high-temperature conditions while maintaining humidity at 50%.	93
Figure 47. Scatter plot of the compressive creep (averaged) of all adhesives.....	96
Figure 48. Creep Compliance and Creep Coefficient Scatter Plots. Creep Compliance over time is on the right, and Creep Coefficient over time is on the left.	98

Figure 49. Reference Creep Compliance and Creep Coefficient Bar Graphs. Shows reference creep compliance on the left and reference creep coefficient on the right for all three samples for each adhesive. The reference creep point is the strain at 672 hours.	99
Figure 50. Average tensile load (surface Class B) vs. displacement. With provided average surface factor (Ks).....	102
Figure 51. Examples of slip test vertical displacement measurement mesh points/vectors	102
Figure 52. Average tensile load (surface Class A) vs. displacement. With provided average surface factor (Ks).....	104
Figure 53. Summary graph of slip surface coefficients (Class B). Numbers indicate a sample of the three best results.	105
Figure 54. Summary graph of slip surface coefficients (Class A). Numbers indicate a sample of the three best results.	105
Figure 55. Individual specimen tensile creep results over time.....	106
Figure 56. Average tensile creep results over time. Includes the final creep for each set of samples at 1000 hr and the linear trend line to 2000 hr.	107
Figure 57. Individual specimen tensile creep clamping force over time	108
Figure 58. Tensile creep average clamping force over time.....	109
Figure 59. Scatter plot comparing compression creep coefficient to tensile creep	113
Figure 60. Scatter plot comparing creep coefficient to compression ultimate stress	113

1 INTRODUCTION

Bridges require repair within the first 20 years of service life, with many designed only to last 50 years. The dilapidation of bridges in the United States has become a widespread, multifaceted challenge. Approximately 30% of bridges are glaring examples of structural deficiency or obsolescence. The causes of degradation vary and may include corrosion, fatigue-induced damage, overloading, design code amendments, deficiencies in design and execution, or inadequate maintenance. Addressing these issues typically involves the choice between repairing or replacing the bridges. Replacement, even of individual components like girders, often proves costly and time-consuming, surpassing the expenses associated with repairs. Hence, there is a pressing demand for innovative, cost-effective approaches to bridge repair to alleviate the financial burdens (Ghaffary & Moustafa, 2020).

Gaps can emerge within steel bridges, occurring between steel plates in bolted connections. Figure 1 or between steel and concrete surfaces, such as between steel-bearing plates and concrete abutments Figure 2. These gaps may arise from corrosion fabrication errors, construction oversights, or long-term service loading. These gaps pose not only durability concerns but also structural issues, impacting load transfer paths and leaving unobservable sections of steel exposed to further corrosion.



Figure 1. An example of a gap repair between a flange on a bridge (Provines, 2022).



Figure 2. An example of a gap repair between a beam end and a concrete abutment (Provines, 2022).

In concrete bridges, cementitious grouts are commonly employed to fill such gaps due to their similar material properties to concrete, high compressive strength, low shrinkage, and cost-effectiveness. Unlike concrete, steel bridges lack an accepted repair technique for these gaps (Rollins, 2015). One potential solution explored by the American Institute of Steel Construction (AISC) involves utilizing structural adhesives as a steel grout to fill these gaps and improve fastened connections (AISC, 2019). These adhesives, including epoxies, chemical fillers, and metal polymers, have been utilized extensively in other industries.

Adhesives can possess fluid/injectable or putty-like properties for use in steel bridge applications to fill small gaps or cracks, as depicted in Figure 3, necessitating minimal surface preparation during the application or viscous/putty-like behavior to pack into more significant gaps (Makevičius et al., 2021). Once cured, they offer high strength, including compressive, adhesive, and shear, while exhibiting low shrinkage. This approach offers a promising avenue for effectively addressing gap-related issues in steel bridges while staying cost-effective, with some reports stating that it is cheaper than other forms of section repairs (Ainge, 2012).



Figure 3. Images of steel connection injected with epoxy (Makevičius et al., 2021)

In a recent repair in Richmond, VA, structural adhesives were used to repair a rusted-out section of the web and flange of multiple girders. The girders had developed rust, mainly on the beam ends and bearings. This is a common repair that occurs due to the permeation of rainwater around expansion joints or ends of bridges where moisture and chlorides can corrode sections of the steel girders Figure 4.

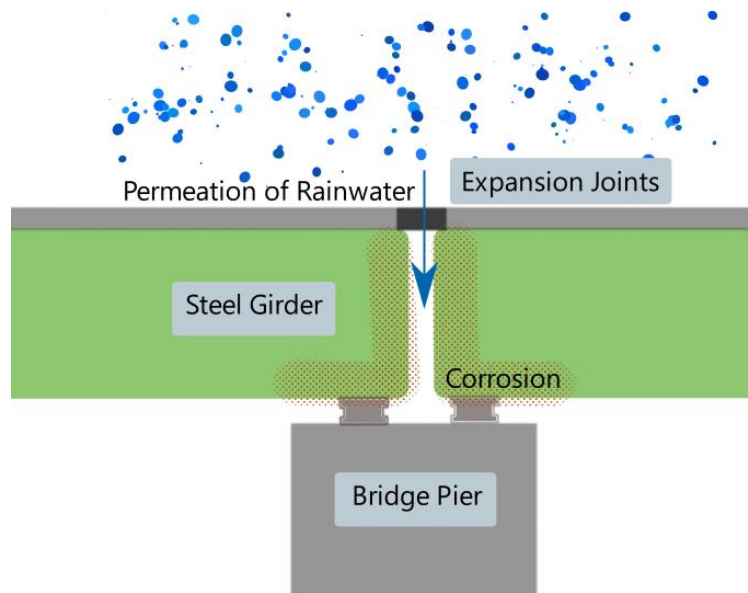


Figure 4. Steel girder expansion joint corrosion illustration

This rust eventually led to section loss in the beams, jeopardizing the bridge's structural integrity. Instead of replacing the beams outright, which would cause considerable slowdowns in traffic and incur a large amount of material and labor costs, the engineers opted for spot repairing the bridge by first descaling all the rust and polishing down the steel, then bolting L-shaped plates over the section loss in the web as shown in Figure 5.



Figure 5. Richmond girder spot repair visit (taken by Joshua Starr)

This method did fix the significant structural deficit of the bridge but left many gaps for further corrosion of the web and used an excessive amount of steel. If the engineers used structural adhesives to assist in the repair, they might be able to reduce steel costs while also providing better preventative measures against further corrosion and creating a more structurally sound repair, as illustrated in Figure 6.

Structural adhesives have recently undergone testing and research for use in structural steel construction. The majority of these studies focused on the tensile or shear behavior of the adhesives. However, for many of the previously mentioned applications of structural adhesives, a primary concern is the compressive behavior of the materials.

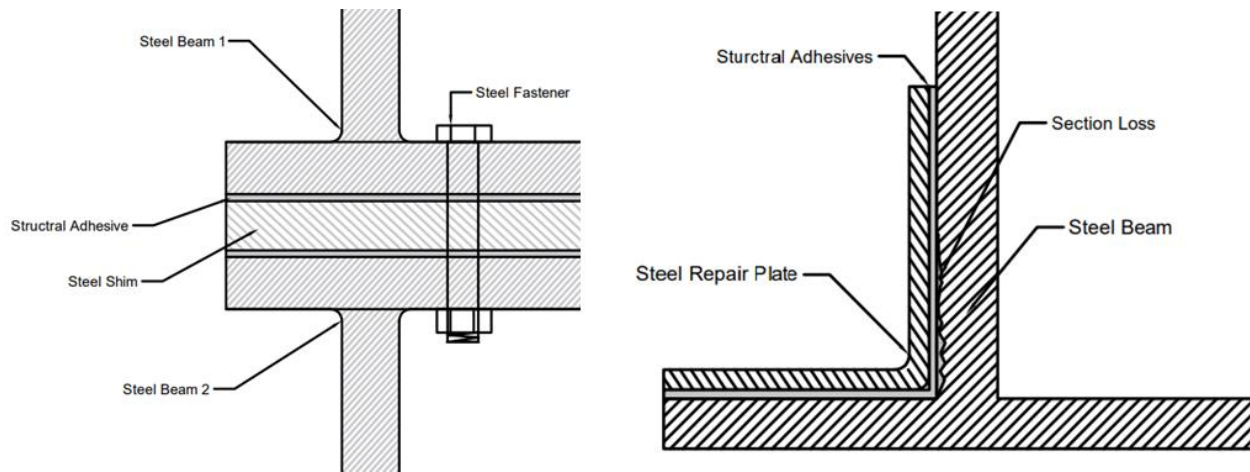


Figure 6. Drawing of steel grouting examples

This thesis aims to evaluate a selected number of structural adhesives for steel grouting and bridge repair while also offering guidance for their specified use. This project includes a literature review of current applications of structural adhesives, with backgrounds on relevant studies on the material properties of structural adhesives, which were introduced first. Then, a comparative analysis of different structural adhesives is conducted for the selection of adhesive materials to be considered in the experimental program. Next, extensive laboratory testing of the selected structural adhesives' compressive load behavior is collected. The experimental tests include both material-level testing, including compressive strength testing and compressive creep tests, and component-level tests, such as slip-critical connection testing and tensile creep tests.

2 LITERATURE REVIEW

2.1 Introduction

Traditional repair methods for repairing steel bridges often involve welding or mechanical fastening, which can be time-consuming, expensive, and disruptive to traffic flow. In response to these challenges, the use of structural adhesives has emerged as a promising alternative for steel bridge repair. The motivation behind the adoption of structural adhesives lies in their ability to address critical challenges associated with traditional repair methods. Structural adhesives offer advantages such as enhanced durability, corrosion resistance, and ease of application by providing high-strength bonding solutions. These adhesives can effectively bond steel components, mitigate stress concentrations, and improve the overall structural integrity of bridges.

This literature review aims to explore the diverse applications of structural adhesives in steel bridge repair and construction, as well as their utilization in other industries, such as aerospace and naval construction. The review will be structured as follows:

- Applications of Structural Adhesives in Aerospace: This section examines the extensive use of structural adhesives in the aerospace industry, focusing on their role in aircraft construction and repair. Topics include the types of polymers used, bonding techniques, and the advantages of adhesive bonding in aircraft design.
- Utilization of Structural Adhesives in Naval Construction: Here, the application of structural adhesives in shipbuilding and maritime infrastructure is discussed. Special attention is given to using fiber-reinforced plastics (FRPs) and adhesive bonding techniques for lightweight, corrosion-resistant vessel construction.

- Structural Adhesives for Transportation Infrastructure: This section explores the application of structural adhesives in transportation infrastructure, particularly in concrete repair and bridge construction. Topics include surface preparation techniques, curing conditions, and material properties of adhesives used in infrastructure projects.
- Behavior and Standards for Structural Adhesives: The behavior of structural adhesives under different environmental conditions, such as moisture and temperature, is examined. Standards and testing methods for assessing adhesive performance and safety considerations are also discussed.
- Health and Safety: The safety concerns associated with working with structural adhesives, including chemical hazards and proper ways to protect workers.

This comprehensive review aims to provide insights into the role of structural adhesives as innovative solutions for steel bridge repair and construction, contributing to the development of sustainable and resilient infrastructure systems.

2.2 Applications of Adhesives

2.2.1 Aerospace

The aerospace industry has been using polymers since 1945 by the British for metal-to-metal, metal-to-composite, or composite-to-composite bonding connected parts. The aerospace industry has been quicker in adopting structural adhesives in their design (Mouritz, 2012), practice. Thermosets and thermoplastic polymers have been observed in airplane construction, with thermoplastics like acrylics used for windshields and canopies. They offer a high-strength, lightweight material that can be transparent. Thermoplastics also provide high resistance to

impacts and are unlikely to fracture. Thermoset plastics like epoxies, often found in fiberglass composites, offer greater strength and stiffness and are the go-to for aircraft structural repairs (Higgins, 2000).



Figure 7. Materials on modern planes (Mouritz, 2012)

As described by Mouritz (2012), structural adhesives are “high-strength glue that bonds together components in a load-bearing structure.” Whether it is an airframe, bridge, or building, this description holds. The most common structural application of adhesives in aerospace is their use on joints, often with fasteners for added safety, providing stronger but lighter connections. Adhesives used in joint bounding lower the cost and weight of connections in aircraft. Using adhesive connection leaves fewer points for stress concentrations and crack propagation due to the

Lessing of drilled holes on parts. It is pointed out that a lot more preparation work is required when using polymer adhesive connections (Admas, 2021)

Table 1. Comparison of the advantages and disadvantages of polymers for structural applications

Thermoplastic	Thermoset	Elastomer
<i>Advantages</i>		
<ul style="list-style-type: none"> • Non-reacting • Rapid Processing • High impact resistance • High Ductility • High fracture toughness • Resists moisture • Recyclable 	<ul style="list-style-type: none"> • Low cure temperature • Low viscosity • Good compression properties • Good fatigue resistance • Good creep resistance • Highly resistant to solvents • Good for composites 	<ul style="list-style-type: none"> • Low cure temperature • High ductility and flexibility • High fracture toughness • High impact resistance
<i>Disadvantages</i>		
<ul style="list-style-type: none"> • Remarkably high viscosity • High processing temperature • High processing pressures • Poor creep resistance 	<ul style="list-style-type: none"> • Long cure time • Low ductility • Low fracture toughness • Low impact resistance • Absorbs moisture • Limited shelf life • Non-recyclable 	<ul style="list-style-type: none"> • Long processing times • Poor creep resistance • Low Young's modulus • Low tensile strength

For this project, using adhesives to strengthen fastened connections within the aerospace industry is a strong suggestion that the use of structural adhesives in civil design and construction

should be taken seriously. With the extensive adoption of polymers like epoxy and acrylics in today's planes in fuselage and wing structures, many people's livelihoods rest on the behavior of these structural polymers.

2.2.2 Navy

In ship construction, as in plane construction, there is a need for lightweight materials. Such materials allow a ship to carry a larger payload, enable higher speeds, and reduce fuel consumption. Most lightweight materials used in ship construction are fiber-reinforced plastics (FRPs). FRP composites for marine applications are generally laminated composites. They consist of several layers of reinforcement fabric in a polymer resin matrix. In the case of sandwich construction, there are two skin laminates with a core between that keeps the laminates in place and provides a shear connection between them.” (Noury et al., 2002). FRP often uses resins like other structural adhesives; these resins can include polyester, vinyl ester, epoxies, and phenolics (Noury et al., 2002). The FRPs are used similarly to carbon fiber in the automobile industry to allow for high-strength, low, low-weight laminate parts that are ideal for performance, mainly in the spots. FRP may provide a vessel with excellent corrosion resistance and less cracking prone. FRP also offers military applications with its non-magnetic (fewer hazards from mines) and low electromagnetic resistance for better stealth. Polymer materials have also been successfully used for piping on vessels to replace steel pipe systems.

When looking at larger vessels, the ship will not be eternally constructed out of light materials like FRP, but other structural adhesives are used to improve vessels. Jointed connections will often use adhesives instead of welding for bolting. This method of joining parts together offers the same advantages as in aerospace design. “Adhesion-bonded joints become more frequently

used in shipbuilding, as they also offer a possibility of joining different materials along with the advantages brought by the adhesion process itself, being cost-efficient and ensuring easy maintenance and repair.” (Panchuck et al., 2021). Adhesive bonding joints offer the added benefit of circumventing the main issue arising from joining two dissimilar metals together, whereby welding would be expensive and fastening connections would lead to significant levels of corrosion, like on the United States Navy’s littoral combat ship (LCS). In the case of the LCS, at the time, the idea of a warship being made of aluminum was first being used by the Navy, Figure 8. The hull is made from aluminum, but the propulsion system is steel, leaving the material more vulnerable to corrosion.

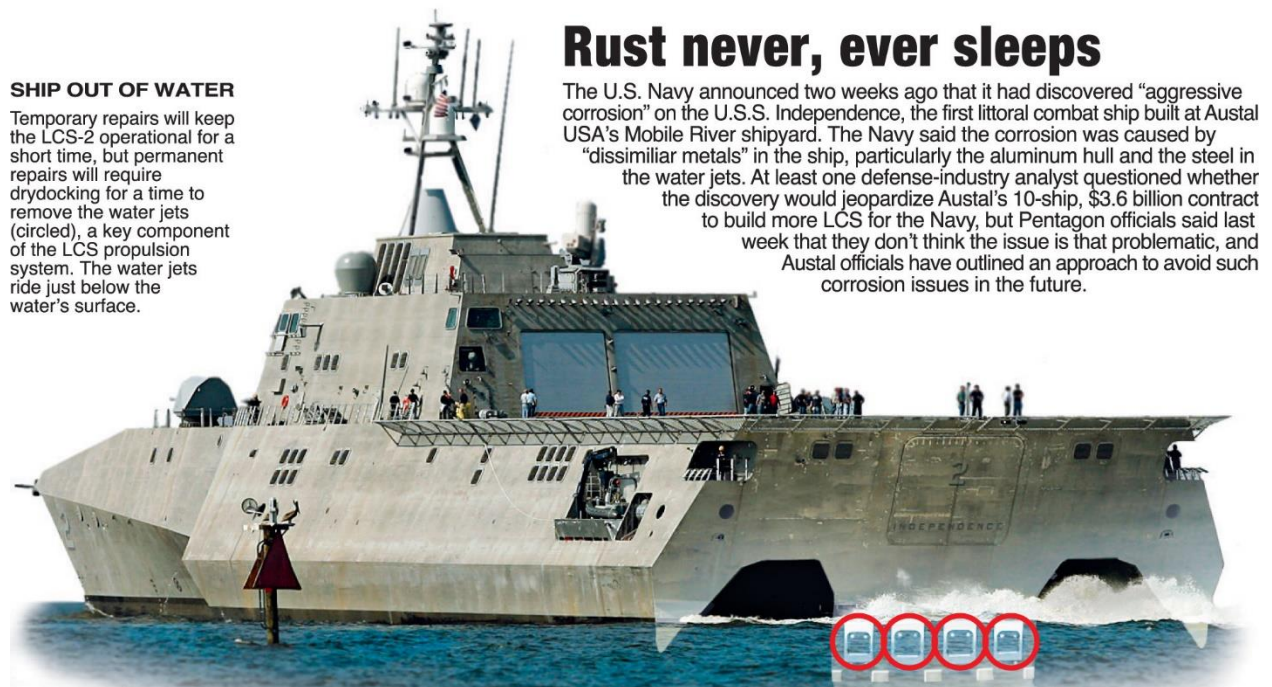


Figure 8. Depiction of the U.S.S. Independence corroding from dissimilar metals (Specker, 2023).

Even though using dissimilar material bonding with adhesives is beneficial, it comes with its own challenges; particular attention must be given to designing joints between dissimilar materials, particularly when combining metals with non-metals, as variations in thermal expansion coefficients can result in significant stresses on the adhesive. Extra care is required when transitioning from welding or mechanical fastening to adhesive bonding in a component's replacement process (Morris, 1994).

2.2.3 Transportation Infrastructure

In transportation infrastructure design, structural adhesives have been used since the 1960s. Many applications have been found for structural adhesives, primarily for their chloride and moisture resistance (Masoudi, 2013). The most widely known uses for adhesives, including epoxy, are used as a protective coating, but newer approaches for high-strength adhesives (structural adhesives) are used as essential structural components in structures. In concrete bridges, epoxy resin has been used to repair cracked and even collapsed bridges. In 1964, an earthquake in Niigata destroyed the Showa Bridge. This bridge was salvaged and repaired with structural adhesives and is still around today, connecting the banks across the Shinano River (Yamazaki, 2020). Other bridges have been restored using structural adhesives for crack repairs on concrete slab decking. When structural adhesives are used in concrete repair, they are treated as grout. The adhesive is mixed fine particles or aggregate that will give the adhesive high compressive strength and 7k low rigidity, having similar behavior to that of concrete while still adhering to it.

Based on findings, the most common use of structural adhesives in bridge repair and construction is in concrete-to-concrete or concrete-to-steel connections, focusing on the adhesive's compressive behavior. Adhesives are used in steel repair and construction, but research suggests

that most applications are made as a form of seal or cover for the steel sections of the bridge or crack filling, not as used as a critical structural part. For crack repair, epoxy can be injected into “dead cracks” for cracks up to 1/8in thick, Figure 9 (Ainge, 2012).

In some cases, steel connections will use structural adhesives coated onto the steel members at a factor or assembly yard before being taken on site, whereby the adhesive is cured, and the members are joined.

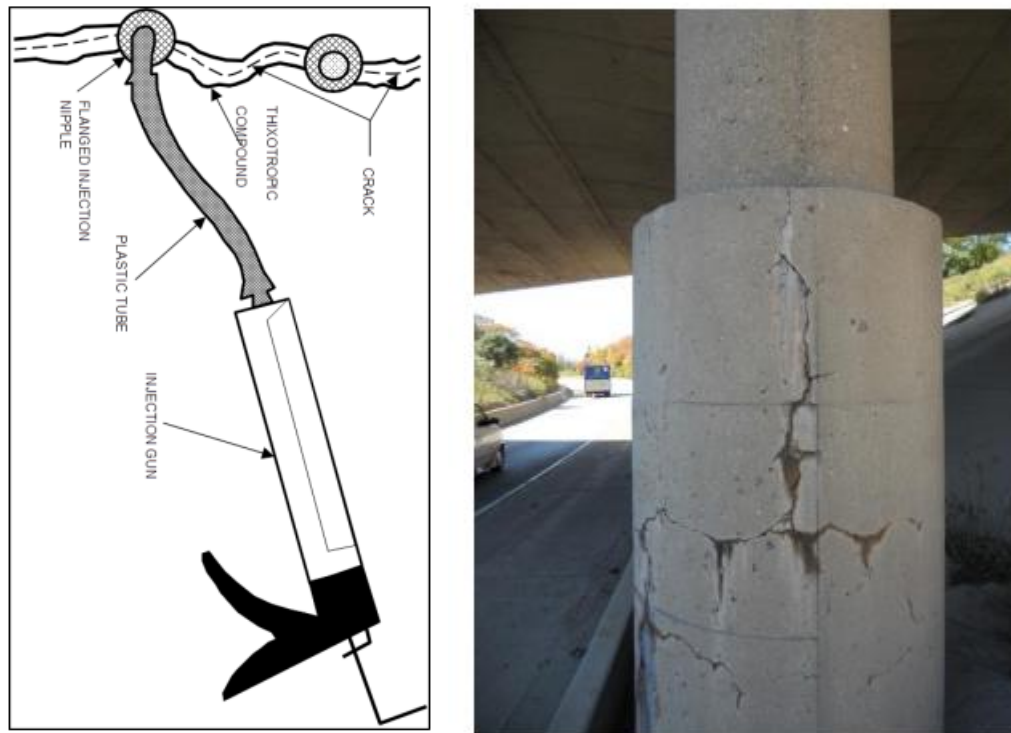


Figure 9. Concrete crack epoxy injection repair (Ainge, 2012)

Injecting bolts with structural adhesives is not a new practice; injection bolts in construction can be done by using a cavity in the bolts to inject resin into the gap between the bolt and fastened structure, Figure 10. This Bolt connection improves load transfer in the bolts and drastically

improves the slip factor of the connection. It has been found to strengthen corroded plates and prevent further corrosion of repaired steel sections on steel girders used on bridges (Gresnigt, 2000).

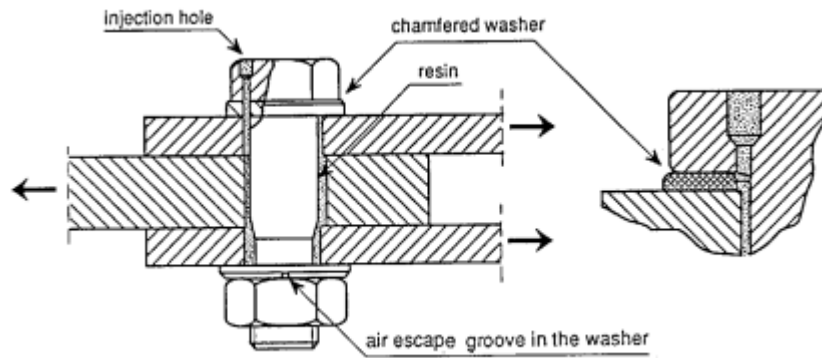


Figure 10. Injection bolt, double lap joint (Gresnigt, 2000)

In one journal entry by Keller et al. (2013), an old concrete bridge spanning the Avancon River in Switzerland must be widened and refurbished. The structural engineers found that using glass fiber-reinforced polymer (GFRP) and balsa to sandwich the deck to two longitudinal steel girders was the optimal solution. They found that using adhesive bonding reduced traffic disruption by 80%. The bridge repair was able to forgo expansion joints, reducing maintenance expenses. Through simulation and lab testing, the engineers of the bridge designed a GFRP-balsa decking structurally adhered together with 90° Z joints through injections.



S

Figure 11. New Avançon bridge, Bex, Switzerland; with the installation of the semi-integral bridge comprising GFRP deck bonded onto steel, longitudinal girders, and supported by cross beams. (Keller et al., 2013)

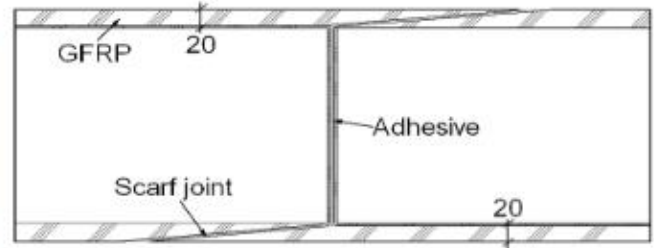
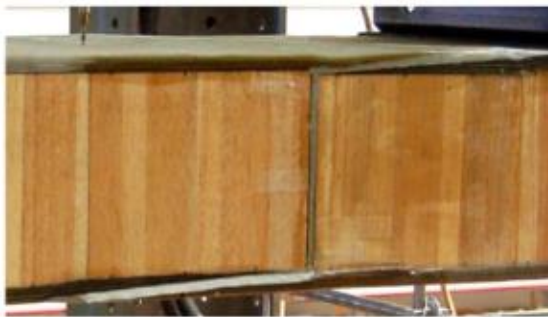


Figure 12. GFRP- Balsa sandwich deck joint. (Keller et al., 2013)

For steel-on-steel joints, it is known that pure adhesive-connected joints are applicable in structural design, though they are not always recommended and should be used with other fasteners. Joints should fail slowly and be easily detected. Also, adhesive connections have been documented to have accounted for unseen defects during their application that can cause premature failure of a connection (Banea & Silva, 2009).

2.3 Behavior and Standards for Structural Adhesives

2.3.1 Surface Preparation

The non-flatness of surfaces at a microscopic scale presents an opportunity for exploitation. Employing a liquid adhesive capable of infiltrating surface roughness, which solidifies, enables mechanical locking to enhance the strength of interfacial bonding (Morris, 1994). Before applying any structural adhesive, some action is necessary to ensure the adhered surfaces are adequately prepared. Dust, grease, water, ink, and residue will all harm the strength of the adhered bond of an adhesive. Therefore, surface preparations are recommended. Surface preparation techniques eliminate contaminants such as dirt, oil, grease, paint coatings, rust, tarnish, and others, facilitating interaction between the applied adhesive and the true contact area of adherence (Panda et al., 2020). Adhesively bonded connections can be powerful while lowering the weight and improving corrosion resistance. Still, the biggest flaw is the interaction between the substrate material and the adhesive. The weakest link in a laminar composite structure is frequently the adhesive bond between the adhesive matrix and the substrate material. This has spurred a growing need to enhance the bonding capabilities of epoxy adhesive joints (Zhang & Huang, 2021).

Imperfections on the surface of the substrate material may lead to gaps in the connections between the adhesive polymer and what it is to adhere to. Stress concentrations start to manifest and lead to fracturing of the adhesive. The connections can fail prematurely with crack propagation due to loss in distributed load area and strength. Latent failures in structural adhesive bolt connections are more challenging to detect than a traditional connection, making surface preparation more paramount. A clean surface is an essential condition for the adhesion of structural adhesives but is not a required condition for bond durability (Banea & Silva, 2009). Rougher

surfaces were found to be better at maintaining adhesion to substrates. In one report, they found that smooth steel surfaces lowered the shear strength of the adhesion by up to 30% for galvanized steel (Machalická et al., 2017).

Parallel to surface preparation, there is a concern about air pockets. Impurities from fluids like air and water can leave voids within the adhesive-filled sections, as shown in Figure 13. Air pockets can develop during the mixing process when air is folded into the adhesive mix or during the application of high viscous structural adhesive. These voids leave a catalyst for stress concentration along the path of stress, lowering the performance of the bond (Park et al., 2010). Tests showed that samples lacking internal voids exhibited failure loads 40.5% and 46.2% higher than those with voids, with adhesive lengths of 25 mm and 30 mm, respectively. The increased thickness of the adhesive section leaves more room for potential voids and lowers the strength. The greater adhesive thickness creates less strength for the bond. This thickness is not easily controlled; in a laboratory, the thickness can be measured and held; in the field, gaps may be problematic to see and non-uniform.

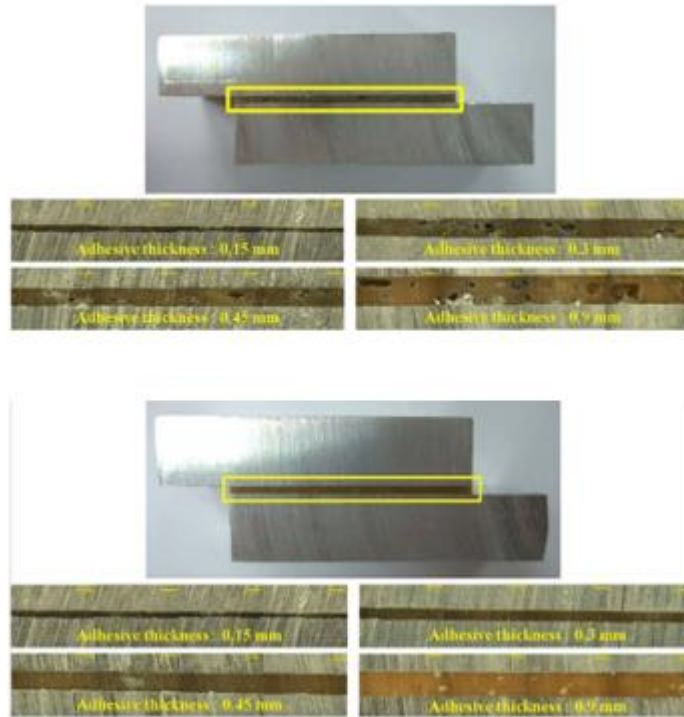


Figure 13. Voids in adhesives: The top image shows adhesives with no insulation when curing, while the bottom image used insulation. (Park et al., 2010)

Surface preparation methods come in many forms, with advantages and disadvantages. Table 2 lists well-known surface preparation methods and their inherent principles at play. The most popular surface preparation is degreasing with immersion/wiping/spray in solvents like acetone or paint thinners like methyl ethyl ketone (MEK) and grit blasting. Many surface preparations are done, leading into other surface preparations; Zhang & Huang (2021) demonstrate this by taking steel sheets that were to be adhered and putting them under a 15-minute ultrasonic cleaning with pure acetone at a constant temperature of 20°C. Subsequently, grit blasting was conducted on the overlapped section of the steel sheets using 60-grit aluminum abrasives, followed by surface cleaning with compressed air. The specific parameters for different surface preparations are

provided in Table 2. Lastly, prior to the application of the prepared adhesive, the blasted steel substrates underwent another round of ultrasonic cleaning under identical conditions to eliminate any residual dust or contaminants from the surfaces.

Table 2. Surface preparation methods for adhesive application on steel (Zhang & Huang, 2021).

Surface Preparation Methods		Working Principle
Degreasing	Vacuum degreasing	Using vapors of degreasing solvent that condense on metals, solubilize content and then drip off.
	Ultrasonic vapor degreasing	Vapor degreasing followed by ultrasonication
	Immersion/spray	Immersing adherend in solvent or spraying solvent of adhered
Mechanical abrasion	Grit blasting	Impinging hard grits on adherend surfaces.
	Acid bath	Immersing material in acids to obtain cavities on the surface.
	Anodization	Formation of coating using the application of voltage between anode and cathode
Physical	Corona treatment	Collision of the stream of charged particles driven by electric fields to the adhered surface.
	Flame treatment	Use of oxidizing flames to treat the surface.
	Plasma treatment	Collision of plasma is obtained by ionizing the air with applied voltage and adhering to it.

A study by Wang et al. (2016) used epoxy resin (without hardener) mixed with a solvent (acetone) as a precoat that can improve the surface area across the substrate; this can be hardened after contact with the two-part epoxy mixed layer of resin (with hardener) if the precoat is thin and has around a 1/10 resin to solvent ratio as shown in Figure 14. A fair amount of testing has been conducted to determine the best surface preparation, but there seems to be no consensus.

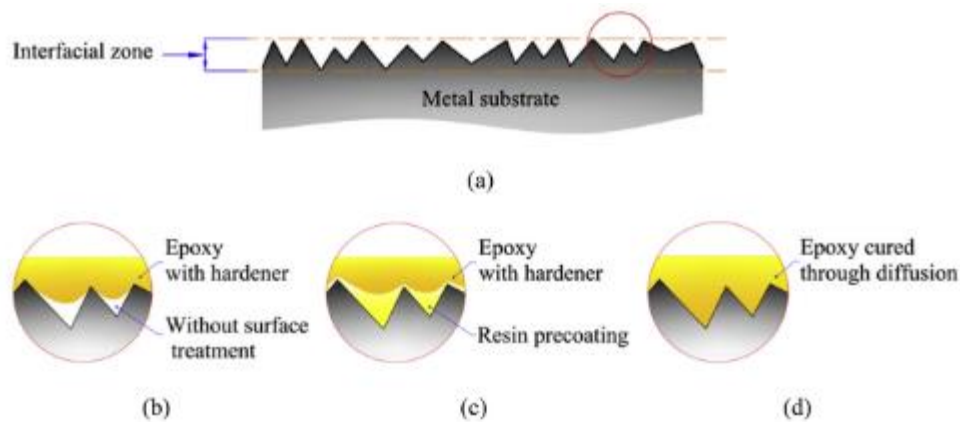


Figure 14. Resin precoating metal substrate before adhesion (Wang et al., 2016)

The method to quickly determine the quality of the preparation substrate surface is by choosing wettability. When a fluid is in contact with soil, there is surface tension; the change in this surface tension can be observed. Wettability refers to the propensity of a fluid to extend over or stick to a solid surface when other immiscible fluids are present. This tendency is typically quantified by determining the contact angle at the interface between the liquid and solid surfaces. The contact angle, denoted as θ_c or the wetting angle, is consistently measured from the liquid phase to the solid surface (Perm Inc., 2016). The closer the contact angle of the water to the substrate is to zero, the better the wettability and the better the surface preparation, Figure 15. Ideally, water should spread out across the substrate surface.

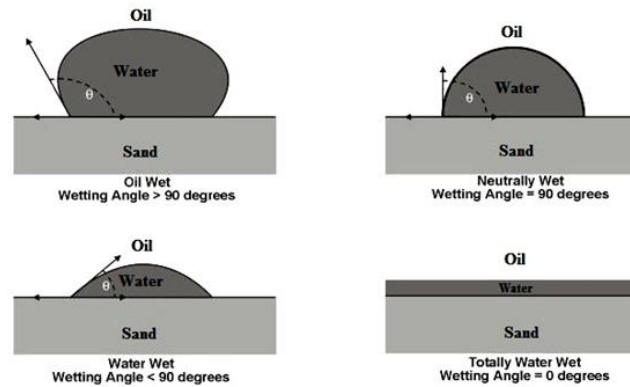


Figure 15. Illustration of wettability (Perm Inc., 2016)

2.3.2 Curing and Environment

In this section, the curing of epoxy resin is discussed. The curing of epoxy resin can be done in various ways: chemical curing (traditional thermal curing), radiation curing (ultraviolet (UV)), and microwave curing. The curing of epoxy resin converts from a fluid into a hard, infusible material. This is done through cross-linking reactions, which lead to a polymer structure. This process typically uses a curing agent (hardener) that causes a chemical reaction that cross-links the resin's polymer chain and increases the adhesive's molecular weight, transforming the resin from a viscous fluid to an elastic gel (gel point). This gel point is where the polymer will no longer flow. Eventually, the resin will continue to go through this chemical reaction till it is a glassy solid when it reaches its glass transition temperature. After curing, while the resin temperature is below the glass transition temperature (T_g), the resin is in a solid; above this limit, the resin will become rubbery. While above T_g , crosslinking of the resin's polymers can continue and increase the strength of the material (Thomas et al., 2014).

The most significant limiting factor for the curing of adhesives is often the glass transition temperature. The T_g , found exclusively in polymeric materials, marks the transition between the glassy and rubbery states. It serves as a crucial benchmark for evaluating the mechanical properties of polymers. Typically, T_g minus 20°C is seen as a threshold temperature for most applications, as significant deterioration in mechanical performance may occur at this temperature level. (Miravalles & Dharmawan, 2007).

Studies have shown that adhesives require longer curing times at lower temperatures, with suggested temperature ranges for epoxy adhesive curing between 35°C to 60°C. This is especially crucial for cold-curing epoxy adhesives (Cruz et al., 2021). In fact, if it is below 0°C, curing the epoxy is impossible. It happens because the resin undergoes vitrification within the network when curing at temperatures lower than the resin's ultimate glass transition temperature (Jahani et al., 2022, p.2). In summary, a high temperature that is below the adhesives glass transition point and a longer cure time increases the strength of the adhesives. Figure 16 Demonstrates some trends for increasing the strength of adhesives like epoxy over cure time. One can see from this figure that lower temperatures drastically slow the relative strength cure of the adhesive, while higher temperatures can improve the strength cure. Given enough time, a cold-sued epoxy will eventually reach its 100% cure strength and level out. Cure temperatures are mostly important for ensuring a structure's readiness for service.

During the mixing and curing process of many adhesives, it is common for gas to accumulate in the adhesive resin, which can cause a reduction in the behavior of the adhesive. Removing air bubbles during the fabrication of exposes improved the quality of the samples and

reduced result inconsistencies. Specifically, the degassing method used without further heating after casting notably enhanced material quality by minimizing trapped air voids. In this report, samples displayed increased stiffness and tensile strength and superior fatigue resistance compared to other sample series (Andrea et al., 2020).

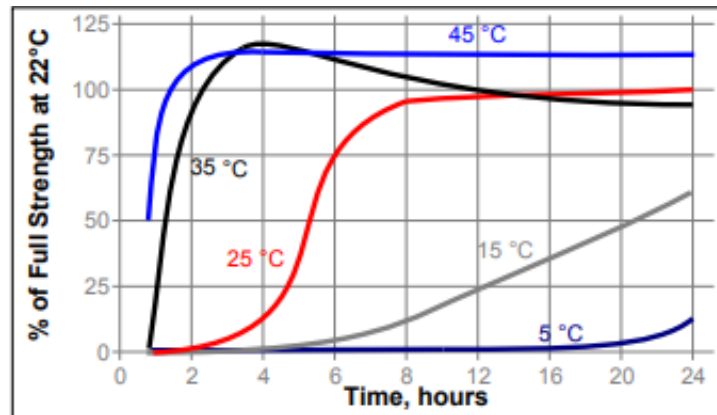


Figure 16. Shear strength development over time at different temperatures. (Loctite, 2022.)

The effect of post-curing and testing temperatures from different epoxies is studied in (Jahani Y et al., 2022). The study found that when testing temperature exceeds T_g significant decrease in tensile strength was observed. Curing temperature below T_g results in greater tensile performance due to the increase in cross-linking within the adhesive's cure. When the cure temperature exceeded T_g the material performance decreased due to thermal degradation. The behavior of epoxy adhesives in compression under different testing temperatures is graphed in Figure 17. The data shows that lower temperatures increase strength and make the adhesive brittle, while higher temperatures decrease strength but lower stiffness, making it soft. The optimal cure and load conditions were suggested to be around 40°C.

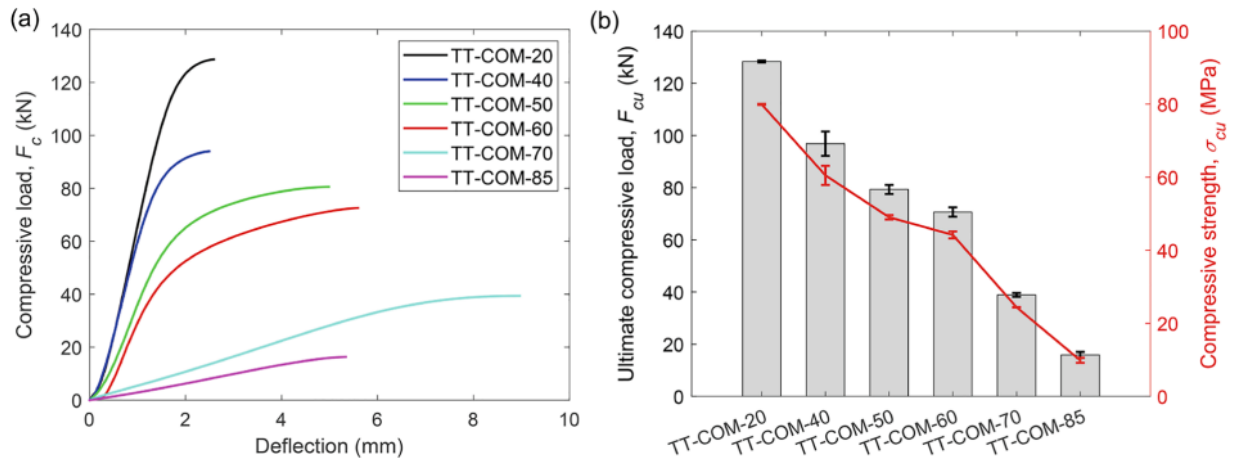


Figure 17. Graph of the effect of testing temperatures on compressive mechanical properties of epoxy resin: (a) Representative load-deflection curves. (b) Compressive strength and ultimate compressive load. (Jahani Y, et al, 2022)

Another environmental concern is adhesive behavior when exposed to high moisture and high chloride environments. Adhesives like epoxies are well known to be a great insulator of water, but this does not mean the adhesives themselves are not effective in corrosive environments. When researching atmospheric humidity effects on curing, one study by Cruz et al. (2021) found that excess atmospheric humidity during curing can compromise the epoxy adhesive and undermine its performance.

In one study by Rudawska (2020), different samples of cured epoxy were exposed to different seawater environments. The results showed that the epoxy was significantly affected by the saltwater, causing delamination and plasticization of the compound with softening of the edges/substrate of the material, Figure 18. Cruz et al. (2021) confirm these conclusions, stating that an irreversible process of chemical degradation and micro-cracking can occur during long-term exposure to moisture and high textures. Water accelerates the aging of epoxies, but less so than other structural adhesives; a fully submerged epoxy specimen will retain 90% of its

interlayer shear strength, while other adhesives, like polyester, will retain only 65%. Layers of structural adhesives that are resistant to moisture will negate most effects of saltwater corrosion, protecting the cured adhesives superstrate. In conclusion to Rudawska's study (2020), states that strength testing outcomes of some types of epoxy adhesive when exposed long-term to environments containing calcium carbonate (CaCO_3) can demonstrate strengthening from the salinity. Depending on the seawater salinity conditions and duration of aging, tested epoxy adhesive formulations with Figure 19 revealed minor compressive strength improvement compared to a lower salinity content water environment.

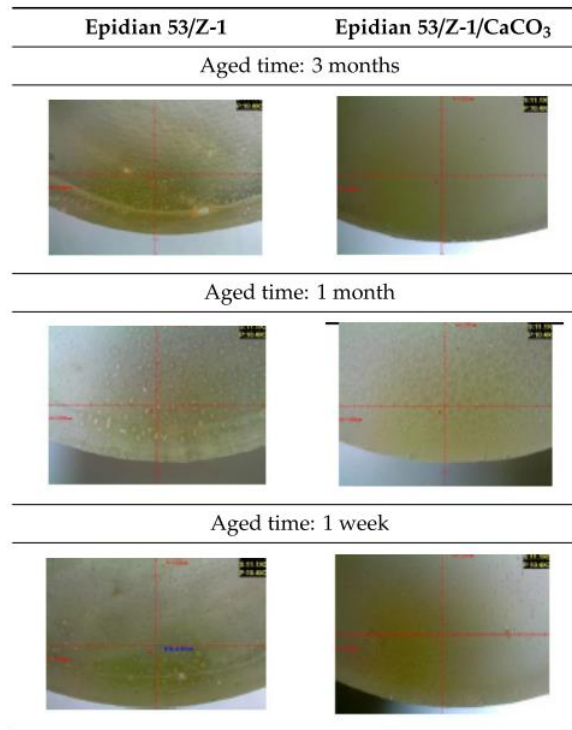


Figure 18. Epoxy samples aged in seawater (Rudawska, 2020)

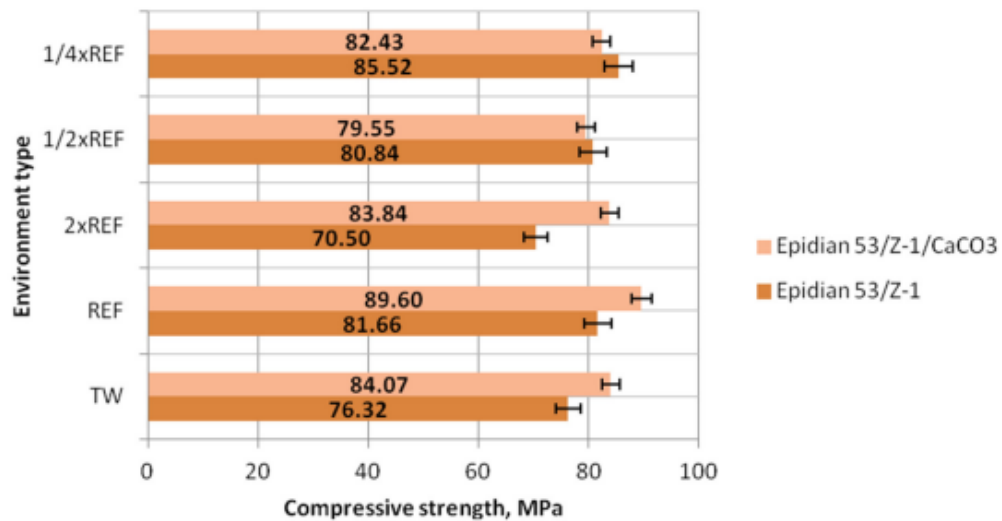


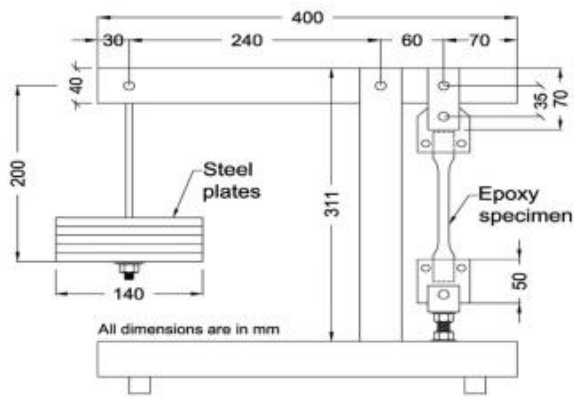
Figure 19. Compressive strength of two different structural adhesives: Epoxies aged in different moisture conditions for three months. TW is tap water, while REF is reference seawater with 2xRED being double the salinity content of reference. (Rudawska, 2020)

A couple of suggested solutions to prevent moisture exposure is to seal the adhesives during and after curing. This could be done using a cover or mold over the adhesives during curing. After curing, the adhesives can be painted to keep out moisture and prevent UV light exposure. Lastly, silicon adhesives are more resistant to moisture and UV damage but are not as rigid and can be used to cover up the core structural adhesives (Zuoa & Vassilopoulos, 2021).

2.3.3 Material Properties

Standards were commonly found for experimental testing of structural adhesives on steel connections: the American Society for Testing and Materials (ASTM) and the International Organization for Standardization (ISO). This study will focus on ASTM standards, but ISO standards will still be recognized, just not tested. For a comprehensive list of ASTM structural adhesive steel connections, go to Appendix T.

A majority of studies tested the tensile performances of different structural adhesives. The tests ranged from obtaining adhesives to ultimate strength performance, yield, and creep behaviors. Many tensile creep procedures followed EN ISO 527-2: 2012 or similar ISO procedures as depicted in Figure 20, using traditional “dog bones.” Quantitative measurements of creep behavior used creep compliance, creep coefficient, or tensile strain (will be discussed more in the following sections). Results found that factors that reduce the creep performance of adhesives were due to high moisture exposure, high or low semaphores, and poor surface preparations (Emara et al., 2017) (Cruz. et al., 2022). Most experimental papers looked at short-term tensile conditions using flat single or double lap shear joint connections like in Figure 21, observing the adhesion behavior of the adhesives (Ozel, 2014) (Morris, 1993) (Banea, 2009).



(a)



(b)

Figure 20. Tensile creep test with details of setup (Emara et al., 2017)

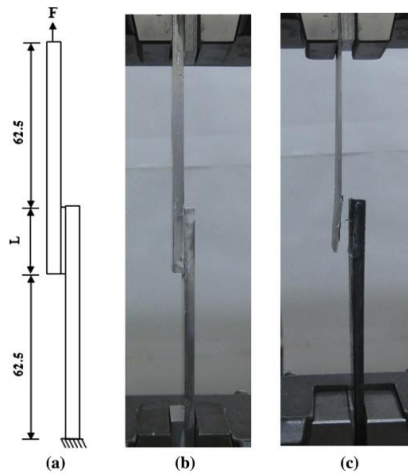


Figure 21. Single lap joint shear test; (a) the boundary conditions, (b) the loading, and (c) the joint failure. (Ozel, 2014)

Slip testing under tension was documented by Gresnigt (2000). The report recorded creep behavior due to tensioned triple plate bolted connections in Figure 22, pre-torqued, then loaded in step increments up to 250 N/mm^2 bearing stresses. Findings concluded that increased temperatures in service loading had a moderate influence on deformation; tests also concluded that creep seemed to flatten out and never reach the displacement failure criteria of 0.3mm after close

to 1600 hrs. of testing. Over longer periods of creep-fatigue joint testing, Sahellie (2015) concluded that epoxy adhesive demonstrates creep resistance appropriate for structural purposes over periods of up to 10 years, provided that the applied shear stresses constitute 12%. In one report comparing tensile strength and creep, it was concluded that a product's performance in tensile strength testing directly reflected tensile creep behavior (Albrecht & Mecklenburg, 1996).



Figure 22. Tensile creep test for injection bolted connection (Gresnigt, 2000)

Some studies, mostly aimed at aerospace development, experimented with the fatigue of adhesive systems. These studies used joint connections under tensile or shear load conditions. In one study, findings indicate that increasing the bond line thickness of adhesives proves to be more efficient in mitigating the fatigue crack propagation rate in joints bonded with the flexible adhesive. Flexible adhesives exhibit more excellent crack resistance owing to their ability to expand their plastic zone when subjected to restrictive substrates. Comparative studies on bulk

adhesive fatigue and fracture using either thin adhesive-bonded specimens or thick adhesively bonded specimens are notably limited in the existing literature (Xu et al., 1996). In Zuo's & Vassilopoulos's (2021) review and in Zhang's (2021) paper, they both found that while the thickness of the adhesives layer affects the fatigue crack growth rate and adhesive joint strength for shear with thicker layers of adhesives lowered crack growth and increase joints strength, fatigue crack growth is also affected by the material, so some adhesives may not follow this trend.

Very few studies have been found exploring compressive structural adhesives or their multi-axial performance. One study looked at the effects of curing and post-curing temperature of compressive strength of epoxies by Jahani et al. (2022), while another study by Rudawska (2020) studied the effects of epoxy adhesive compressive strength when aged in salt water and found that some epoxies aged in salt water provide mechanical strengthening. Another document discussed the characteristics of flexible adhesives; in this regard, they mentioned that during volumetric testing, the assumption that rubber-like adhesives could be treated as incompressible was false. Flexible adhesives are compressible, and volumetric terms should be included in material testing standards (Duncan & Croker, 2023). Studies of structural adhesives were mainly aimed at inspecting the behavior of structural adhesive joints in shear or tensile load conditions. With the assumption that tensile and compressive behavior would be equivalent due to their isotropic nature, it is essential to note that no data was found to confirm this. However, it seems to be a common assumption. In other reports, FRP resins may diverge from being isotropic. Most papers did not focus on bulk adhesive material testing and seemed to lean more toward adhesive joint testing.

The classification of adhesion joint failures includes adhesive failure, cohesive failure, thin-layer cohesive failure, fiber-tear failure, light-fiber-tear failure, stock-break failure, or mixed failure. Modes are depicted in Figure 23. The primary research failure modes are adhesive failure, whereby the adhesives lose hold on the substrate surface, and cohesive failure, where the structural adhesives themselves fail (Sullivan & Peterman, 2024)

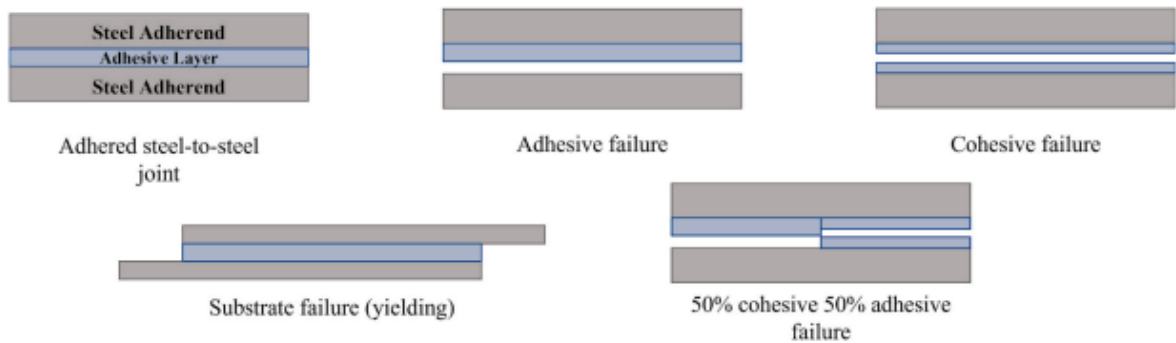


Figure 23. Possible failure modes in bonded joints (Sullivan & Peterman, 2024)

For adhesive-metallic joints, the most common failure for well-made metallic joints is with the adhesives (cohesive failure) rather than the interface with the adherend and adhesive (adhesive failure); this is only common in ideal lab conditions with proper joint preparation; otherwise, failure seems to be due to delamination, not adhesives failure (Adams & Comyn, 2000), this makes bulk material testing of specimens less informal to engineers when design for shear and tension. In comparison to failure to compress, delamination is less of a concern.

2.4 Safety and Hazards

There are a few hazards and safety concerns from using structural adhesives. Structural adhesives are usually formed through chemical reactions, with the associated chemicals being potentially harmful when uncured or during mixing. Many chemicals are used within the selected adhesives for this study, but in the context of state, Table 3 summarizes the different adhesives and the safety concerns associated with them. The tables of chemicals collected from the manufacturers provide safety sheets, with the chemical hazards and characteristics provided by the Centers for Disease Control and Prevention (CDC) through the Nations Institute for Occupational Safety and Health (NIOSH, 2020) pocket guide to chemical hazards. In summary, all the adhesives used have essential safety concerns that should be considered before interacting with them. All adhesives must come with safety data sheets that address the safety concerns associated with the product and need to be reviewed (NIOSH, 2020).

Table 3. Key chemical safety concerns (NIOSH, 2020)

Adhesives	Symptoms	Chemical	Formula	Protection
"All"	irritation eyes, skin with deep pain; nausea, vomiting; abdominal pain; resp distress, cough; cyanosis; reproductive effects; [potential occupational carcinogen]	<i>bisphenol- (epichlorohydrin)</i>	C_3H_5OCl	Skin: Prevent skin contact Eyes: Prevent eye contact, eyewash Wash skin: When contaminated Breathing: Respirator
HP	irritation eyes, skin, nose; dizziness, drowsiness; dermatitis; In Animals: liver, kidney damage	<i>solvent naphtha (petroleum)</i>	C_nH_{2n}	Skin: Prevent skin contact Eyes: Prevent eye contact, eyewash Wash skin: When contaminated Breathing: Respirator
CFL, HP	irritation eyes, skin, mucous membrane, upper respiratory system; dermatitis, skin sensitization; eye, skin necrosis; cough, dyspnea (breathing difficulty), pulmonary sensitization	<i>Diethylenetriamine or bis(2-Aminoethyl)amine</i>	$(NH_2CH_2CH_2)_2NH$	Skin: Prevent skin contact Eyes: Prevent eye contact, eyewash Wash skin: When contaminated Breathing: Respirator
HP	irritation eyes, skin, respiratory system; cough; skin, mucous membrane burns; dermatitis; conjunctivitis; liquid: frostbite	<i>m-phenylene-bis (methylamine)</i>	CH_3NH_2	Skin: Prevent skin contact (solution)/Frostbite Eyes: Prevent eye contact (solution)/Frostbite Wash skin: When contaminated (solution) Breathing: Respirator
MFL, MP	irritation of eyes, nose, throat, and respiratory system; lacrimation (discharge of tears); cough; wheezing, dermatitis; [potential occupational carcinogen]	<i>Formalin (formaldehyde)</i>	CH_2O	Skin: Prevent skin contact Eyes: Prevent eye contact, eyewash Wash skin: When contaminated Breathing: Respirator

To protect the user of the adhesives, it is recommended that the user go through the GHS classification and labels per OSHA standards and take proper precautions. Personal protection equipment (PPE) should be used before interaction with the adhesives. This can be determined based on the hazardous ingredients in the adhesives and the OSHA PPE recommendations (OSHA,

2023). This includes wearing eye protection, gloves, air respirator, and fully covering clothing. Figure 24 demonstrates the PPE used when preparing test specimens.

It is also worth mentioning that thermosetting polymers, such as epoxy resins, can be flammable, especially before and during the curing process (Yin et al., 2022). Therefore, taking proper precautions to mitigate or prevent adhesive fires is crucial. This includes ensuring adequate ventilation and avoiding the presence of ignition sources during the application and curing of epoxy adhesives. Additionally, storing epoxy adhesives in a cool, dry place away from heat sources can help reduce the risk of fire hazards.

During the current study, for eye protection and lung protection, the individuals who were responsible for interaction, mixing, and molding the adhesives (mixer) used a full-face respirator (3M 6000) with a (FM)/(OV)/P100 cartridge filter. The full-face respirator keeps irritable fluids away from the eyes and keeps both fine particles and organic vapors, including formaldehyde, out of the lungs. As recommended, Butyl or Nitrile with a thickness of 6-8 mil (double layering gloves are valid) were used and discarded every 20 minutes after contamination due to the penetration of the chemicals in the adhesives. Lastly, the mixer wore full body protection to protect his/her arms and legs from direct chemical contact.



Figure 24. PPE for long-duration interaction with uncured structural adhesives

After the mixer prepares the samples, any excess unmixed adhesives that will not be used later should be mixed/cured to neutralize them. After the epoxy adhesives are cured, they are considered harmless, can be interacted with without PPE, and can be disposed of via landfill without concern. A strong solvent like acetone or mineral spirits can dissolve the resin if the adhesives spill.

3 SELECTION OF ADHESIVE MATERIAL

3.1 Selection of Adhesive Class

Prior to conducting experimental testing, a compilation of potential adhesives suitable for this project was assembled. The principal criteria guiding the selection of adhesives for the project include the following: the adhesive must be manufactured in the USA, with preference for those used by VDOT in previous projects; it must be an established, commercially available product (not a prototype); it must be feasible for field repairs of bridges; and it must demonstrate adherence to both steel and concrete surfaces.

To narrow down the list of adhesive materials, a discussion is needed to determine what type of adhesive can be used for this project. In Table 4, there are seven classes of commonly used adhesives. Starting with phenolics, polyimides, and bis maleimides, all three adhesives suffer from the need to cure under high pressure. High-pressure curing is not only difficult but expensive to do for on-site repairs. VDOT is also unfamiliar with using these adhesives, so for the focus of this study, these three adhesives will be excluded. Next, looking at more familiar adhesives like polyurethanes and silicones, both are considered low-strength adhesives, so they are not desirable as structural adhesives. While both polyurethane and silicon are easy to cure and cheap, they are more designed for low mundane applications like mold making and exterior/floor coatings. Acrylics look promising; they do have some familiar usage as structural adhesives (Panda et al., 2020) and are easy to use and apply. As stated in the name, Anaerobic needs to be cured in oxygen-absent environments, having on-site repair issues and zero found usage from VDOT in the past.

Cyanoacrylates offer a low range of serviceable temperatures and do not offer water, salt, and air insulation, leaving concerns for possible corrosion effects after the repair.

As a result, the final options are epoxy and acrylic adhesives. Acrylics are more straightforward to mix, cure, and prepare surfaces for; they also have the bonus of being a polymer resistant to UV light, an excellent choice for repairing surfaces with a large amount of direct light exposure. However, epoxy offers tremendous advantages over acrylic: it offers better performance under stress than acrylic, it is still relatively easy to use (depending on the added aggregates and mix ratio), and it is low cost (Banea & Silva, 2009). Epoxy structural adhesives offer minimal shrinkage upon curing, low susceptibility to creep under continuous load, high strength and rigidity, effective chemical resistance, broad operation/cure temperature ranges, and excellent gap-filling capabilities (Morris, 1994). Unaltered epoxies tend to be brittle, resulting in limited impact resistance and peel strength. However, numerous modified formulations are widely utilized to enhance these attributes notably. Epoxy adhesives also have the advantage of being well-known in the engineering world and being used in both marine and aerospace engineering. They have been used frequently for different applications by VDOT in the past. Moving forward, only epoxy adhesive is selected for testing and final discussions.

Table 4. Typical classes of adhesives (Banea & Silva, 2009)

Class	Comments	Stress Behavior	Service Temperature (°C)	Cure
Epoxy	Affordable and easy to use	High strength and temperature resistance	-40 to 180	One part is cured with thermal energy. Two-part cure at room temperature.
Cyanoacrylates	Poor insulation to temperature and moisture	Moderate strength	-30 to 80	Fast cure in minutes upon exposure to moisture at room temperature.
Anaerobic	Inconvenient curing	Moderate strength	-55 to 150	Cure in the absence of air and oxygen at room temperature.
Acrylics	Poor fatigue performance, but easy to bond with surfaces	Moderate strength	-40 to 120	Cure through a free radical mechanism
Polyurethanes	Poor stress behavior	Low strength, flexible	-200 to 80	Room Temperature
Silicones	Poor stress behavior, with long cure times but excellent insulation	Low strength, flexibility, high temperature, and chemical resistance	-60 to 350	Cure with high temperature and pressure
Phenolics	Inconvenient curing, short-term bonding	High strength for short periods of time, poor thermal shock resistance	-40 to 175	Room Temperature
Polyimides	Inconvenient curing, difficult to use	Moderate strength, high thermal shock resistance	-40 to 250	Cure with high temperature and pressure
Bismaleimides	Inconvenient curing, brittle	Ridged with low-peel	-50 to 200	Cure with high temperature and pressure

3.2 Selection of Properties

A database was organized using epoxy adhesives from conference discussions with other Department of Transportation researchers' experience and structural adhesives used in VDOT projects within the past four years. Some additives were not directly used in documents from the literature review but were of the same manufacture, and the adhesive was like what had been used in previous studies. The database includes the details on the properties of each epoxy, with the top

6 adhesives being selected for lab testing. A more in-depth database that used many of the same adhesives was published by Sullivan and Peterman (2024). The properties documented by each company are not uniform, so some properties, like elastic modules or creep behavior, were often not recorded in the documentation. Most technical documentation provided by the companies that produced and evaluated their adhesives followed ASTM standards for properties like ultimate compressive strength and tensile strength. For products like MM1018 from Diamant, the company's headquarters is in Germany, and their standards follow ISO. These standard differences will be discussed more after this project's testing results. Publicly accessible technical data sheets obtained all information regarding the initial material review or though requested information from the adhesive companies.

The desired usage of the epoxy adhesive is to fill or repair gaps between steel plates/members on bridges. Ideally, the adhesive should behave similarly to steel (or as close as possible). The primary loading concern for this type of repair is from compression; the adhesive should have high compression yield strength, high compression ultimate strength, and a high elastic modulus. The high compression yield strength will reduce the likelihood of the adhesive undergoing plastic deformation. During elastic deformation, any strain can be unloaded back to zero. Past yield strength deformations cannot be fully unloaded, so some form of permanent internal strain will remain in the adhesive. Ultimate strength is the peak stress that the adhesive can handle before it starts to fail (strain does not gain with stress); this is critical for the integrity of the bonded connection from the adhesives. The last material property of elastic modules pertains to compressibility, which is undesirable as it might lead to additional slippage. Therefore, high-

elastic modules can minimize the compressibility of adhesives and prevent the occurrence of more slips in applications such as slip-critical connections.







Other criteria that seemed imprudent during initial material selection were the viscosity and workability of the epoxy. The high viscous adhesive would have a more pudgy/gel consistency, while the lower viscous adhesive would behave more like an oil. The adhesive fluid, while within a more gel form, was inferred to be better for repairing surfaces where a member would need to be fixed with a plate connection whereby the gel would be able to hold to the surfaces on even ceilings while also being less exposed to air pockets when the two-steel surface are pushed into contact. The oil adhesive fluid was inferred to be best for use as an injectable, whereby the premixed adhesive could be pulled easily into tiny gaps in member or plate connections between steel.

Workability is the definition of how long an adhesive takes (once it has started mixing if a two-part adhesive) before the adhesive is too ridged to be considered a fluid and will, therefore, become unworkable. This is important for on-site effectiveness. Having an adhesive with a short workability might offer a faster soft cure time to allow the connection to hold a load sooner (not total service loading). A short workability will make it hard to mix and give little time for applying the adhesive. This workability will also become faster the more extensive the batch of adhesive is and the higher the temperature of the environment. For initial adhesive consideration, workability time will be set for a range of time between 10 minutes and 2 hours.

3.3 Selection of Initial Materials

The project's initial adhesives selection included six structural adhesives, with this list being narrowed down further after material testing. The adhesive materials to be considered in the experimental program were selected based on their viscosity and strength, given that the adhesives have acceptable working time and usable temperature range. This narrowed down the top-performing products into two viscosity classes, i.e., injectable and Puddy form, as documented in Table 5. The project team chose injectable and puddy adhesives with the highest strength characteristics for the top three companies. These companies included COPPS industries and their K-082 Rapid Strength Grout (CFL) and K-009 High-Performance Grout (CP), Diamant's with their MM1018 Fluid (MFL) and MM1018 Puddy (MP), and lastly, Sikas USAs with their well-known Sikadure-32 Hi-Mod (HFL) with Sikadure-31 Hi-Mod Gel (HP).

Table 5. Initial adhesive selection.

Product Name (Acronym)	Company	Comp Modulus (GPa)	Comp Strength Standard	Comp Strength (MPa)	Load limit (kN)	Elastic Modulus (MPa)	Tensile Strength (MPa)	Flexural Strength (MPa)	Creep (mm/mm)	Viscosity	CTE (mm/m m/°C)	Working Time at 22°C (min)	Mix Ratio (A / B)
Sikadur-31 Hi-Mod Gel (HP)		3.861	ASTM D-695	86.2	13.3	10345	22.76	42.07	N/A	PUTTY	N/A	60	1/1 Vol
Sikadur-32 Hi-Mod (HFL)		14.48	ASTM D-695	84.1	13.3	3724	47.59	48.28	N/A	SYRUP	N/A	30	1/1 Vol
MM1018 FL (MFL)		N/A	ISO 604	89.6	26.7	69	88.97	N/A	1.10 E+0 0	OIL	1.98E-5	89	21.3/1 Mass
MM1018 P (MP)		N/A	ISO 604	110.3	17.8	10	88.97	N/A	5.92 E-02	PUTTY	1.98E-5	20	79/21 Mass
K-009 HP (CP)		N/A	ASTM D-695	131	22.2	N/A	31.03	63.45	1.62 E-03	SYRUP	"Good"	30	10/1 Vol
K-082 (CFL)		2.461	ASTM D-696	86.7	13.3	N/A	30.34	N/A	N/A	PUTTY	N/A	9	1/1 Vol

Based on the information collected from the manufacturers, among the six materials in Table 5, MM1018 FL (MFL) was the highest performer in compression strength for the injectables, and MM1018 P (MP) was the highest performer for the putty category. Note, that most of the selected adhesives have a simple volume mix ratio of one to one, except those from Diamant. The different adhesives have working times ranging from 10 minutes to 1-½ hours. This good range of workability will be discussed further in the following sections. Most adhesives were advertised as being curable from 4.4°C to 71.1°C (40°F to 160°F), and both the Copps company's products (CP and CFL) only advertised a range of 15.6 to 37.8°C (60° to 100°F).

4 EXPERIMENTAL PROCEDURE AND METHODOLOGY

4.1 Experimental Procedures

4.1.1 Compressive Strength

Compressive testing for rigid polymers, including structural adhesives, follows testing guidelines from ASTM D695-15 (ASTM, 2023). The ASTM-specified specimens are 12.7×12.7×25.4mm (0.5×0.5×1.0in) rectangular prisms (ASTM, 6.2). The process for the preparation of the specimens first includes molding and curing the adhesives in a silicon mold. The mold must be primed with an epoxy/silicone release agent (Stoner Zero Stick and MG Chemicals 8329 Epoxy Mold Release) to ensure easy separation from the mold. The ASTM does not dictate how the mold is used or constructed; molds for epoxy can be made from multiple plastic materials. These materials include silicon, acrylic, and polyethylene. Molds can also be made from metals like steel and aluminum with a generous amount of release agent or wax.

Once the two-part epoxy is mixed adequately, as documented by the producers' technical sheet, the epoxy is applied to the mold cavities and placed in a controlled environment to allow the epoxy to cure at the desired temperature and humidity. The conditioning of the test specimens follows procedure A of ASTM D618-21 (ASTM, 2021). The curing time is seven days, as stipulated, and the curing and testing conditions follow the testing matrix. Table 6.

Table 6. Compressive test matrix

Variable	Number of Tests	Conditions
Adhesives	6	Adhesive Selection based on Section 4
Test Temperature	3	Cold: 4°C (40°F), 50% Humidity Lab: 22°C (73°F), 50% Humidity Hot: 43° (110°F), 50% Humidity
Replicates	3	For averaging data
Total	54	Loaded To Failure

After the samples are cured for six days, they are removed and then cut to the desired size via a water jet cutter, Figure 25. The samples are then placed back into their environmental chambers for an additional 24 hours before starting compression testing.



Figure 25. Compression silicone molds and water jet cutting

Before compression testing, the samples are seated in a displacement-controlled manner via a Material Testing System (MTS) hydraulic press that holds a 100-kN (22-kip) loading cell, as illustrated in Figure 26, the MTS can record the displacement of the hydraulic press using its built-

in LVDT sensors, but to reduce interference in displacement due to the stiffness of the press, a laser extensometer is also used Figure 26. The laser extensometer is set up to measure the displacement between the reflective tape attached to the top/bottom of the samples.



Figure 26. MTS compression test setup and laser setup.

The hydraulic press is lowered until close to 1mm from the top of the sample, then lowered at a rate of 20 mm/min (0.75 in/min) till a seating force of 20-450kN (5-100lbs) is steady. The displacement is then zeroed, and the compression tests are performed at a 1.27 mm/min (0.05 in/min) loading rate. The test runs until the samples fail, with real-time displacement and force data being recorded. Failure in compression is determined to be when the force on the sample drops by more than 5 kN (1 kip) from the ultimate peak force/stress or the sample starts to stiffen and regain strength due to puddy effects.

Compressive strength testing provides the ultimate strength/strain, yield strength/strain, and behavior under compressive loads. Each of the previously listed material properties can be recorded by measuring the displacement and force applied on an adhesive test specimen.

4.1.2 Compressive Creep

The compressive creep test gives us an understanding of the adhesive's behavior under sustained compressive load. The creep tests follow ASTM C1181/C1181M-17 (ASTM, 2018) guidelines and provide the displacement of the adhesive samples that occurred under constant compressive load over 28 days. ASTM C1181 stipulates that the creep adhesive samples consist of 4-inch (101.6mm) diameter cylinders with a 1-1/8in (28.575mm) diameter center hole. All adhesive specimens are then housed in a rig that is two 4 ½ in by 4 ½ (114.3mm) and 1 in (25.4mm) thick square loading plates of high carbon steel with also a 1-1/8 in (28.575mm) center hole as well as four ¼ in (6.35mm) diameter measurement holes with being on only on one plate, as shown in Figure 27.

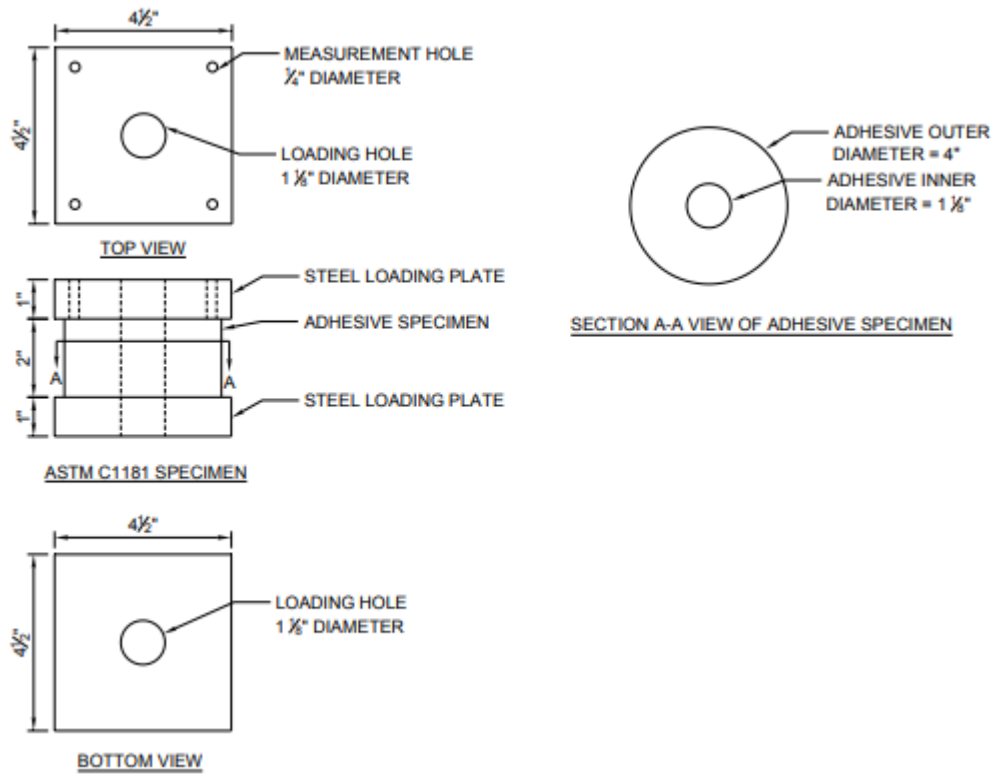


Figure 27. Drawing of ASTM C1181 creep test specimen

To prepare the specimens, a custom high-carbon steel mold was made using stacking plates of 1 thick steel that can be fastened together using four tightening nuts/bolts on each corner. The inside of the mold is generously insulated with wax; other release agents can be used, but Turtle wax offers more protection against the uncured adhesive from leaking due to its thicker consistency. The two-part adhesives are mixed and poured through the top hole in the mold (if fluid) or plastered in (if it is a puddy), Figure 28.



Figure 28. Compression creep mold pictures

Following ASTM guidelines, the mold with the curing adhesive sets at lab conditions for at least 24 hours before the mold is disassembled. The hardened adhesive is placed into an environmental chamber for seven days until cured. Environmental chamber settings are set for 43°C (110°F) at 50% humidity (H). On the sixth day of the cure, the specimen is removed, and a center hole is cut through the adhesive sample via a water jet. After cutting, the specimen is put back in the environmental chamber to finish the cure.



Figure 29. Compression creep assembled rig with cured adhesive specimen

The specimen is measured and placed in its compression creep rig, as shown in Figure 29. The rig has a 1 in (2.54 cm) diameter rod with a tightened nut that runs down the rig's center. The bolt has four spring washers that are 2.9 by 5.7 cm (1 1/8 by 2 1/4 in.) being 4.0 mm (0.159-in.) thick, with a spring rate of 27,300 kg/cm (153,000 lb/in.), spaced by equivalent flat washers, as depicted in Figure 30. This rig is then seated on an MTS hydraulic press with a 100-kN loading capacity (10 kip minimal capacity) so that the load is applied to the top of the bolt and held by the steel plate on the bottom of the rig.

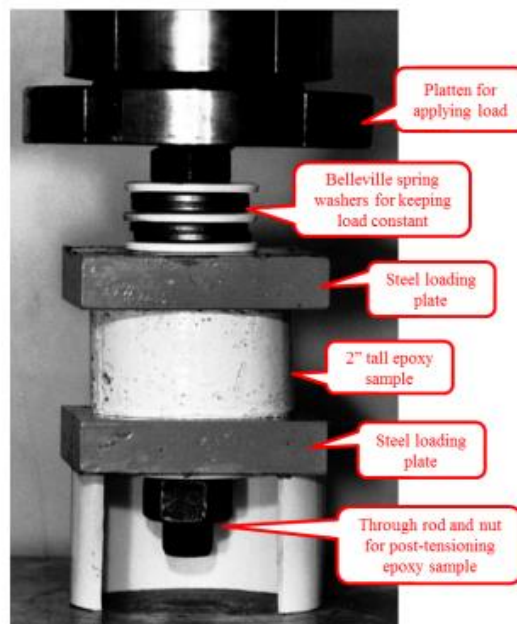


Figure 30. Example of creep test setup (ASTM C1181)

The desired constant creep force P is determined via Equation 1, based on the desired stress on the specimen of 2800 kPa (400 psi). The rig is loaded in 450 N (100 lbs) increments until the desired force of 20.5 ± 0.22 kN (4.6 kips ± 50 lbs) is reached. After reaching the load requirement, the tension nut is hand-tightened till it is snug-tight before the rig is unloaded and removed from

the MTS frame. This nut tightening should keep a constant stress of 2800 kPa by the tension in the nut and bolt.

$$P = S \left(\frac{\pi D^2}{4} - A \right)$$

Equation 1. Load requirement for designed compression stress for creep (ASTM C1181)

Following the application of creep stress, the displacement of the specimen is documented by using calipers between all four corners of the sample's top and bottom loading plates to be taken as an average sample depth. The rig is placed at 43°C (110°F) at 50% humidity for a different set of periods listed in Table 7. ASTM recommends measuring and loading in cycles like this Table 7. The rig will slowly relax and lose stress over time as the adhesives strain due to creep, so the specimen's displacement must be measured, reloaded, and remeasured over increasingly longer increments. ASTM directs the rigs to be placed in lab conditions 24 hours before measurements or loading, regardless of environmental conditioning. After the creep schedule has run its course for 672 ± 12 hr for each set of specimens, the test is concluded. The stress should be far below the adhesive's yield strength for failure to occur, but if specimens fail or crack, new specimens need to be created and re-run.

Table 7. Compression creep exposure periods

Total Environmental Exposer Time (hr.)	Time For Environmental Exposer for Cycle (hr.)	Cycle Number	Time For Specimen Relaxation at Lab Conditions Before Test
24	24	1	24
48	24	2	24
120	72	3	24
168	48	4	24
336	168	5	24
672	336	6	24

4.1.3 Short-Term Compressive Slip

Compressive slip testing follows guidelines from *Specification for Structural Joints Using High Strength Bolts* (RCSC, 2020, p. 77). The slip tests used four different adhesives with two separate steel surface types. The steel types used were A588 steel with a class A surface of organic zinc coat with a mill of 0.35 ($m=0.35$) and a class B surface sandblasted A588 $m=0.50$. The curing and testing of the samples were done under standard lab conditions. The summary of the test matrix is given in Table 4.

Table 8. Test matrix for short-term compression slip testing

Variable	Number of Tests	Details
Adhesive Type	4	Determined Based on Task 1 and Task 2 results.
Thickness	2	3.175 mm (1/8 in) 12.7 mm (1/2 in)
Surface Finish	2	Class A ($m=0.35$) Class B ($m=0.50$)
Replicates	5	

The compression slip test specimens consist of the selected three pieces of steel with a dimension of 4 x 4 inches (10.2 x 10.2 cm) and a depth of 5/8 inches (15.875 mm). The steel has a centered 1-inch (25.4 mm) diameter hole placed 1-1/2 inches (3.81 cm) from one end. The specimens for this test will have two different gaps of adhesive layers depending on if the used adhesive is putty-like or injectable, with putty adhesive having a 1/2 in (12.7 mm) gap and injectable having a 1/8 in (3.175 mm) gap to reflect their real-world application better. The entire specimen will have a hole to allow fasteners to run through and an overhang for an applied load from one path to two paths in double lap shear, Figure 31.

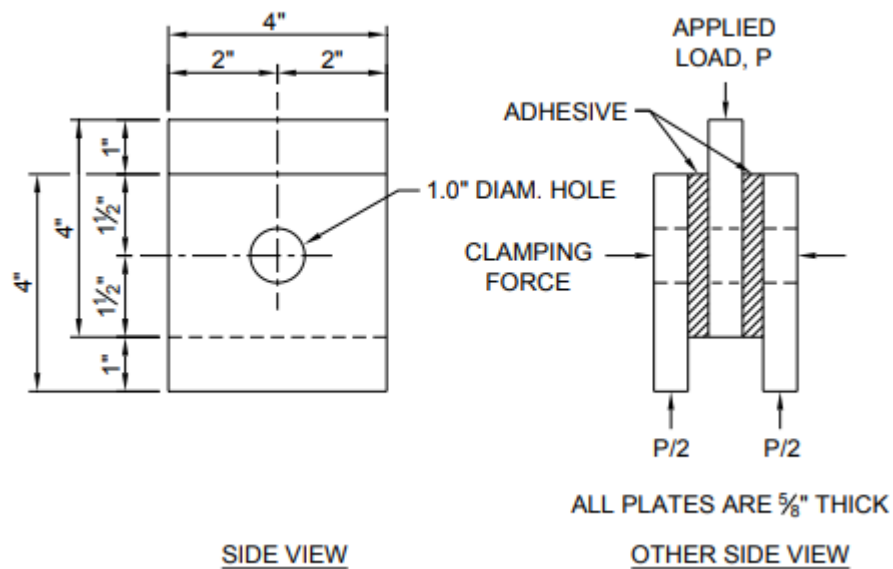


Figure 31. Compression slip test specimens

Adhesives are mixed and then poured into empty caulking tubes, which are injected into the gaps in the plates made by the molds. The specimens are then cured for seven days under lab

conditions before removing the mold and being prepared for testing. If the samples are to be used for short-term compression slip testing, the samples are spray painted with black and white paint to prepare a reference for generating a digital mesh with a digital imaging camera (DIC) that is used to measure displacement, as shown in Figure 12. Testing of the samples is prepared by passing a 3 ft (~90 cm) threaded 7/8 in (~22 mm) high-strength steel rod with 150,000 psi (~1 GPa) tensile strength attached to a center hole jack with a 100kip external load cell, as shown in Figure 32.

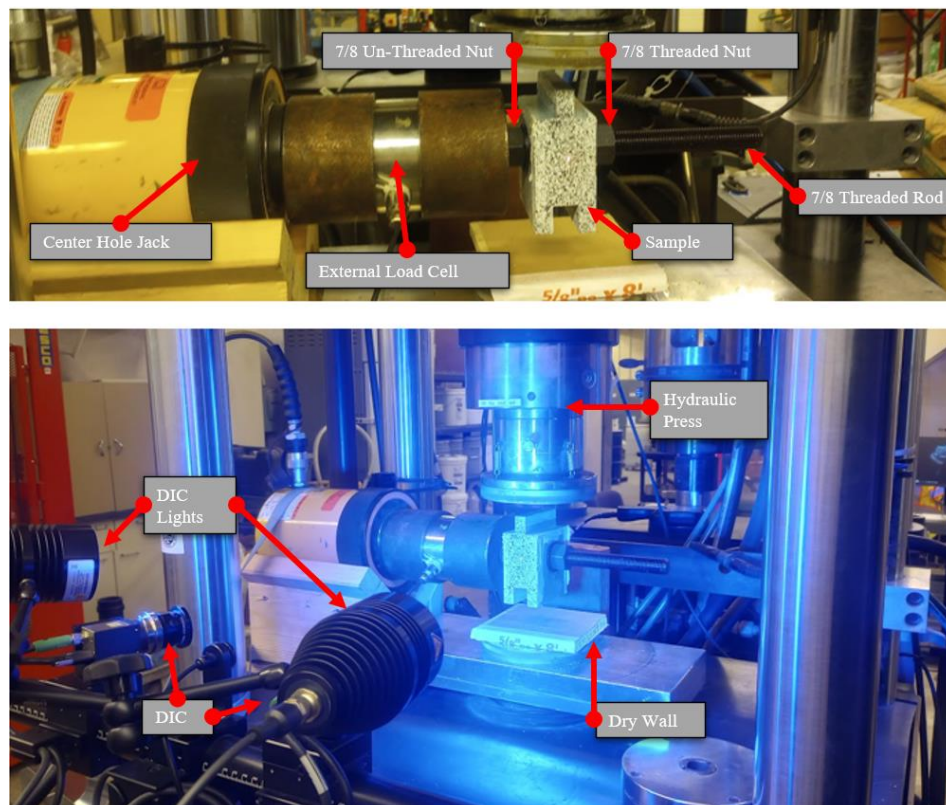


Figure 32. Picture of compression slip test assembly

After being assembled, the center hole jack is loaded to 5 kips to apply a clamping force to the specimen. The specimen is then seated with the DIC being calibrated before compressive loading. Seating uses a piece of 5/8 in. drywall to help ensure a better load path before testing. The

hydraulic press is lowered to hold the specimen under close to 25 lbs., then the center hold jack is loaded to the desired clamping force that will be maintained for the test: 50kips. (~222 kN) The specimen is then unseated from the hydraulic press, and the drywall is removed. The hydraulic press is then reseated back to 25 lbs (100 N). The drywall allows the specimen to have a uniform load and some freedom of movement to align itself with the hydraulic press's plates during seating. However, the drywall will interfere with the slip test results and cannot be used. Loading is done at a rate of 0.003 in/min (0.0762 mm/min), with monitoring of the clamping force to ensure it stays between ± 0.5 kips (± 2 kN) through the tests and that loading stays below 25 kips/min (111 kN/min). RCSC specifies that the tests are concluded when the sample slip or the displacement exceeds 0.04 in (~1 mm). RCSC gives examples for analyzing the compressive test data to determine slip load and different types of slip, as replicated in Figure 33.

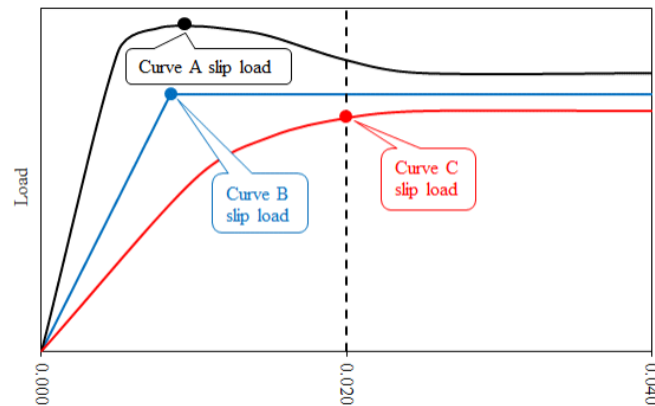


Figure 33. Definition of slip loading (Province & Abebe, 2020)

The slip coefficient is calculated using slip load and clamping load in Equation 2 using a slip load: Max load at or before 0.02 in (~0.5 mm) displacement.

$$k_s = \frac{\text{slip load}}{2 \times \text{clamping force}} = \frac{P_s}{T_s}$$

Equation 2. Compressive slip coefficient

4.1.3.1 Slip Test Molds

The samples are made using two different molds made of cut acrylic sheets that, when assembled along with the specimen's steel plates, set a fixed distance between the plates and leave injection ports and venting holes for injecting adhesive. Figure 34. The mold has two sidings with injection ports, air holes, and peg holes where acrylic or polyethylene spacers are inserted between the two sidings; all parts were cut from one sheet of cast clear ½ inch acrylic. All acrylic is sprayed with a release agent before use. When the steel plates are inserted, and a 1 in diameter bolt is passed between the steel, the spines will be inline and level to each other with the desired gap thickness. The 3/8-inch bolts with nuts are passed between the four corners and then hand-tightened to ensure fit.

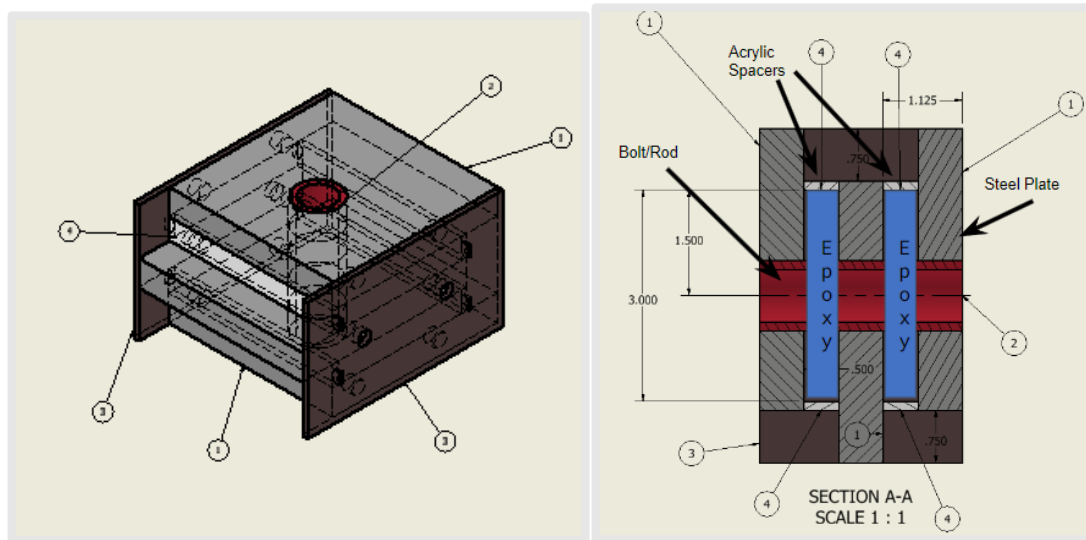


Figure 34. Sketch of slip molds (Joshua Starr)

Before injection of adhesive, a caulking gun with silicon or acrylic caulk should be liberally applied to the gaps and corners of the steel plates to prevent leakage during injection and curing of layered adhesive. This is more critical for lower-viscosity adhesive.

4.1.4 Long-Term Tensile Creep

The tensile creep procedure follows RCSC (RCSC, 2020, p. 88) with specified imperial units. Each tensile specimen consists of three 4 x 7 x 5/8 in (10.16 x 17.78 x 1.5875 cm) thick A588 steel plates of class B surface with two 1 in. diameter holes drilled 1 1/2 inches from either end. The specimens will have a layer of cured adhesives between the plates: 1/2 inch (12.7 mm) for puddly adhesives and 1/8 inch (3.175 mm) for injectable adhesives. The assembly follows the arrangement shown in Figure 35.

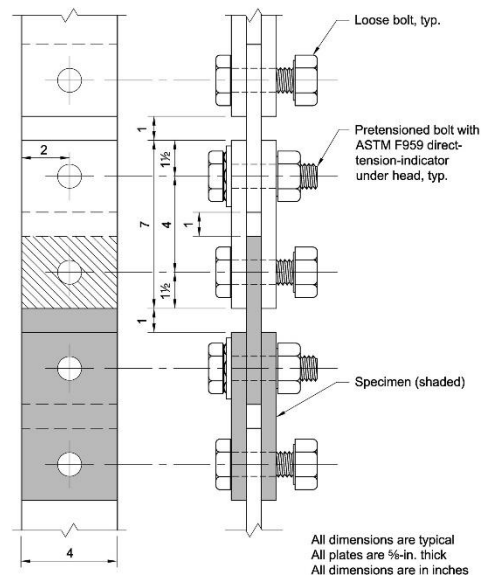


Figure 35. Sketch of tension creep test specimens (Jason Provines)

The specimens will mold together with the adhesives, as in the slip-testing specimen. The specimens are then conditioned/cured for 7 days before the start of creep testing. The matrix for the creep tests, including all the different conditions, is included in Table 9.

Table 9. Test matrix for tension creep testing

Variable	Number of Tests	Details
Adhesive Type	4	Determined Based on Task 1 and Task 2 results
Thickness	2	3.175 mm (1/8 in) 12.7 mm (1/2 in)
Replicates	3	Tested for at least 1000 hours

Before setting up the test, each set of specimens undergoes a sequential process after conditioning. Each specimen has a 4-6 ft (~150 cm) threaded 7/8 in (~22 mm) high-strength steel rod with 150,000 psi (~1 GPa) tensile strength inserted through the center hole of the specimen (between the layered adhesive). Lubrication is coated on each bolt's thread to ensure smooth nut torquing. The center-holed load cell (450 kN) will be placed in the bolt assembly with a washer contacting the top of the plate and the pressure plate of the load cell. An ASTM A490 nut is then hand-tightened in contact with the other side of the load cell. The bolt assembly of each specimen is laid out in Figure 36.



Figure 36. Tensile slip plate specimen

Once the bolt assembly is finished, each specimen is then torqued till the load cell on the bolt assembly reads 50 ± 0.5 kip (222 ± 2 kN) for the desired clamping force that would be used in the field. A high-strength vise with a torque multiplier is used to apply the clamping force on the

plates, as shown in Figure 13. This is repeated two more times for the same specimen type.



Figure 37. Tensile slip plate clamping

The three specimens are arranged in a "daisy chain," end to end. The specimens are connected with loose A490 7/8 in (22 mm) diameter bolts 4-5 inches long (10-12 cm) to ensure an in-line load path. An addition plate may be used to attach the chain to the creep frame on each end. The final chain should be assembled and attached to the frame as depicted in Figure 38.



Figure 38. Tensile slip plate rig assembly

Two displacement dial gauges are magnetically attached to each specimen, one for each side, measuring the document between the center plate and the front plate, center plate, and back plate. In total, this is a six-dial gauge per daisy chain. Each dial gauge is zeroed before loading the chain in tension.

To determine the load at which the specimens will be sustained at, the following equation for vertical load R , assuming a standard slip coefficient k_s of 0.5 and a clamping force T of 50 kips (222 kN), providing a desired tensile load of 33 kips (148 kN):

$$R = \frac{2k_s T}{1.5}$$

Equation 3. Tensile creep vertical load

A hydraulic jack, attached to four threaded rods 2 ft (~60 cm) threaded 7/8 in (~22 mm) high-strength steel, loads the chain in tension. Hand-tightened bolts secure the rods until the desired load is reached. The tensile load is measured at the top of the frame from a 100 kip (2000 kN) center hole load cell that is set between the chain connection and the frame.

To properly load the chain, the hydraulic is extended to within 1% of the designed tensile load before each of the four bolts above the jack is hand-tightened before the hydraulic is unloaded. The process may need to be done 1-3 times to ensure the required tensile load is kept. The dial gauges are recorded within 30 min. of tensile loading.

Through the test, the load reading of the clamping and tile forces is required every 30 minutes, with displacement readings manually recorded daily (excluding weekends and holidays). If the tensile load drops below 1% of 33 kips (148 kN) at any point during observation, the chain is reloaded to the desired load, and dial gauges are rerecorded. This is critical within the first five days of testing. The tests run for at least 1000 hours before ending.

5 EXPERIMENTAL RESULTS AND DISCUSSIONS

5.1 Testing Results

5.1.1 Compression Test Results

The compressive strengths of six different adhesives under three different curing environments are determined, and the stress vs. strain results are presented in the appendix. The summary of each group of adhesives and their respective ultimate stress and peak strain is graphed in the figures below. The results from each epoxy type at different curing conditions are replotted to enable a closer performance evaluation of each epoxy.

Figure 39 shows the compressive strength of HFL and HP adhesives. The compressive strength at room temperature provided by the manufacturer was also indicated in the plot with a horizontal dashed line. The HFL shows a compressive strength value very close to its specified strength by the manufacturer when it is cured at 23°C or 43°C. However, the compressive strength of this epoxy decreases by more than half when the curing temperature is 4°C. On the other hand, the putty version of this epoxy (HP) exhibited a compressive strength of 104.6 MPa and 109.6 MPa at curing temperatures of 23°C or 43°C, respectively. This was higher than the advertised compressive strength of 85 MPa. When the curing temperature is 4°C, the compressive strength of this adhesive is measured as 74.6 MPa, only 15% lower than the advertised strength. When looking at the Sikadure-32 and 31, the consumer's advertised strength aligns well with the record strengths. This was due to the easy mixing ratios of the two-part adhesives and the fact that the temperature effects on the strength were not too drastic.

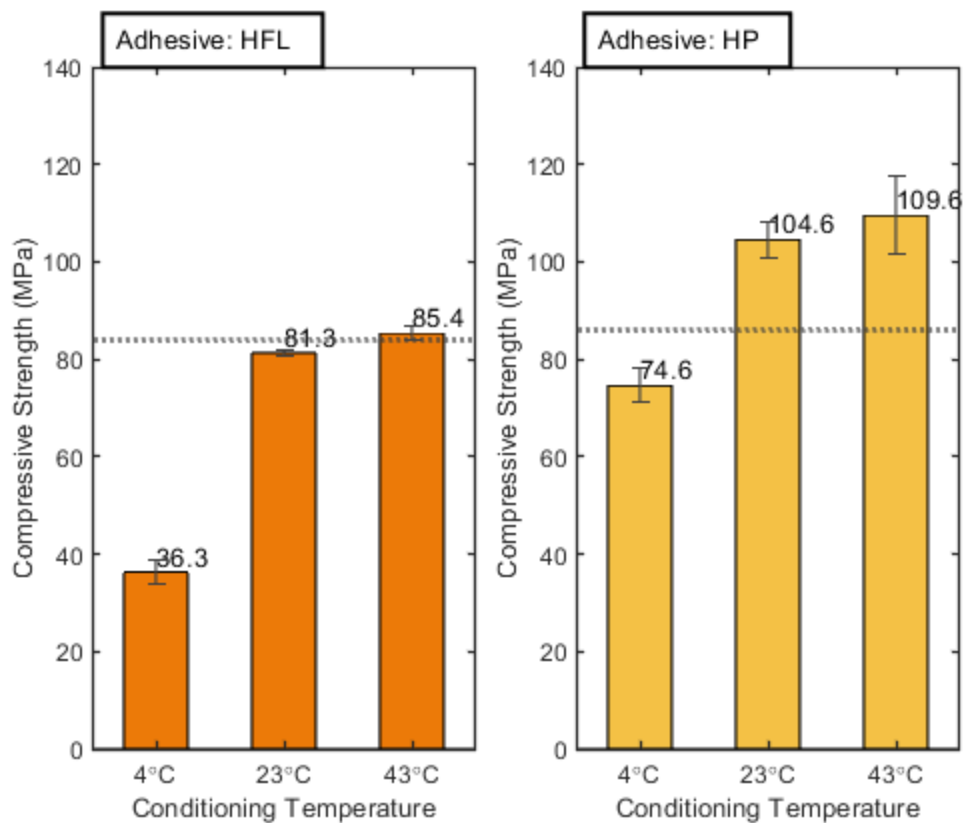


Figure 39. Bar graphs of the compressive ultimate strength of HFL (Sikadure-32 Hi-Mod) and HP (Sikadure-31 Hi-Mod Gel) based on different curing and testing temperatures. Bar graphs compare cure conditions to the advertised strength from the provider.

Figure 40 shows the compressive strength results for adhesives CFL and CP. At room temperature, the strength of the adhesive seems to perform equivalent to or better than documented. The CFL seems sensitive to colder temperatures and shows a 33% drop in strength. CFL has a minor gain in strength at higher temperature conditions, having 97 MPa in lab conditions and 112 MPa in hot conditions. HP holds up well under cold conditions while still having 70 MPa of strength, only 13% less than the lab-conditioned 80 MPa. While MP performance is not spectacular when compared to other adhesives, underperforming CFL, it keeps very close to its manufacturer's specified strength of 12.5 MPa. It is important to note that CFL (COPPS Industries K-009) had a

ratio of resin to hardener of 10-1, making it a bit harder to work with and mix, most notably with small batches.

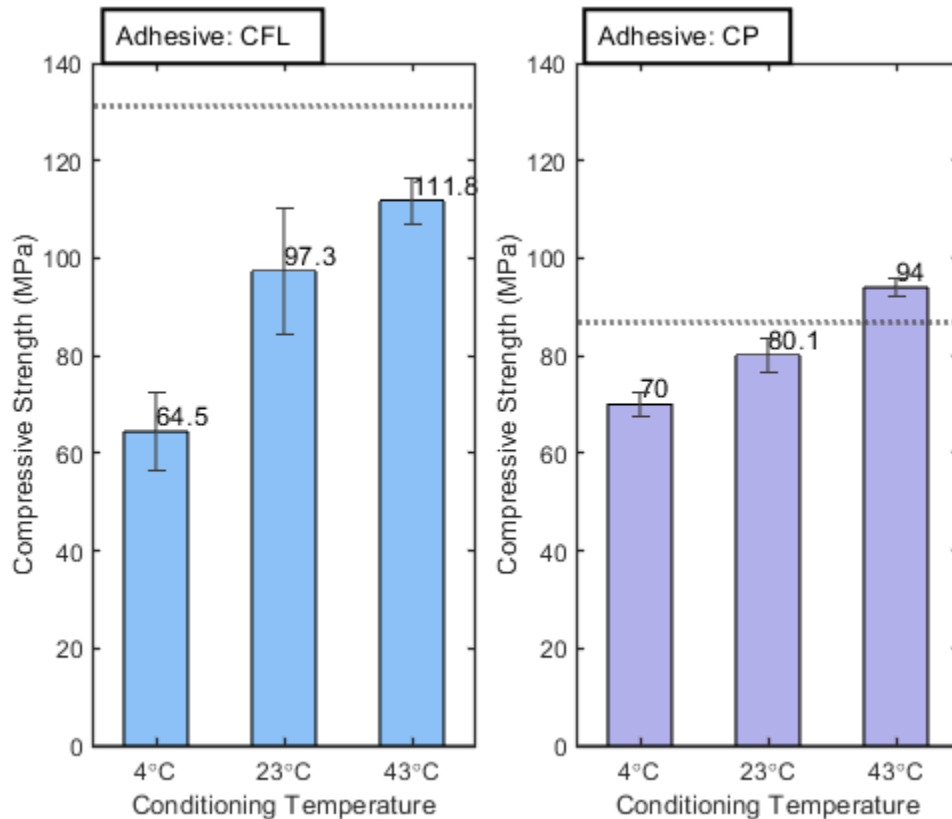


Figure 40. Bar graphs of CFL (K-082) and CP (K-009) compressive ultimate strength based on different curing and testing temperatures. Bar graphs compare cure conditions to the advertised strength from the provider.

MFL and MP strengths are graphed below in Figure 41; MFL's manufacturing strength was specified to be 159 MPa (23 ksi). Both adhesives have the same trend between the three condition ranges. MFL drops a bit more to 58 MPa at 4°C from 100 MPa at 23°C while only increasing to 115 MPa at 43°C. MFL also has more variation between the data than MP, with an ultimate strength of 66 MPa at 4°C up to 91 MPa at lab conditions and 124 MPa at 43°C. MP shows greater strength at low and high temperatures and better reflects the manufactural

specification. This difference in performance could be due to the difficulty of its two-part mix ratio; with MP having a mix ratio of resin to hardener 79-21 per mass (A-B) and MFL having 21.3-1 (A-B).

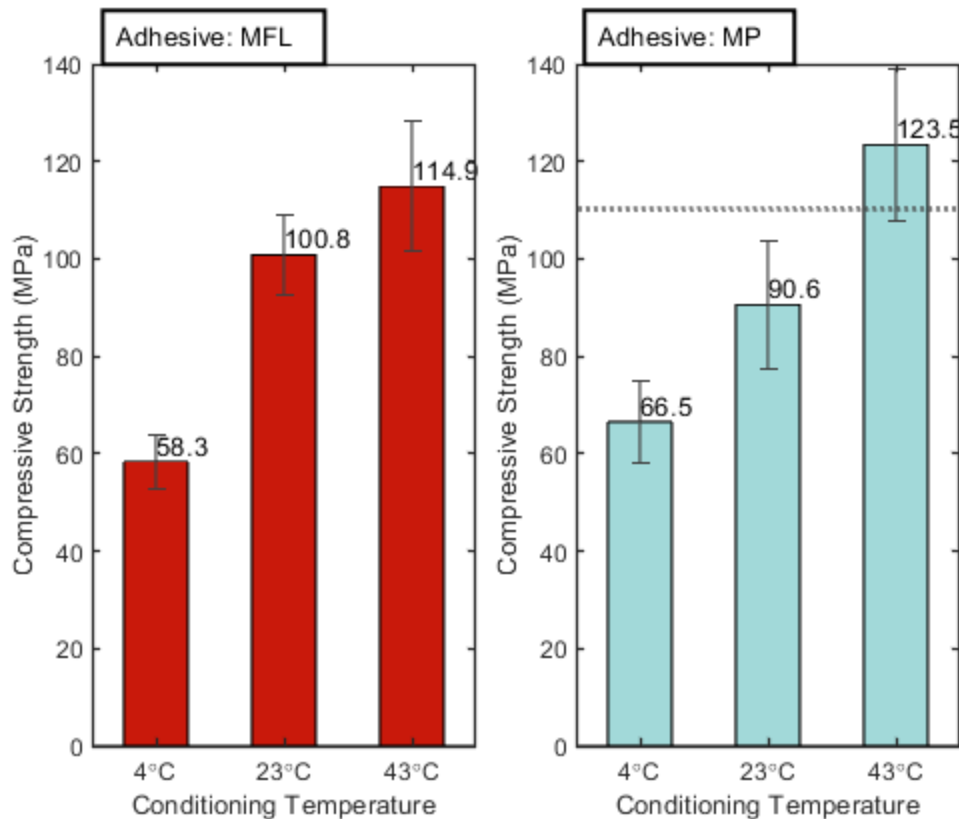


Figure 41. Bar graphs of the compressive ultimate strength of MFL (MM1018 FL) and MP (MM1018 P) based on different curing and testing temperatures. Bar graphs compare cure conditions to the advertised strength from the provider.

The MFL (MM1018 FL) did not perform close to what was specified, even though testing was redone with multiple different shipments of the adhesive that were pre-checked by the manufacturer. It is worth discussing that both MFL and MP use steel aggregate in their resin components; while this would allow for better tensile strength performance, the aggregate made mixing the adhesive the most difficult of all the adhesives. A power drill with a concrete mixing

paddle is needed to prepare mixes with the resin (part A), which needs to be mixed for over 10 minutes to get the stuck aggregate off the bottom of the can (a paint can mixer would work), maybe even more if it is the MFL. This is very important because the steel aggregate proved enormous benefits for its compressive strength when starting early testing, and great care should be taken to premix components of adhesives prior to mixing if they are using aggregates. Then, after the resin is added to the hardener (part B), the mix needs to be mixed with a drill again for at least 3 min; all this mixing leads to an excessive amount of air being trapped in the mix, further reducing its performance.

Similarly to K-009, the advertised strength was significantly high, and the MM1018 was very difficult to mix; it had a large mix ratio with a heavy amount of aggregate that was not dispersed throughout the resin and required thorough mixing of the two-part adhesive. Also, the first batch of MM1018 FL had a compromised hardener that led to uncured adhesive. The complex mixing of MM1018, the overly optimistic advertised strength, and quality control concerns make this product an unappealing adhesive.

The results from each epoxy type at different curing conditions are summarized in bar graphs that compare the average ultimate compressive strength determined in the testing with standard deviation bars. The results show significant changes in the compressive strength due to temperature curing. With curing temperature, the colder curing conditions led to lower compressive strength, while the samples cured at higher temperature conditions led to more strength for the cure period given. It will be discussed later that both strains and stress need to be

inspected to determine whether weather conditions led to better or worse performance for the adhesive.

The poor performers are HFL and CP. HFL, while performing acceptably at 23°C, did not gain a notable amount of strength at high temperatures. Also, HFL was very sensitive to 40°F cure condition and was not a prime candidate. CP did not show any vast issues besides the fact that its relative strength in most categories was relatively low.

The selected adhesives did well at the high temperature of 43°C. HFL did not gain much more ultimate strength at the highest temperature, and its yield strength decreased significantly. It is inferred that when the adhesive is designed to cure it at higher temperatures, it will become more malleable and flexible, having an undesirable behavior then leading to more plastic deformation in the adhesive.

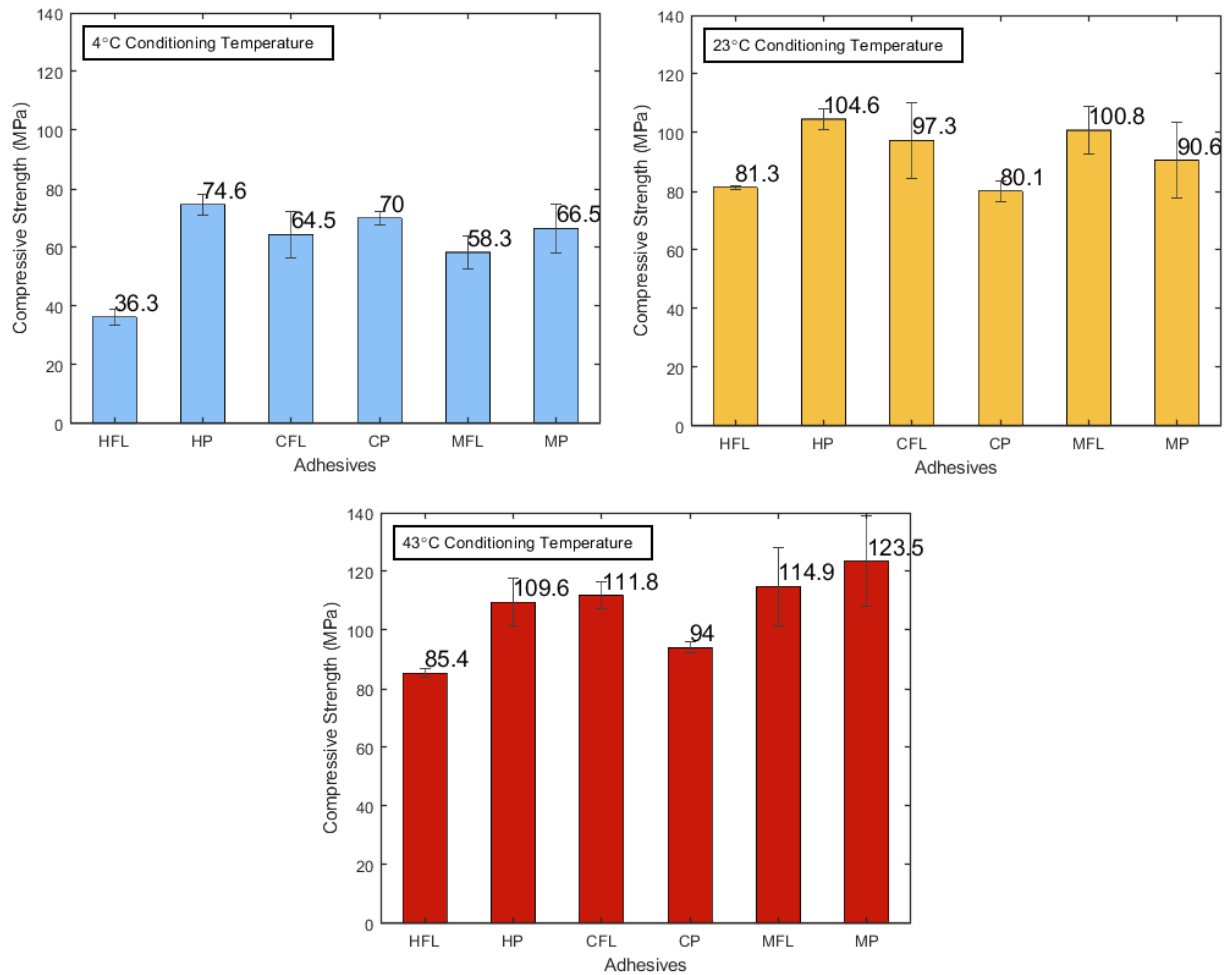


Figure 42. Averaged compressive ultimate and compressive yield strength bar graphs of all adhesives

In Figure 43, the peak strain at ultimate strength is shown in comparable bar form with standard deviation bars and recorded average strain from all tests of the adhesive at all three cure conditions. The results illustrate which adhesive deforms well or not; a material can have a high ultimate strength but could have a high strain. At 4°C cure, MFL shows high strain with a large deviation due to slow curing, making the adhesive not fully cured yet. This may indicate insufficient curing in low-temperature conditions, possibly due to the limited cure time (7 days) and the slowed chemical process caused by the low temperatures impeding the curing mechanism.

At 23°C cure, CFL shows a larger strain in comparison to the others. 43°C cure reveals CFL to start struggling as it seems to be pushing its max cure temperature range but still hardening. Also, at high temperatures, HFL jumps to large deformation; this manifests as softening when the conditions surpass the glass transition temperature (T_g). The glass transition temperature is when an amorphous material transitions from a rigid, glassy state to a rubbery state. This transition occurs as the polymer chains in the adhesive shift from a more ordered to a less ordered state, resulting in the adhesive becoming less stiff and brittle while becoming more pliable and weaker. This phenomenon is evident in the shortening of the material's elastic deformation range and the elastic region's elongation, as demonstrated in Appendix I.

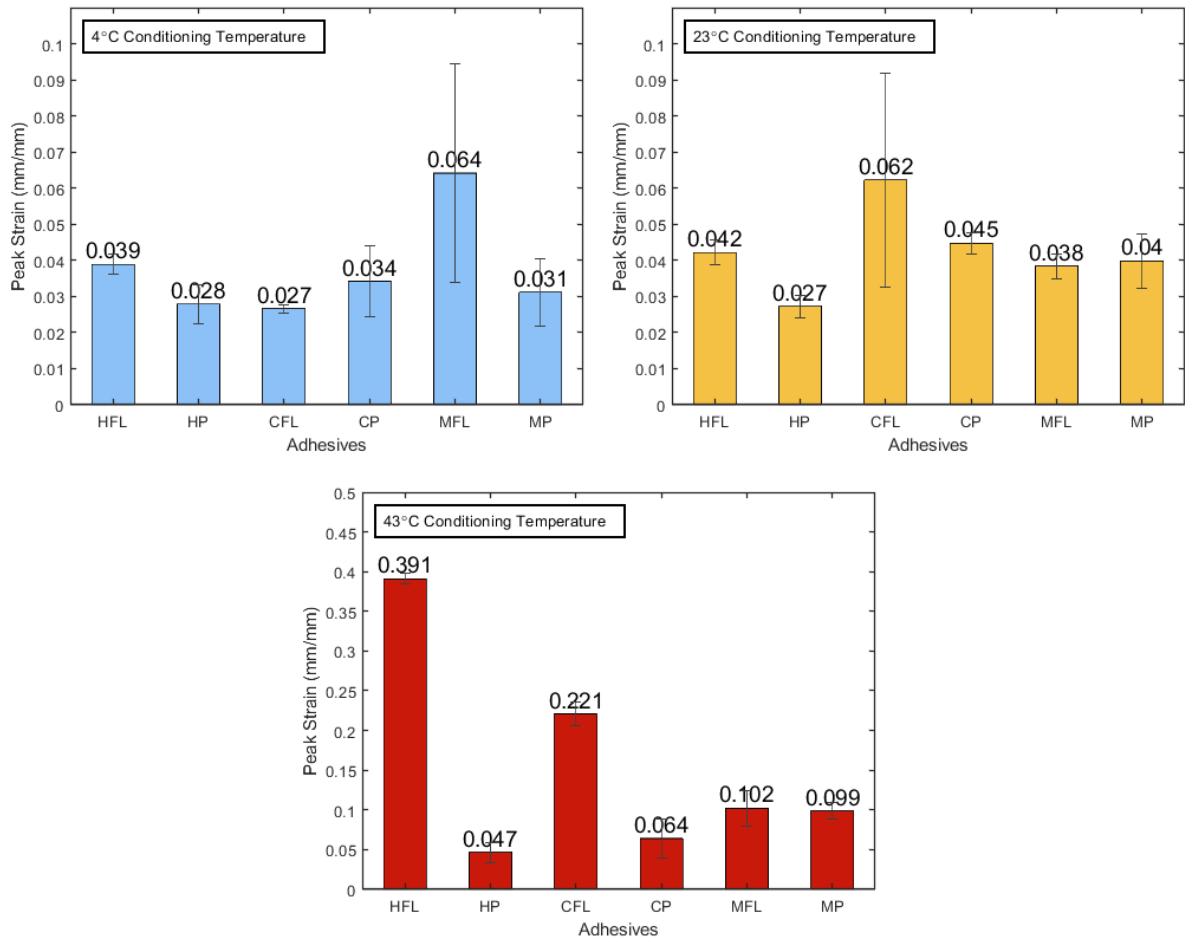


Figure 43. Averaged compressive ultimate peak strain and bar graphs of all adhesives. Peak strain is the strain at max stress.

The following graphs show peak strain during compression testing for each group of adhesives to compare temperature effects between the fluid and puddly classes. Figure 46 strongly indicates that HFL does not perform well under high temperature curing due to the T_g point being reached. HP shows that there is not much of a difference between 4°C and 23°C cure peak strain, with the increase in strain at 43°C cure due to the increase in ultimate stress, not softening.

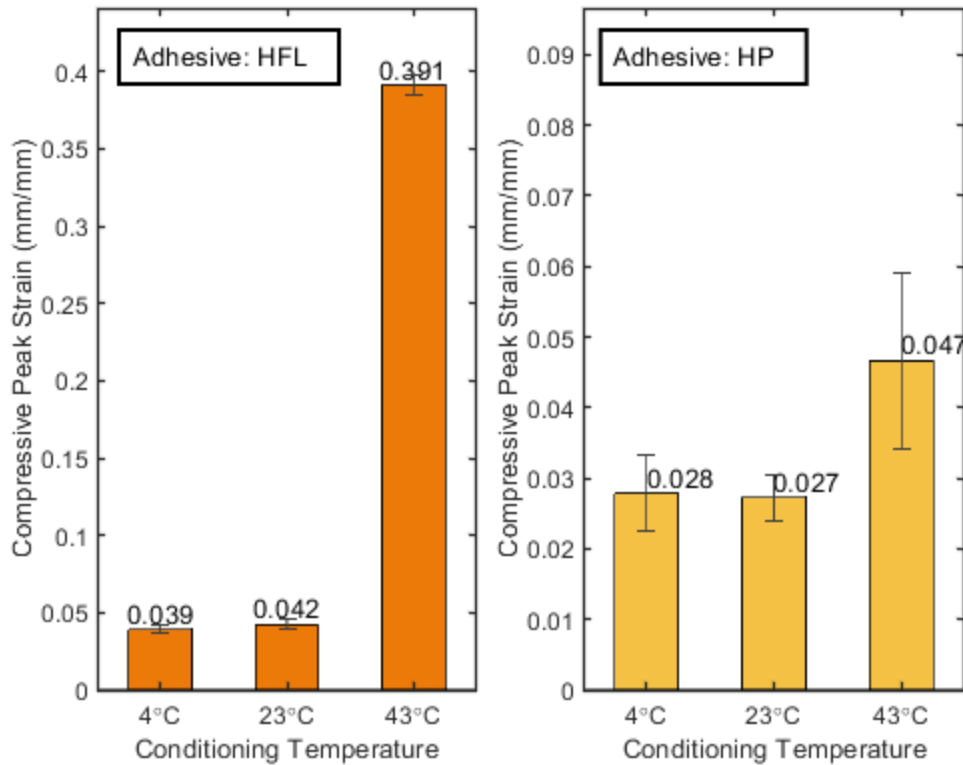


Figure 44. Comparison of compression peak strain for Sikadur-31 Hi-Mod Gel (HP) and Sikadur-32 (HFL) at three different temperatures under a range of low to high-temperature conditions while maintaining humidity at 50%.

Under room temperature conditions, CFL displays a substantial strain with a notable standard deviation, Figure 45. This is attributed to variations in mix batches, where air pockets and bubbles in the adhesive mix, resulting from overmixing or inadequate air removal, could influence the observed strain. With elevated temperatures (43°C), both HFL and CFL exhibit extremely high strains at peak, clearly illustrating adhesives surpassing their glass transition temperature. Additionally, an extension of the plastic region can be observed from the stress vs. strain data in Appendix C. In Figure 45, CP shows a steady increase in peak strain as cure temperature increases.

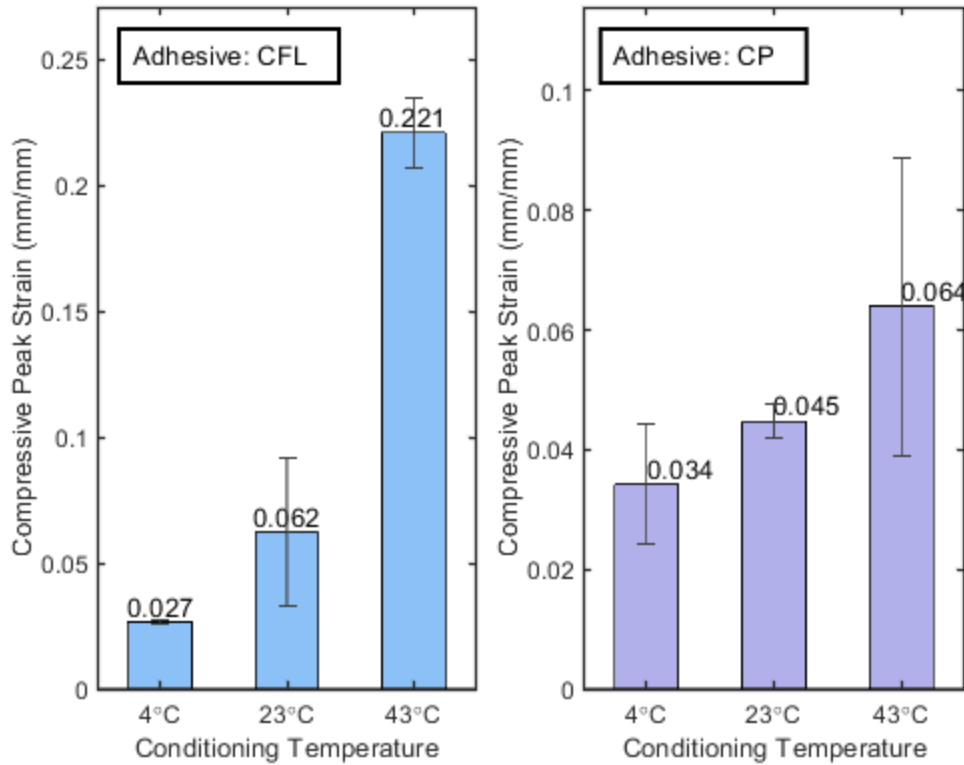


Figure 45. Comparison of compression peak strain for Copps K-082 (CFL) and K-009 (CP) at three different temperatures under a range of low to high-temperature conditions while maintaining humidity at 50%.

The analysis of Figure 46 reveals distinctive characteristics of MFL compared to other adhesives. MFL exhibits a significantly higher standard deviation and strain deflection at low and high temperatures. This behavior can be attributed to several factors, primarily associated with variability in the mixing process and the quality control of the hardener component. One contributing factor to the observed variance is the intricate nature of the MFL and MP mix. It is characterized by a notably large mix ratio, surpassing even that of MP. Additionally, the resin part of the mix is densely packed with aggregates, particularly steel. This unique combination of a high mix ratio and a dense aggregate content makes the MFL mix inherently challenging. The

variability introduced during mixing and the intricate composition of the adhesive contribute to the observed fluctuations in strain behavior and a higher standard deviation.

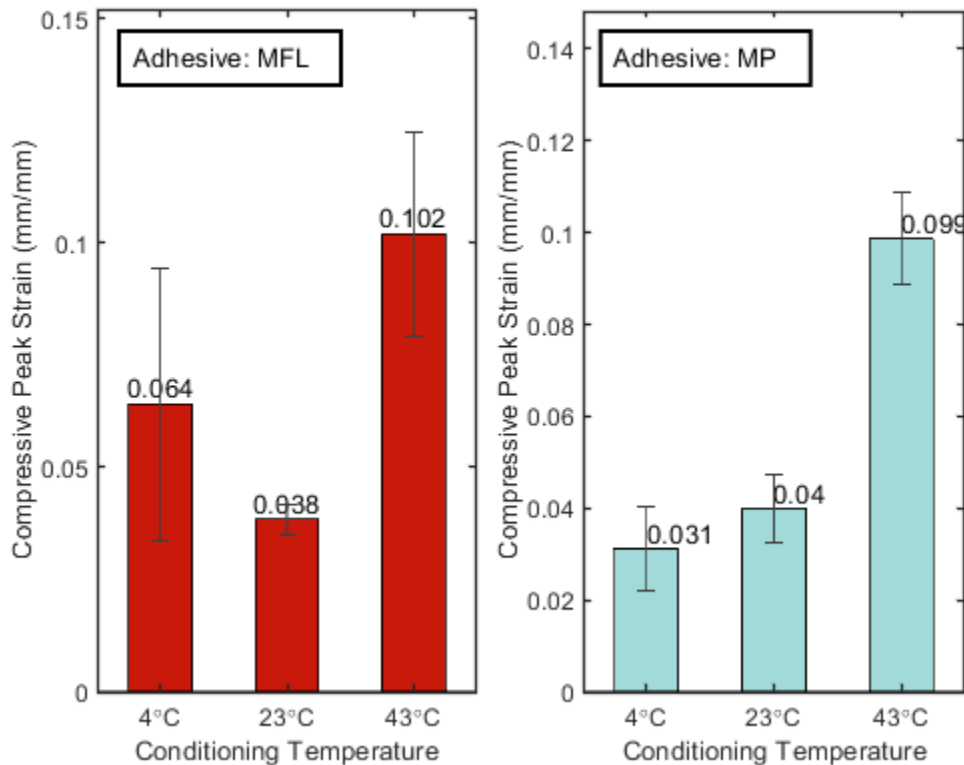


Figure 46. Comparison of the compression peak strain for Diamant MM1018 FL (MFL) and Diamant MM1018 P (MP) at three different temperatures under a range of low to high-temperature conditions while maintaining humidity at 50%.

It is crucial to acknowledge that MFL and MP are not straightforward adhesives and demand a high level of expertise for their effective utilization. Users, especially those handling MFL or MP, should possess extensive experience, employ proper mixing equipment, and be well acquainted with the intricacies of the product. Due to its complex composition and demanding mixing requirements, MFL and MP are best suited for application by experienced personnel who can ensure the accurate preparation of the adhesive for optimal performance.

Table 10 and Table 11 are summary tables with all the ultimate strength and peak strain averages for each cure condition and a rough average of the relative strength and peak strain for each adhesive, including all condition ranges for use and comparing average results.

Table 10. Average compressive strength for each cure condition summary table

Adhesive Name	Cure Condition At 50% Humidity (°C)	Ultimate Strength σ (MPa)	σ STD	Peak Ultimate Strain ϵ	ϵ STD
HFL	4	36.30	2.56	0.0389	0.0027
	23	81.31	0.49	0.0422	0.0034
	43	85.37	1.36	0.3910	0.0068
CFL	4	64.45	7.87	0.0266	0.0011
	23	97.34	12.93	0.0622	0.0295
	43	111.85	4.71	0.2210	0.0142
MFL	4	58.34	5.66	0.0641	0.0303
	23	100.80	8.20	0.0384	0.0034
	43	114.93	13.37	0.1020	0.0228
MP	4	66.54	8.30	0.0311	0.0093
	23	90.59	13.01	0.0398	0.0075
	43	123.46	15.52	0.0987	0.0100
CP	4	70.04	2.33	0.0342	0.0100
	23	80.09	3.49	0.0447	0.0028
	43	94.01	1.88	0.0640	0.0249
HP	4	74.62	3.41	0.0279	0.0055
	23	104.58	3.61	0.0272	0.0032
	43	109.55	8.00	0.0466	0.0125

Table 11 Average compressive strength for all conditions summary table

Adhesive Name	Ultimate Strength σ (MPa)	Peak Ultimate Strain ϵ
HFL	67.66	0.1574
CFL	91.21	0.1033
MFL	91.36	0.0682
MP	93.53	0.0566
CP	81.38	0.0476
HP	96.25	0.0339

5.1.2 Compression Creep Test Results

The creep compression results Figure 47 show a scatter plot of the average strain vs. time of the raw creep data during the tests of all samples. Creep testing revealed that two adhesives had significantly worse behavior under sustained compression loading. CP and HFL had more than double creep displacement compared to the averages of the remaining adhesives. Large creep displacement is undesirable for an adhesive. Ideally, the strain behavior of the adhesive should follow closely to the strain behavior of the structural material the adhesive is fastening together.

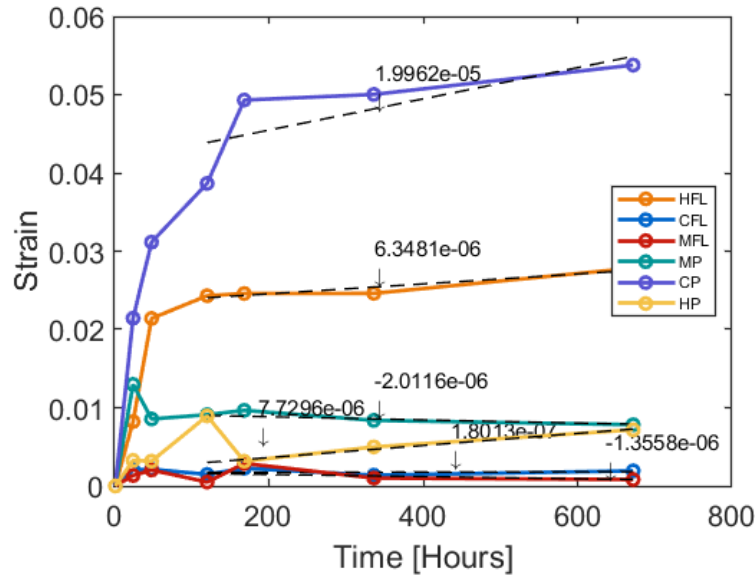


Figure 47. Scatter plot of the compressive creep (averaged) of all adhesives.

When looking at the four lower creep adhesives, the strain does not increase significantly over time for adhesive CFL and MFL. The high viscous adhesives of MP and HP seem to have large jumps and dips in strain. The significant dips could be from air pockets/gaps in the specimens.

The results from the creep test are quantified in terms of creep coefficient and creep compliance. Both measurement points follow a similar research paper by Emara et al. (2017). Creep compliance (J) is a measurement that represents the deformation ability of a material under constant stress in terms of a creep modulus. A more considerable J value means the material deforms more under sustained stress, while a smaller value means that the material is stiffer. The creep compliance is calculated by using strain ε at time (t) with respect to a constant applied stress σ :

$$J(t) = \varepsilon(t)/\sigma$$

Equation 4. Creep compliance

The creep coefficient (creep factor) is a ratio that shows the tendency of the material to deform over time at a constant load beyond its yield point, with a more significant creep coefficient indicating larger deformation from creep. The creep coefficient at time (t) is based on the instantaneous strain $\varepsilon(t_0)$ and strain $\varepsilon(t)$ at a time (t):

$$\phi(t) = \frac{\varepsilon(t) - \varepsilon(t_0)}{\varepsilon(t_0)}$$

Equation 5. Creep coefficient

While creep coefficient and creep compliance are related, they are related non-linearly inversely; a high creep coefficient should mean low creep compliance (Cruz et al., 2021).

ASTM C1181 has a procedure and approach that leaves many inaccuracies in the test, making it initially challenging to conclude. ASTM C1181 measurement procedure is taken only at a handful of data points throughout the 28 days of exposure. Furthermore, spars direction on how to interpret the data is given, leading to the approach for using creep coefficient and creep compliance as used in the papers by Emara et al. (2017) and Cruz et al. (2021). In many data points, significant inaccuracies from human error could occur from two events: (i) the loading technician did not tighten the nut with enough torque to properly hold the compressive force required, leading to a drop in the strain over the next handful of points and (ii) human error occurred during the hand measurement of strain that gave a higher or lower strain than what should have been recorded. As observed, the data is not measured in real-time and is measured over a really short time, meaning that drawing any trend lines for secondary creep behavior is inconclusive. However, qualitative

data can be compared if the data is average and the study observes the final points. Individual sample creep coefficient over time can be found in Appendix U too Appendix Z

The creep compliance in Figure 48 shows a significant difference in the trend of the average data. Some data points may be imprecise or inaccurate due to human error. However, generally, creep compliance and coefficient increase over time, and the final value can be treated as the creep coefficient and compliance of reference to be used to conclude.

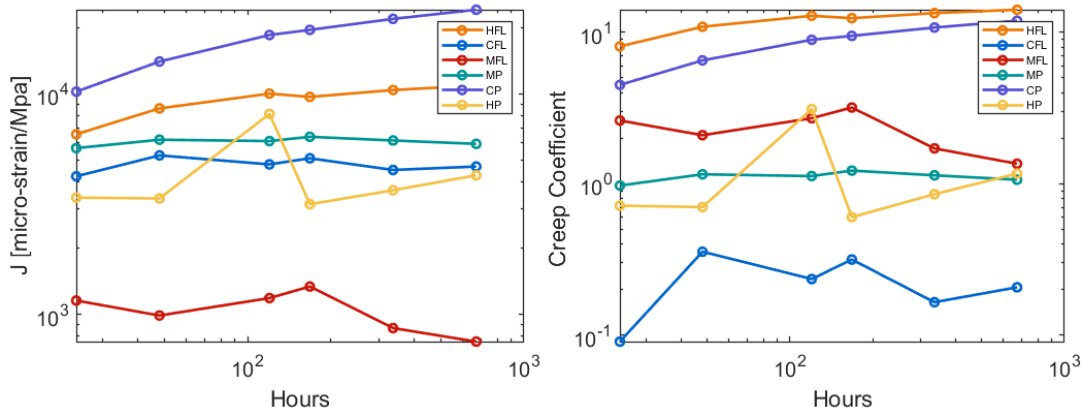


Figure 48. Creep Compliance and Creep Coefficient Scatter Plots. Creep Compliance over time is on the right, and Creep Coefficient over time is on the left.

Furthermore, summarizing the creep compliance and coefficients at the instantaneous endpoints at 672 hr ± 24 , notable comparisons can be made from the results that reflect the adhesive performance. In Figure 49, creep compliance indicates that CP and HFL are underperforming and deform more from compressive creep, while CFL and MFL perform very well. The creep coefficient data reflects the same trends and the creep compliance with variation between samples, primarily due to differences between initial and final sample depths.

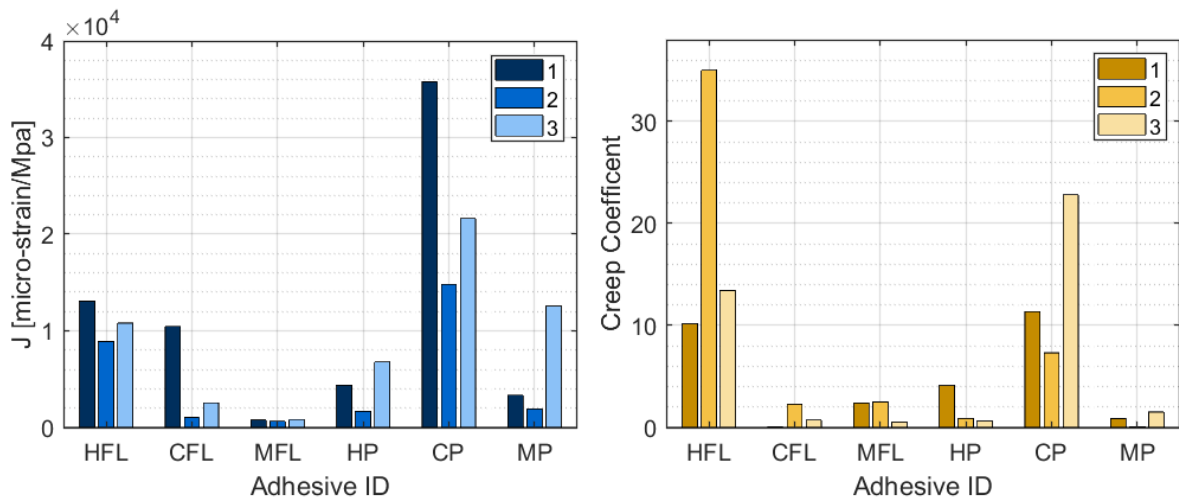


Figure 49. Reference Creep Compliance and Creep Coefficient Bar Graphs. Shows reference creep compliance on the left and reference creep coefficient on the right for all three samples for each adhesive. The reference creep point is the strain at 672 hours.

Overall, the best compressive creep performers are CFL and MFL, with lower creep coefficient/compliance values, while the notable bad performers were HFL and CP. It is worth noting that even though the creep coefficient/compliance is low for HP and MP, their initial strain after loading (at the first hour) is very high. The puddy-like adhesive shows more instantaneous creep after loading than the injectable fluid adhesives, meaning that the puddy adhesives generally have the worst behavior from primary creep. Table 12 and Table 13 summarizes creep testing results.

Table 12. Specimen summary of creep coefficient and compliance.

Adhesive Name	Specimen ID	Specimen Creep Coefficient ϕ	Specimen Creep Compliance J ($\mu\text{m/m/MPa}$)
HFL	HFL1	10.14	13,062
	HFL2	35.00	8,883.1
	HFL3	13.42	10,863
CFL	CFL1	0.0634	10,440
	CFL2	2.286	1,041.5
	CFL3	0.7121	2,566.7
MFL	MFL1	2.40	774.66
	MFL2	2.50	639.67
	MFL3	0.5417	843.94
MP	MP1	0.8608	3,325.5
	MP2	0.04938	1,931.9
	MP3	1.512	12,546
CP	CP1	11.37	35,777
	CP2	7.316	14,830
	CP3	22.80	21,620
HP	HP1	4.105	4,373.6
	HP2	0.8974	1,672.5
	HP3	0.6216	6,772.6

Table 13. Average summary of creep coefficient and compliance

Adhesive Name	Initial Strain	Final Strain (t=672hr)	Average Creep Coefficient	Average Creep Compliance ($\mu\text{m/m/MPa}$)
HFL	1,993.5	30,113	14.11	10,916
CFL	1,0698	1,2918	0.2075	4,682.8
MFL	880.93	2,076.5	1.357	752.73
MP	7,930.1	16,371	1.064	5,934.5
CP	5,133.9	66,416	11.94	24,076
HP	5,438.8	11,788	1.167	4,273.2

5.1.2.1 Narrowed Adhesive Selection

The initially proposed project stated that 4 adhesives would be chosen and tested in both material and structural. In order to give more options for promising adhesives, initial material testing was done with 6 selected adhesives, with the 4 best-performing of the 6 being selected for further structural testing. From analyzing results from compressive creep and compressive strength testing, it is evident that the two worst performing were HFL and CP due to their deficient performance in both categories. Going forward, HFL and CP will be excluded from testing.

5.1.3 Slip Test Results

The force vs. displacement data for all four adhesives and their samples for different steel surfaces are plotted to analyze the slip test results. Displacement represents the maximum measured vertical displacement of the specimens during testing from four sets of reference points, as illustrated in Figure 51. Appendix S shows the five individual runs for each adhesive type for the 50CR steel slip connections. Figure 50 is the summary scatter plot for the average of the 5 specimens under slip testing. The plot shows a 0.5 mm (0.02 in) dotted y-line that indicates slip

criteria. The surface coefficient (k_s) and their average are also shown for the five tests. The slip was determined to be the point of max force before or at 0.02 in displacement from RCSC specifications.

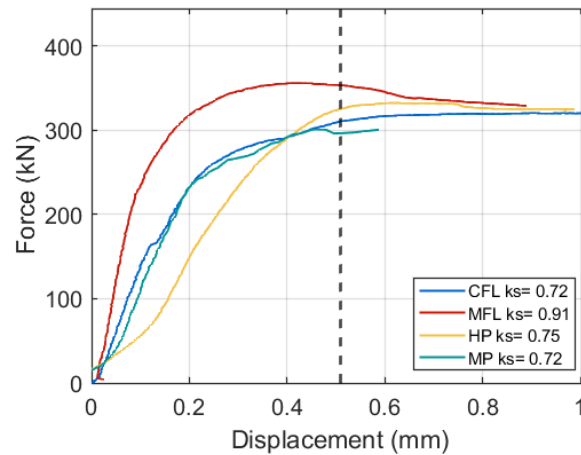


Figure 50. Average tensile load (surface Class B) vs. displacement. With provided average surface factor (K_s).

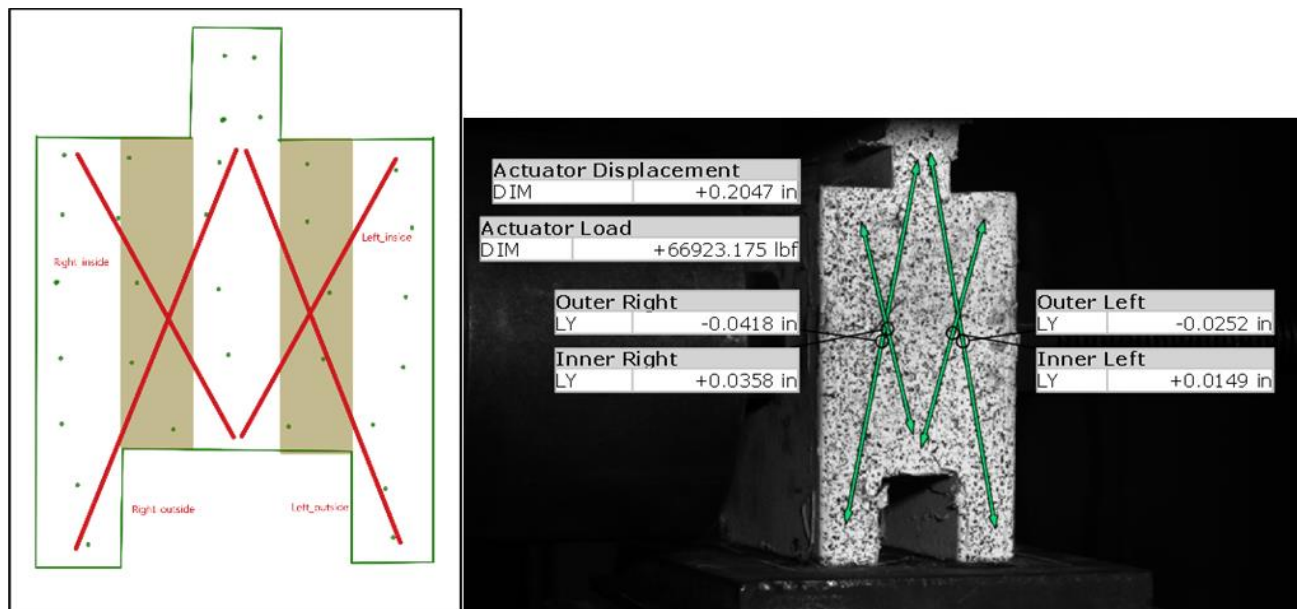


Figure 51. Examples of slip test vertical displacement measurement mesh points/vectors

Many adhesive individual trials follow similar trends, with the occasional outlier. Outliers like CFL1 and MFL2 occurred due to seating issues when loading, while outliers like MFL3 and HP5 were due to defects within the samples. It is important to note that none of the outliers change the average measured surface factor enough to be of issue.

The overall trends of the adhesives when loaded in a slip-critical connection are summarized in Figure 50 and Figure 52. The average slip data indicates an improvement in the connection between the steel and the adhesive used, as in a previous report from Provines and Abebe (2020). The 50CR clean mill scale A490 steel (class B) has a surface factor of 0.50 while the lowest reported adhesive factor is 0.71, proving that the use of adhesive will be beneficial for slip-critical connections if the clamping force is maintained chiefly. Figure 53 summarizes the surface coefficients with a bar graph from all the tests using class B steel. The dotted horizontal line marks typical unadhered slip connections' expected surface factor performance. MFL is shown to be the best performer of the four adhesives by 30% with a surface factor of 0.91, while the rest seems to sit around ~0.70. Based on our findings, the thickness of the adhesives between the plates does not seem to affect the performance if the clamping force is held constant, as thicker layers of adhesives lose more clamping force from creep. All averaged slip testing results for both surface classes are in Table 14.

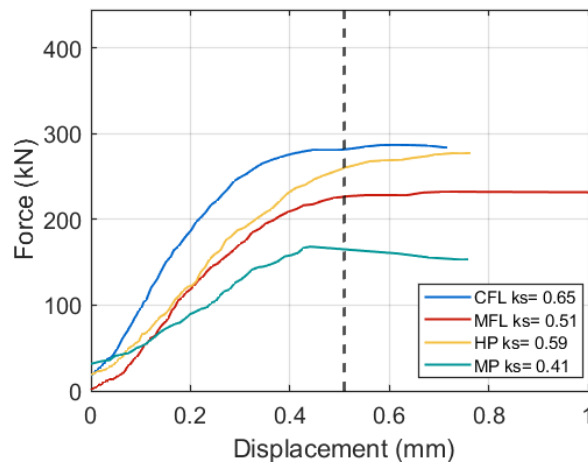


Figure 52. Average tensile load (surface Class A) vs. displacement. With provided average surface factor (Ks).

The m=0.35 scale A490 steel with zinc coating (class A) has a nominal surface factor of 0.35, and the lowest-performing adhesives were shown to have a surface factor of 0.41, with some achieving 0.65. This still reflects an improvement in slip criticality on adhered connections vs non-adhered. Overall, class A still performed worse in slip condition testing when looking at Figure 54; this was expected due to the smooth surface of the zinc-coated steel versus the rough-coasted class B steel. One crucial issue to note was that in some samples, the adhesives would not adhere to one of the plate surfaces during molding/curing, which harmed testing results. This happened with about one in every 5 samples for all four selected adhesives.

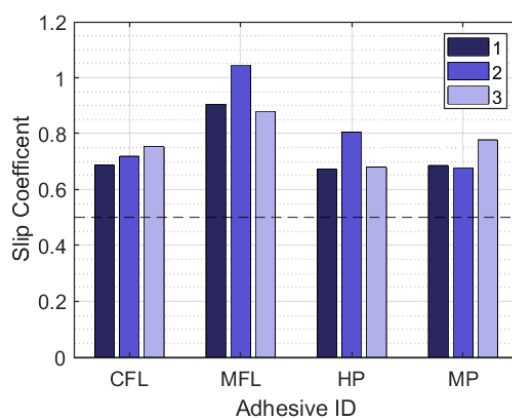


Figure 53. Summary graph of slip surface coefficients (Class B). Numbers indicate a sample of the three best results.

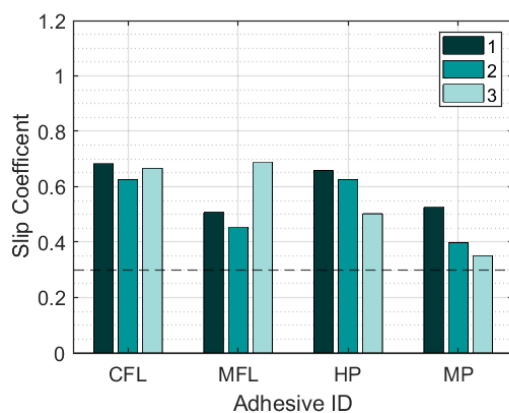


Figure 54. Summary graph of slip surface coefficients (Class A). Numbers indicate a sample of the three best results.

Table 14. Summary table of slip testing

Adhesive Name	Class A Slip Coefficient	Class B Slip Coefficient
CFL	0.65	0.72
MFL	0.51	0.91
MP	0.41	0.72
HP	0.59	0.75

5.1.4 Long-Term Tensile Creep Results

Creep vs. time data for all three species for the three selected adhesives was plotted and compared; due to time limitations and delays, only three sets of samples ran for the entire 1000 hrs; therefore, MFL results were excluded. Figure 55 graphs the creep vs. time for all three samples of each adhesive on separate plots at lab conditions over 1000 hrs. on a constant tensile force after the sample's fasteners were tortured to achieve set clamping force from testing specifications; this force was not held constant through the test.

The performance of different samples varied, with one sample in the batch diverging from the others. The outliers would be due to different losses in clamping force between the samples and differences in the sample's adhesive mixture.

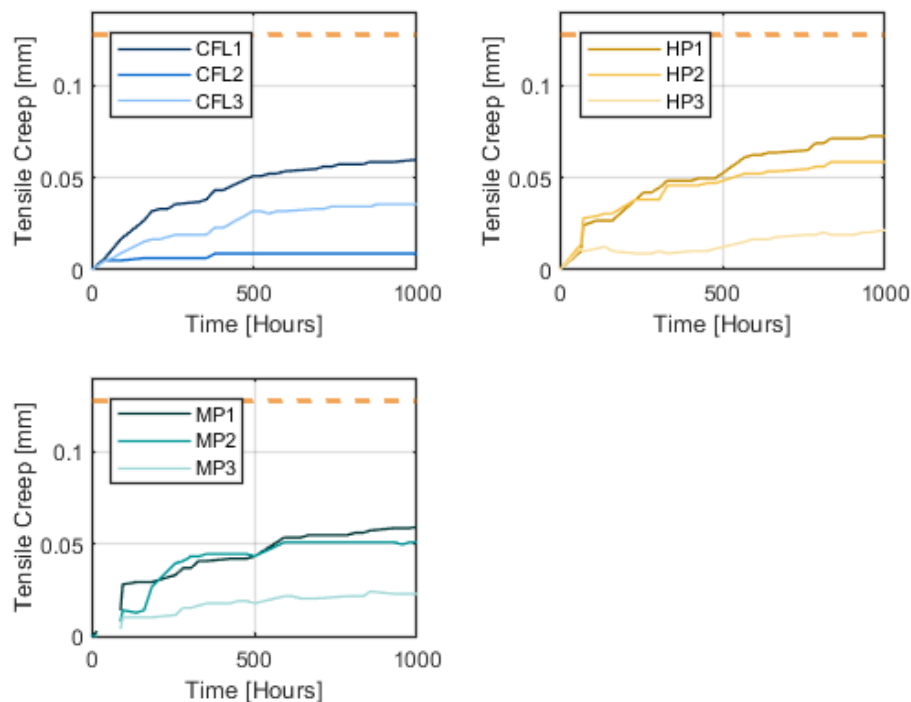


Figure 55. Individual specimen tensile creep results over time

The average tensile creep data for each set of specimens is in Figure 56. The figure shows similar slip vs. time plots for the four adhesives without failing the tests at 0.127 mm slip limit: The final creep only reached, on average, 0.044 mm. A significant initial creep occurs throughout the test, with large deformation occurring in the first 100 hrs., then it settles into a second creep phase.

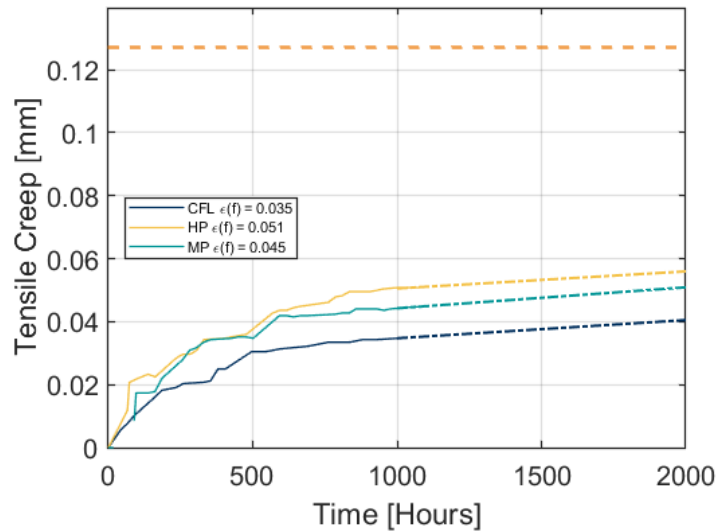


Figure 56. Average tensile creep results over time. Includes the final creep for each set of samples at 1000 hr and the linear trend line to 2000 hr.

It is important to note again that the clamping force from the tension bolts on the samples changed throughout the test, changing the actual slip coefficient of each sample during the test. The clamping force vs. time is plotted in Figure 57 for all three samples for the four selected adhesives under lab conditions. Clamping of the specimens is done 30 minutes before the test

starts; the time of zero indicates the start of tensile loading, not immediately after clamping. Again, one sample in each set diverges from the rest in its trend, following the creep vs. time plots.

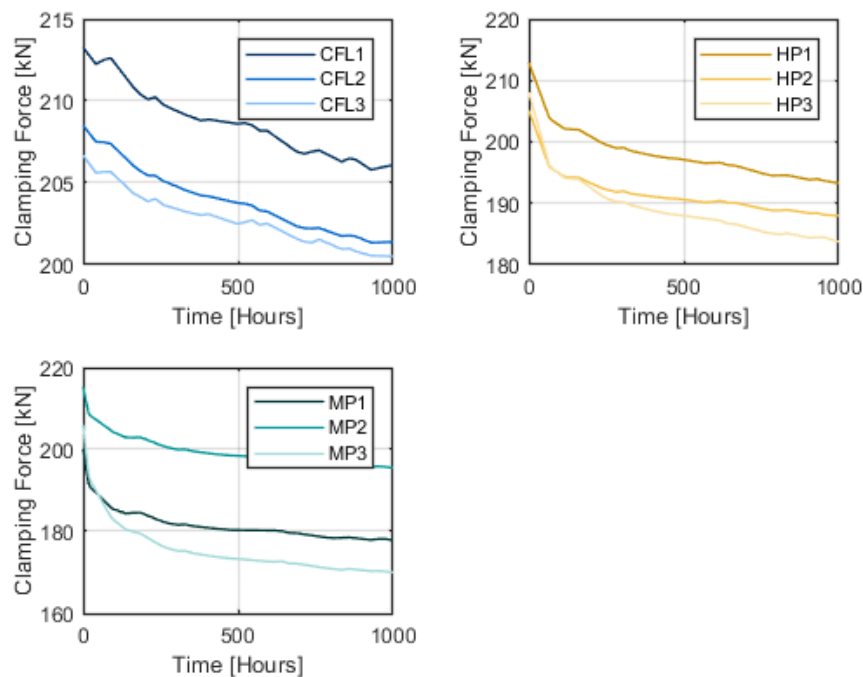


Figure 57. Individual specimen tensile creep clamping force over time

Figure 58 plots the average clamping force of the sets of samples over the 1000 hr. tensile creep test. This shows a divergence in the trends of each adhesive, with the thicker layered MP and HP dropping more clamping force through the test than the other two adhesives. The clamping force trend follows the creep over time, with CFL performing the best in the results. This is reflected in the summary Table 15.

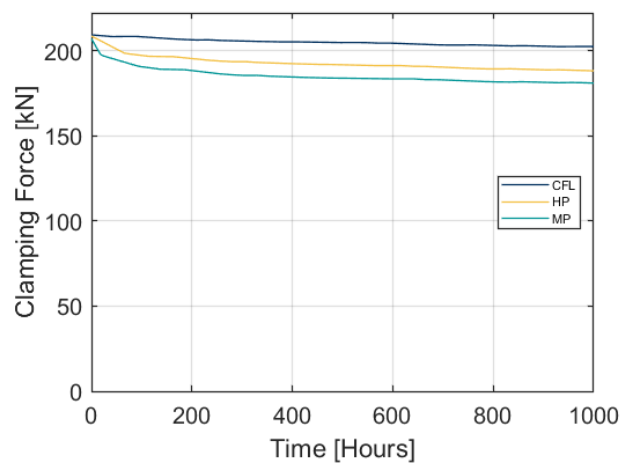


Figure 58. Tensile creep average clamping force over time

Table 15. Tensile creep summary

Adhesive Name	Layer Thickness (mm)	Creep at t=1000hr (mm)	Final Clamping Force (MPa)
CFL	3.175	0.035	202.57
MFL	3.175	--	--
MP	12.7	0.045	180.89
HP	12.7	0.051	188.33

5.2 Discussions on Test Results

The various properties of different structural adhesives studied in this report are summarized in Table 16. The color symbols indicate the percentile range of the result: red is below 33% of the average, green is above 66% of the average, and yellow is within 33% of the average. Check marks are used for pass-fail criteria. It is unrealistic to pick one ideal adhesive, as different adhesives have different pros and cons. This discussion will go through the general performance of each adhesive.

- HFL – The adhesive revealed poor behavior in all compressive testing but showed some stiffness to resist strain at lower temperatures. The compressive creep behavior was also deficient. While it was the most affordable and straightforward to handle of all the adhesives, its poor performance excluded it from tensile creep testing.
- CFL – The product had great compressive results. It also did the best under compressive creep and tensile creep. The adhesives were relatively affordable and not too tricky to work with. One of the best adhesives in the selection.
- MFL – Performed mostly well in compressive testing but is relatively soft and deformed more than the other adhesives under initial compressive loading. Under longer compressive loads, the adhesives performed well and became among the best performers.
- MP – Has excellent compressive behaviors and is one of the best performers under instantaneous compressive loading. It also did well in compressive creep. Tensile creep tests revealed that the adhesive passes the displacement limits, but a large amount of initial

relaxation occurred, causing a large amount of clamping force to be lost, and because of this, it displayed higher displacement than other adhesives.

- CP – The adhesives did below average in compressive testing, but it did show that it was reasonably stiff in short-term compression. The creep behavior of CP was not encouraging and was the second worst performance in this test. The adhesives' inferior performance excluded them from tensile creep testing.
- HP – Revealed decent short-term compressive behavior except at higher temperatures. The compressive creep results were acceptable, and tensile creep behavior was found to be reasonable. This adhesive ranks as the second most affordable among the selected options, presenting only minor challenges in application.

Table 16. Comparison of various properties of studied structural adhesives.

	HFL	CFL	MFL	MP	CP	HP
Compressive strength, 4°C [MPa]	● 36.30	● 64.45	● 58.34	● 66.54	● 70.04	● 74.62
Compressive strength, 23°C [MPa]	● 81.31	● 97.34	● 100.80	● 90.59	● 80.09	● 104.58
Compressive strength, 43°C [MPa]	● 85.37	● 111.85	● 114.93	● 123.46	● 94.01	● 109.55
Strain at peak strength, 4°C	● 0.0389	● 0.0266	● 0.0641	● 0.0311	● 0.0342	● 0.0279
Strain at peak strength, 23°C	● 0.0422	● 0.0622	● 0.0384	● 0.0398	● 0.0447	● 0.0272
Strain at peak strength, 43°C	● 0.3910	● 0.2210	● 0.1020	● 0.0987	● 0.0640	● 0.0466
Compressive creep coefficient (t=675hr)	● 14.110	● 0.208	● 1.357	● 1.064	● 11.940	● 1.167
Surface Factor (class A)	N/A	● 0.65	● 0.51	● 0.59	N/A	● 0.41
Surface Factor (class B)	N/A	● 0.72	● 0.91	● 0.71	N/A	● 0.72
Tensile creep max displacement (t=1000hr) [mm]	N/A	✓ 0.035	N/A	✓ 0.045	N/A	✓ 0.051
Tensile creep clamping force loss (t=1000hr) [MPa]	N/A	● 19.84	N/A	● 41.52	N/A	● 34.08
Affordability	●	●	●	●	●	●
Ease of application	●	●	●	●	●	●

To compare the results from both bulk (material) testing and joint (structural) testing, scatter plots were constructed to find relationships between different selections of data. The table below, Figure 59, plots the three samples tested in tensile creep in relation to compression creep. The results show a distinct linear trend between the three pairs of averaged data sets. There is a positive correlation between compressive creep behavior and tensile creep behavior for the selected structural adhesives. An in-depth discussion relating tensile creep to ultimate strength cannot be done due to the different thicknesses of the adhesive tests when under creep. Further research into adhesive thickness is needed.

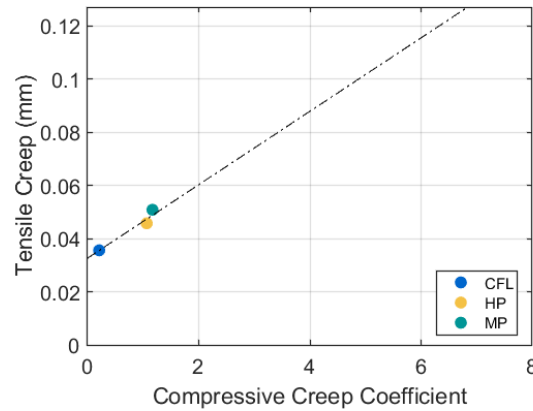


Figure 59. Scatter plot comparing compression creep coefficient to tensile creep

In Figure 60 the graph plots all 6 samples' averages (for lab conditioning) of compression ultimate stresses to compressive creep coefficient. The plot reveals a linear relationship between structural adhesives' ultimate stress and compressive creep behavior; higher ultimate stress in compression would mean lower creep under sustained load.

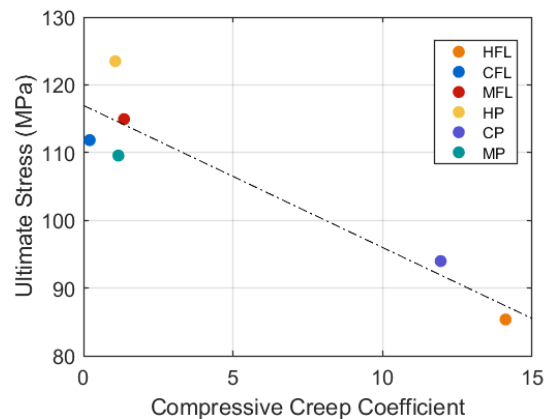


Figure 60. Scatter plot comparing creep coefficient to compression ultimate stress

6 CONCLUSION AND RECOMMENDATIONS

This thesis explores the use of structural adhesives for maintaining steel bridges, particularly focusing on a technique called "steel grouting" to prevent crevice corrosion and improve load capacity. By conducting various experimental tests and analyses, such as examining compressive strength and how adhesives behave under sustained pressure in different environments, the study aims to understand how these adhesives perform. Tests on slip and tensile creep further explore adhesive behavior in bolted connections and prolonged stress situations. Moreover, the study includes a thorough review of existing literature and field investigations to supplement the experimental findings. After extensively researching the performance of selected structural adhesives for bridge repair, the findings of this study give insights into how different adhesives behave under various conditions.

The compression test results offer detailed insights into how curing and service conditions affect the compressibility of structural adhesives. Epoxy adhesives, for instance, can show significant strength increase with more extended curing periods and higher temperatures. Temperature conditioning is most important during the first 7 days of curing, with other papers suggesting up to 30 days. It suggests picking times of the year that offer advantageous conditions for curing or providing an isolated environment for the adhesive to cure onsite.

Certain adhesives like HFL and HP, have low T_g and should be watched for temperatures approaching the glass transition temperature point when curing. Epoxy structural adhesives will display undesirable stress vs. strain behavior at high temperatures, including 43°C, reducing yield strength and increasing plastic deformation. These findings stress the importance of considering

curing and operating conditions when selecting adhesives for structural applications. It also stresses the importance of knowing the operation temperature ranges for an adhesive to ensure consistent behavior throughout its lifespan. The adhesive that will be used for steel repair in external structures should have well-documented operation capture ranges, including T_g point, ideally being tested before large-scale usage.

Further analysis of specific epoxy types reveals variations in compressive strength based on curing temperatures. While some adhesives maintain manufacturers' specified strengths across different conditions, others deviate significantly, such as MFL, MP, and CFL. The study suggests that before using adhesives on a project, testing of the average strength of adhesives should take place to ensure material behavior. HP, CFL, and MP emerge as top performers, demonstrating consistent strength across various temperature environments.

Compression creep testing underscores the critical role of adhesive selection in applications involving sustained compression loading. Adhesives like CP and HFL show significantly higher creep displacement, indicating poor performance under prolonged compression. In contrast, CFL and MFL demonstrate minimal creep, making them favorable choices for applications where long-term stability is crucial. Few manufacturers list their product's creep performance, so testing of creep behavior in both tension and compression is suggested prior to large-scale use of a product. Testing should record the creep coefficient and aim to have a coefficient of less than 2.0 for 2.8 MPa loading over at least 500 days. In addition, the current ASTM C1181 has several shortfalls as a standardized test, such as not requiring continuous data collection during creep testing, which is highly suggested for future tests.

In slip test results, improvements in slip connection performance between steel and adhesives are evident, particularly in slip-critical connections. Standard steel on steel slip connection using class B steel has a surface factor of $m=0.50$, while adding adhesives provides a surface factor improvement ranging from $m=0.71$ to $m=0.91$. MFL stands out as the top performer among tested adhesives, improving the surface factor to 0.91 and highlighting its suitability for enhancing slip connections. Interestingly, the thickness of adhesives does not significantly impact performance, provided the clamping force remains constant. It is suggested that thinner layers of adhesive should be applied to reduce loss in clamping slip load from the torqued bolted connections and limit possible voids in the gaps. Also, the slip-bolted connection is suggested to be over-torqued by 12% to leave room for load drop due to initial creep.

Long-term tensile creep testing offers insights into the complex behavior of adhesives under sustained tensile loading. While all adhesives exhibit initial creep, CFL shows the most favorable performance, maintaining stability over extended periods. Clamping force dropped throughout testing, mostly in the first 100 hours; these negative influences adhesive behavior, leading to more significant slippage of the connections, with thicker adhesives like MP and HP experiencing greater force loss over time. This more significant loss in clamping force is primarily due to thicker layers of adhesives having more impactful compressive creep. Again, the findings suggest that thin layers of adhesive should be used when possible, and the loss of clamping force needs to be considered.

For comparison of data between material and structural tests, the selected adhesives show a linear relationship between creep compression behavior and ultimate compressive strength. Based

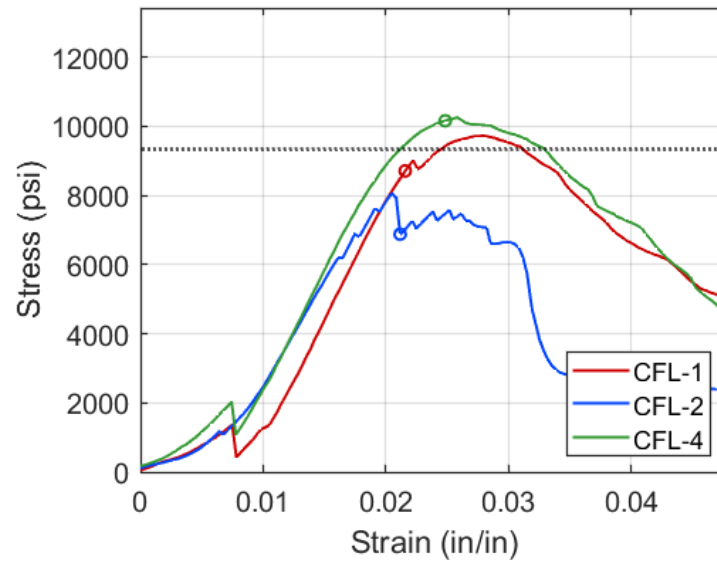
on these findings, it is concluded that the creep behavior of adhesives can be inferred based on the compressibility of the adhesives. It is suggested that the ultimate compressive strength of the structural adhesives be above 110 MPa (lab conditioning). Comparing compressive creep to tensile creep releases a linear correlation between the two; a better compressive creep coefficient reflects less tensile creep. It is suggested for a compressive test following ASTM C1181 at ~2.75MPa load at 60°C 50% H to have a creep coefficient of less than 6.00. In summary, an ultimate compressive strength of 110 MPa or higher should ensure good behavior in tensile slip and compression creep.

This study underscores the critical importance of meticulous adhesive selection and consideration of environmental factors in structural adhesive applications for bridge repair. Adhesives like HP and MP exhibit promising performance characteristics, while others like HFL and CP may pose challenges due to inferior creep and strength properties. This study only includes 4-6 different adhesives for three different companies; there are countless other structural adhesives on the market, and more studies need to be taken to narrow down extensive selections of approved adhesives for use.

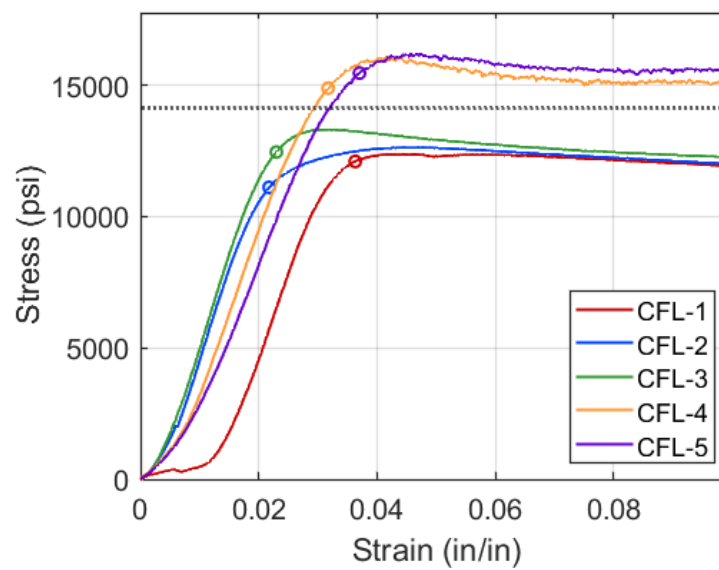
Several important areas for further exploration are suggested based on the insights gained from the literature review and our experimental results. These include conducting more extensive compressive and tensile creep tests over longer timeframes, possibly spanning up to a year. It is crucial to investigate how factors like water, chloride, thermal wear, and radiation damage affect the performance of structural adhesives. Additionally, there is a need to study how adhesives behave under different types of loads, both in bulk and joint setups. Furthermore, we should explore how using different types of epoxy aggregates impacts the performance of materials. To

ensure effective steel-adhesive connections, it would also be beneficial to thoroughly study the surface preparation methods for commonly used bridge steels. An in-depth life cycle analysis (LCA) would be informative considering the environmental impact. Continuous research and development efforts are necessary to refine adhesive formulations and application techniques, ensuring better performance and longevity in real-world bridge repair scenarios.

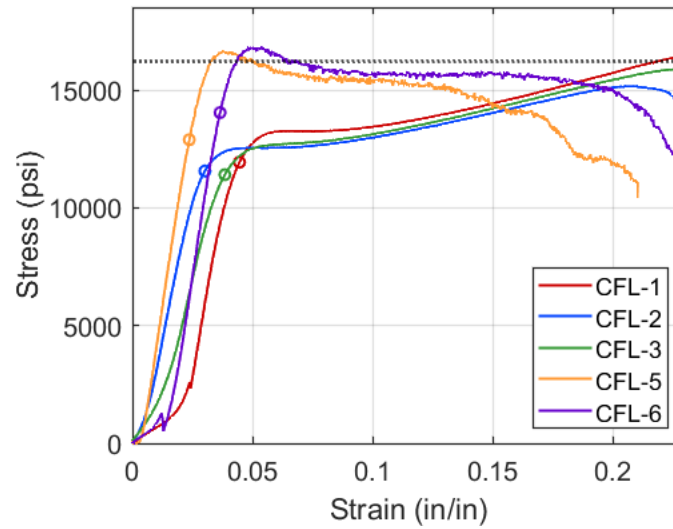
APPENDIX



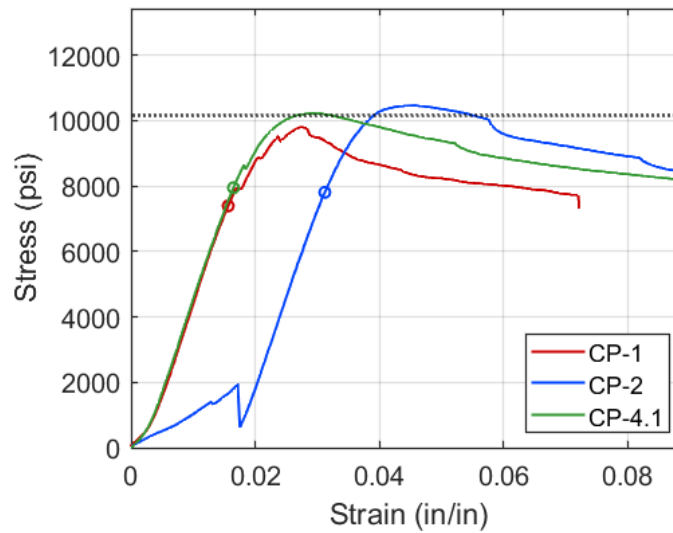
Appendix A. Compression Results for CFL at 4°C



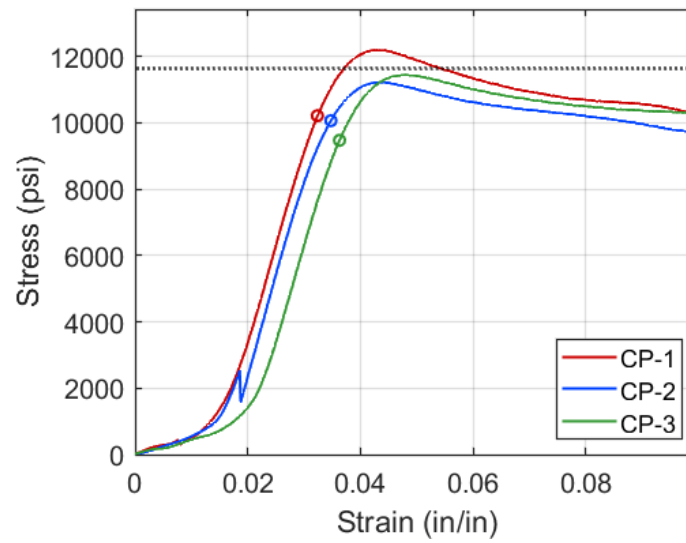
Appendix B. Compression Results for CFL at 23°C



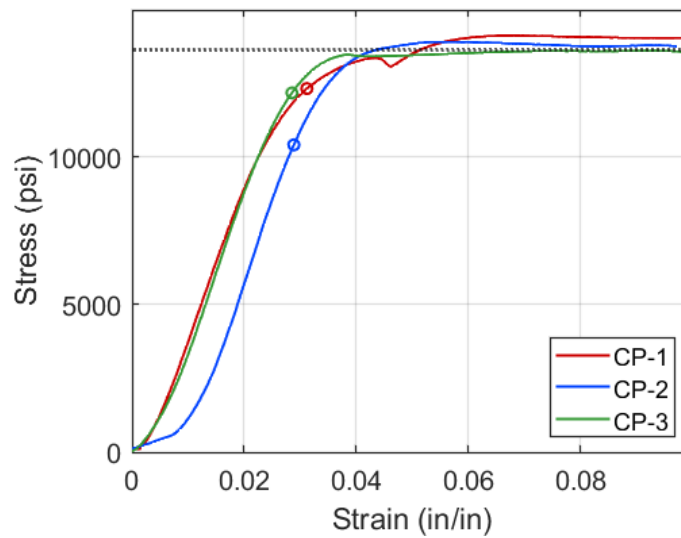
Appendix C. Compression Results for CFL at 43°C



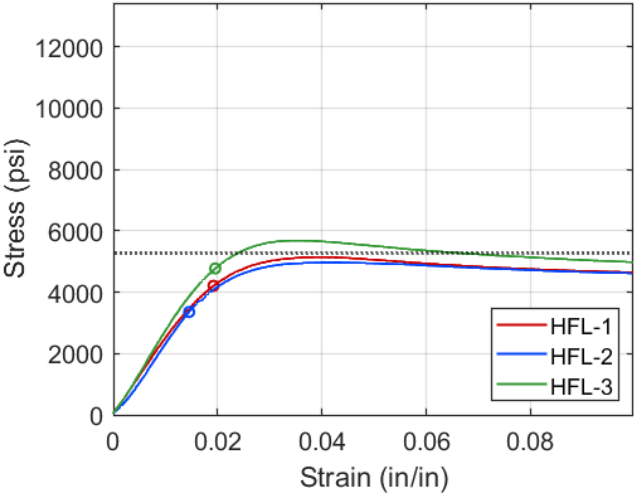
Appendix D. Compression Results for CP at 4°C



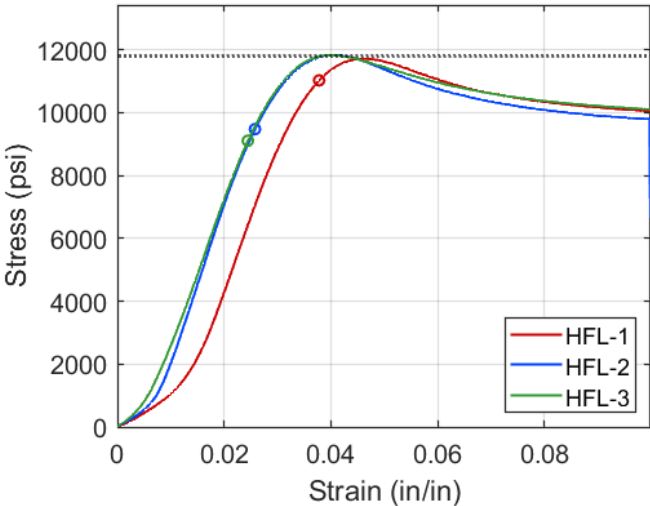
Appendix E. Compression Results for CP at 23°C



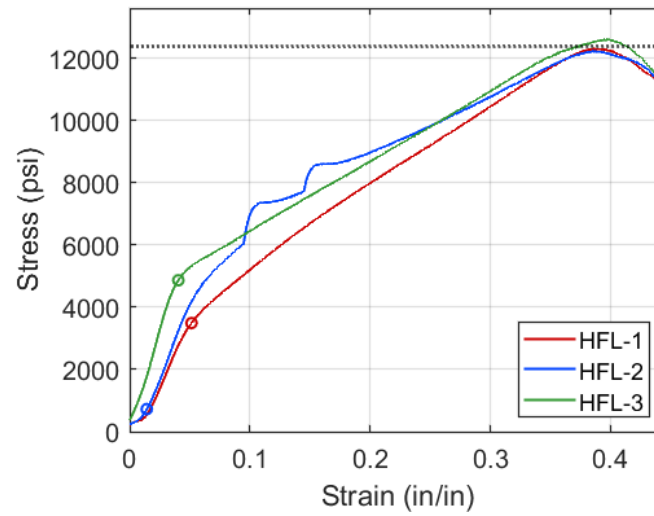
Appendix F. Compression Results for CP at 43°C



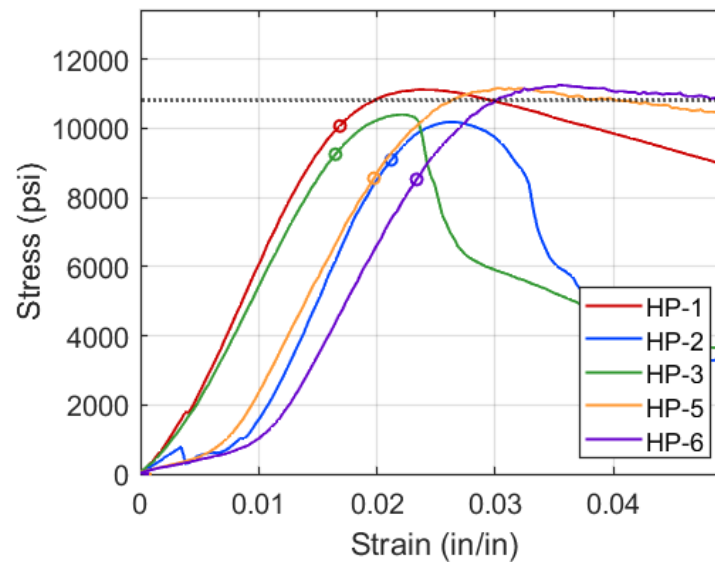
Appendix G. Compression Results for HFL at 4°C



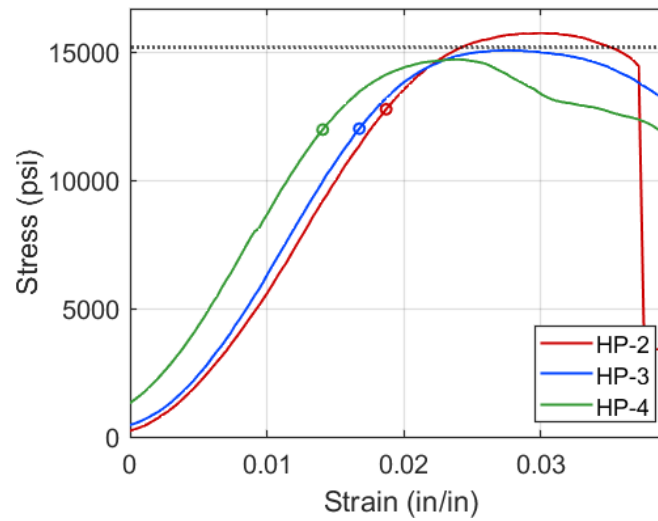
Appendix H. Compression Results for HFL at 23°C



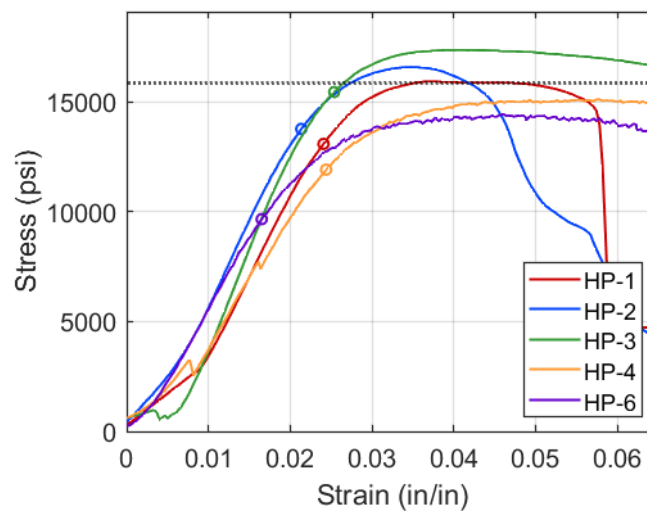
Appendix I. Compression Results for HFL at 43°C



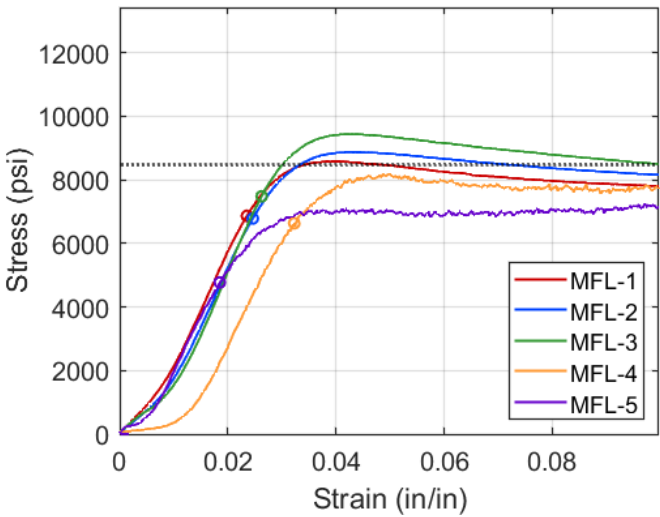
Appendix J. Compression Results for HP at 4°C



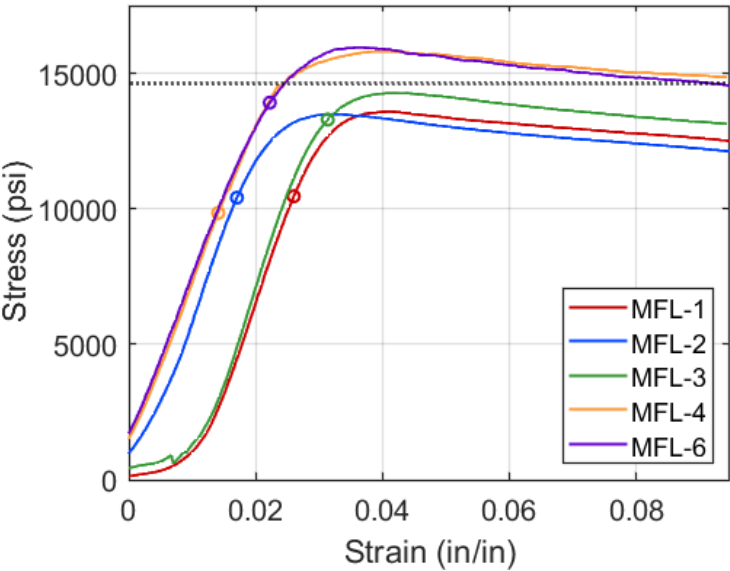
Appendix K. Compression Results for HP at 23°C



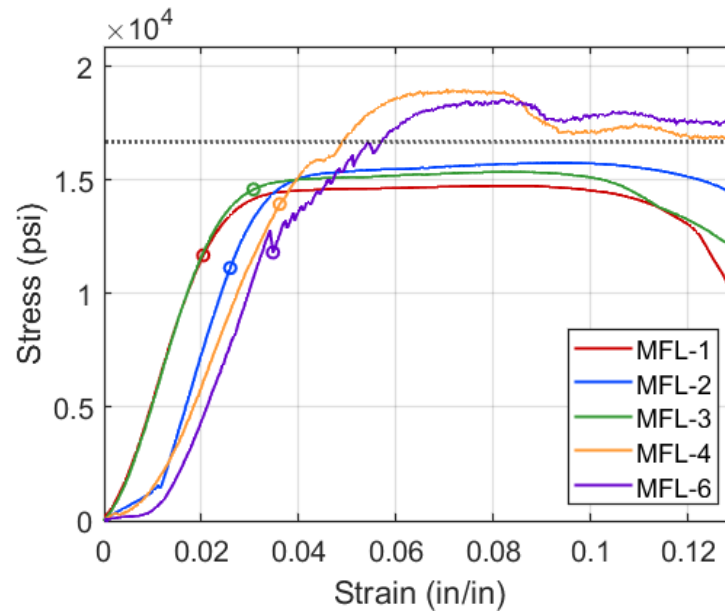
Appendix L. Compression Results for HP at 43°C



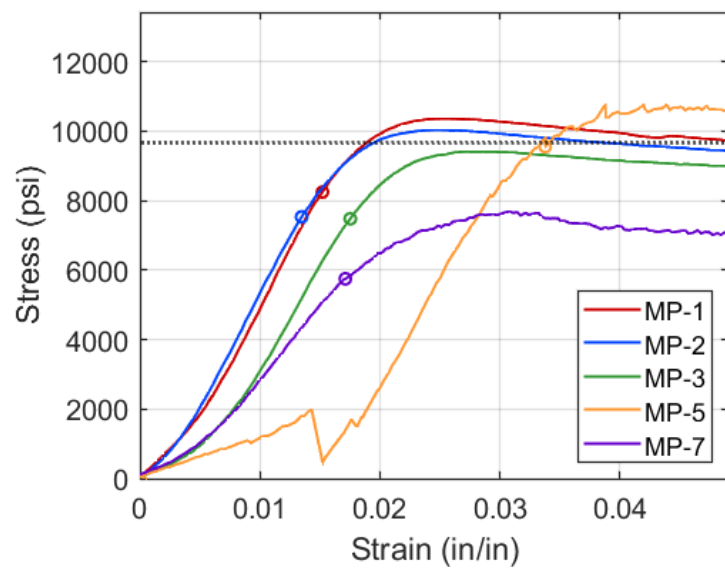
Appendix M. Compression Results for MFL at 4°C



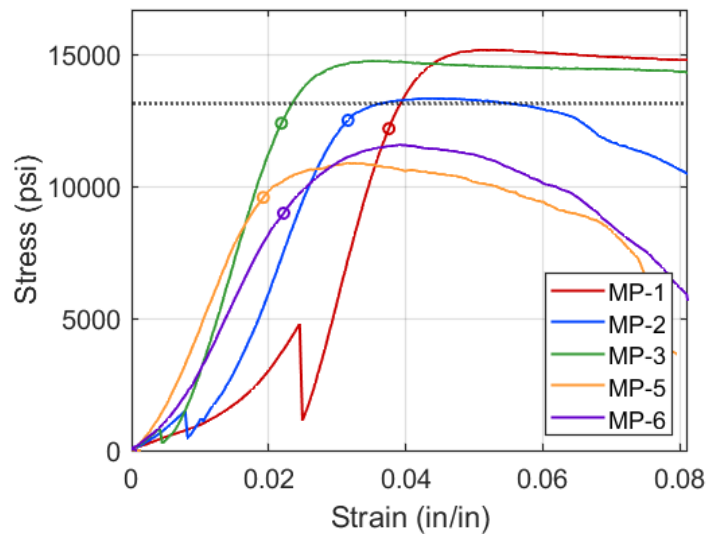
Appendix N. Compression Results for MFL at 23°C



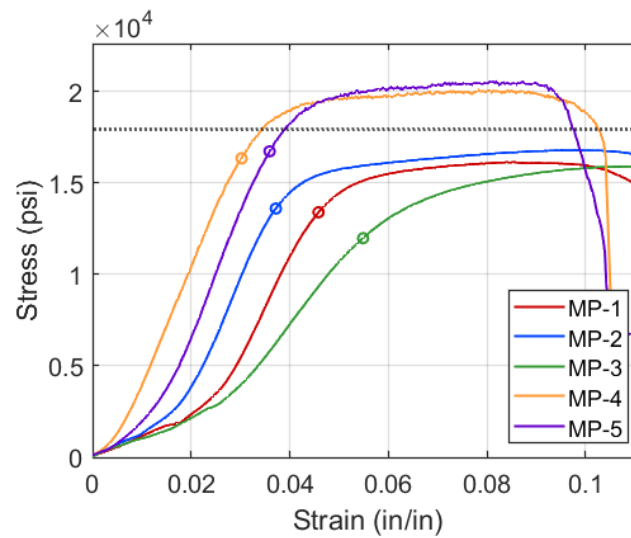
Appendix O. Compression Results for MFL at 43°C



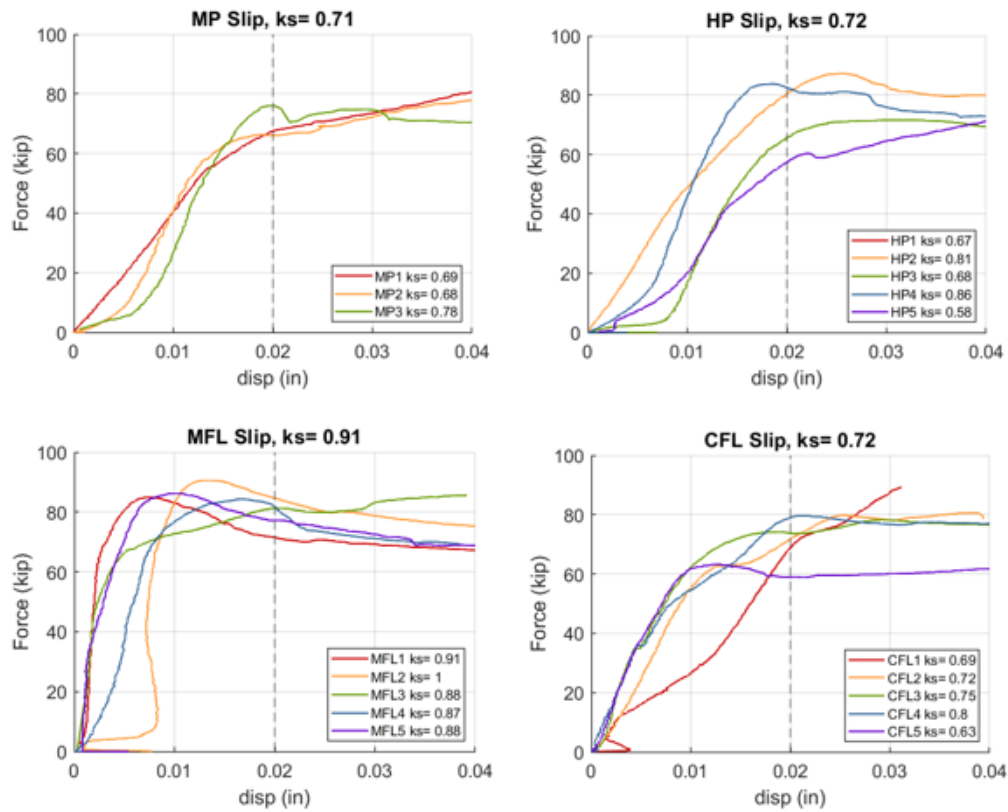
Appendix P. Compression Results for MP at 4°C



Appendix Q. Compression Results for MP at 23°C



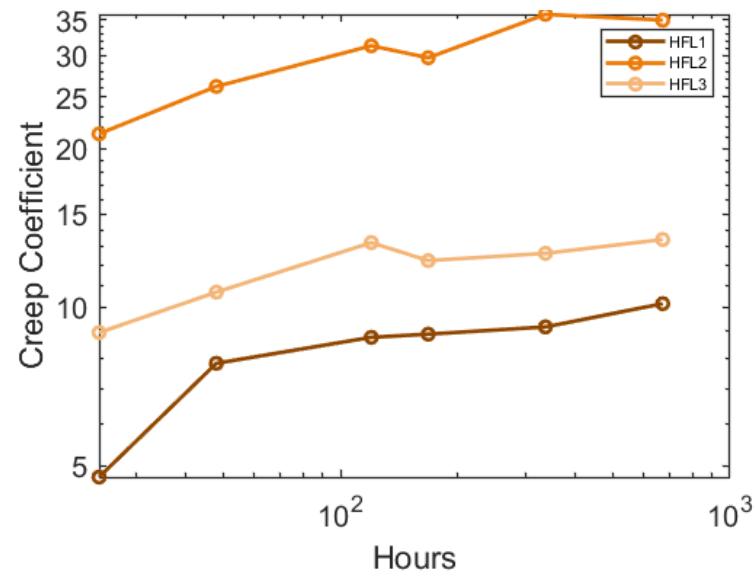
Appendix R. Compression Results for MP at 43°C



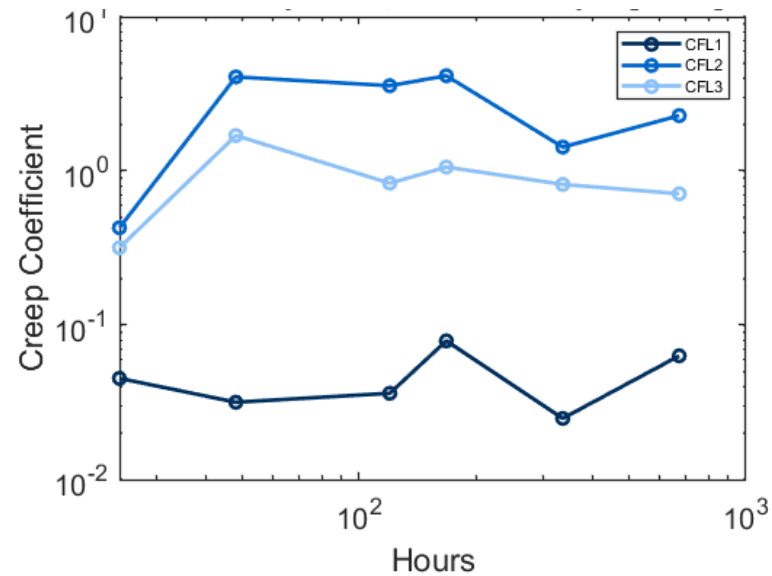
Appendix S. Slip Tests Individual Results for 50CR Steel. Individual surface factor (k_s) is listed in the ledger.

Appendix T. ASTM Standards for Steel Adhesive Connections (Provided by Dr. Kara Peterman & Kathleen Sullivan, 2024)

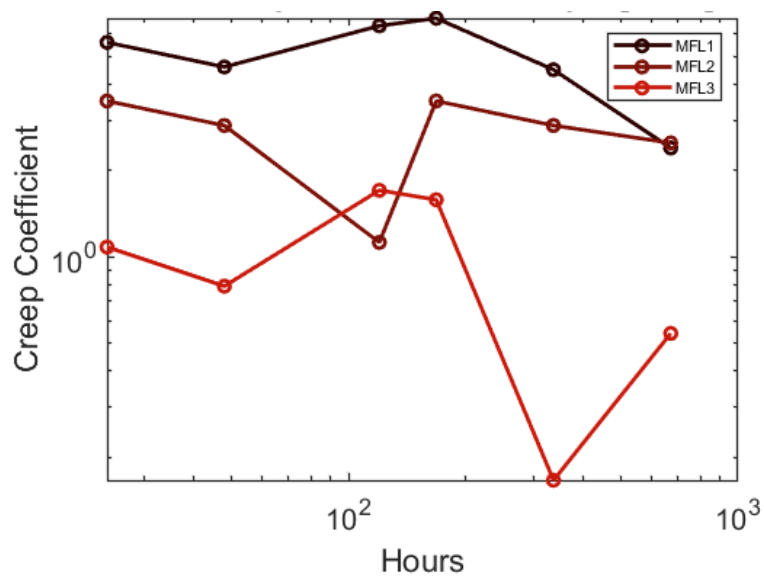
Standard	Description
D897-08	Standard Test Method for Tensile Properties of Adhesive Bonds
D905-08	Standard Test Method for Strength Properties of Adhesive Bonds in Shear by Compression Loading
D907-15	Standard Terminology of Adhesives
D950-03	Standard Test Method for Impact Strength of Adhesive Bonds
D1002-10	Standard Test Method Apparent Shear Strength of Single-Lap-Joints Adhesively Bonded Metal Specimens by Tension Loading (Metal-to-Metal)
D1062-08	Standard Test Method for Cleavage Strength of Metal-to-Metal Adhesive Bonds
D1151-00	Standard Practice for Effect of Moisture and Temperature on Adhesive Bonds
D1183-03	Standard Practices for Resistance of Adhesives to Cyclic Laboratory Aging Conditions
D1780-05	Standard Practice for Conducting Creep Tests of Metal-to-Metal Adhesives
D1828-01	Standard Practice for Atmospheric Exposure of Adhesive-Bonded Joints and Structures
D2095-96	Standard Test Method for Tensile Strength by Means of Bar and Rod Specimens
D2293-96	Standard Test Method for Creep Properties of Adhesives in Shear by Compression Loading (Metal-to-Metal)
D2294-96	Standard Test Method for Creep Properties of Adhesives in Shear by Tension Loading (Metal-to-Metal)
D2295-96	Standard Test Method for Strength Properties of Adhesives in Shear by Tension Loading at Elevated Temperatures (Metal-to-Metal)
D2651-01	Standard Guide for Preparation of Metal Surfaces of Adhesives Bonds
D2919-01	Standard Test Method for Determining Durability of Adhesive Joints Stressed in Shear by Tension Loading
D3166-99	Standard Test Method for Fatigue Properties of Adhesives in Shear by Tension Loading (Metal/Metal)
D3433-99	Standard Test Method for Fracture Strength in Cleavage of Adhesives in Bonded Metal Joints
D3528-96	Standard Test Method for Strength Properties of Double Lap Shear Adhesive Joints by Tension Loading
D3808-01	Standard Test Method for Qualitative Determination of Adhesion and Adhesives to Substrates by Spot Adhesion
D4501-01	Standard Test Method for Shear Strength of Adhesive Bonds Between Rigid Substrates by the Block-Shear Method
D4896-01	Standard Guide for Use of Adhesive-Bonded Single Lap-Joint Specimen Test Results
D5656-10	Standard Test Method for Thick-Adherend Metal Lap-Shear Joints for Determination of the Stress-Strain Behavior of Adhesives in Shear by Tension Loading
D6465-99	Standard Guide for Selecting Aerospace and General-Purpose Adhesives and Sealants



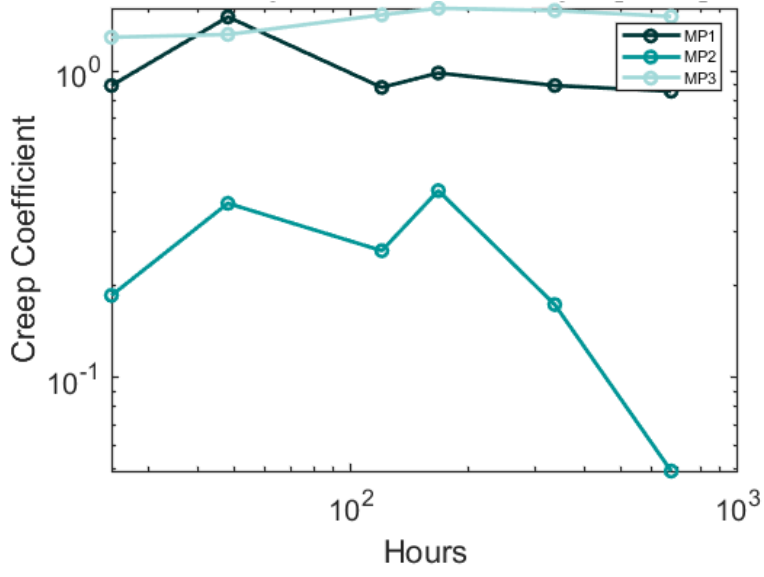
Appendix U. HFL samples creep coefficient over time in log-log



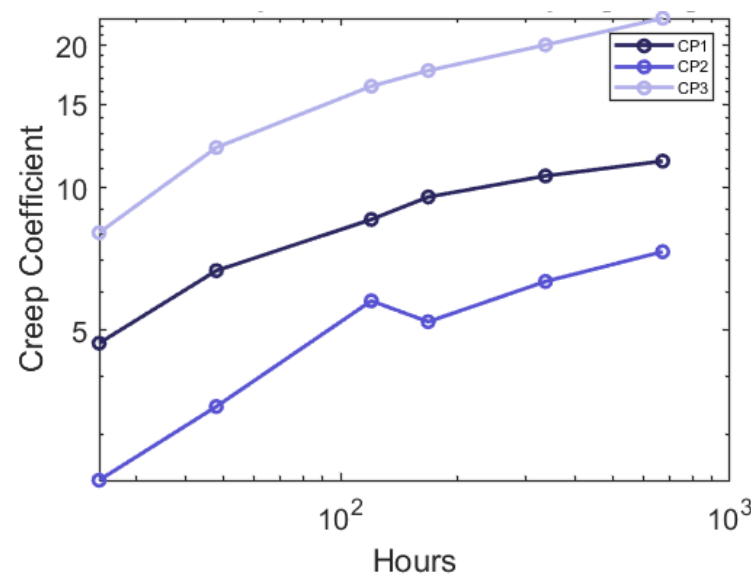
Appendix V. CFL samples creep coefficient over time in log-log



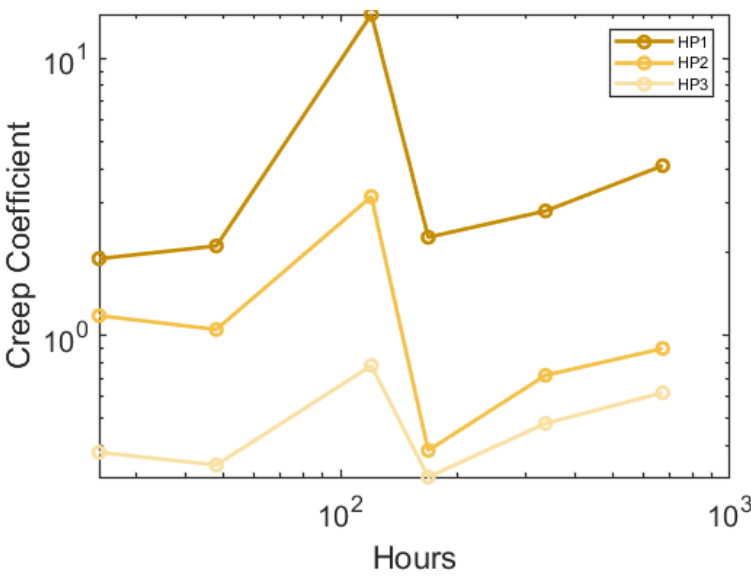
Appendix W. MFL samples creep coefficient over time in log-log



Appendix X. MP samples creep coefficient over time in log-log



Appendix Y. CP samples creep coefficient over time in log-log



Appendix Z. HP samples creep coefficient over time in log-log

REFERENCES

- Adams, R. D. (2021). *Adhesive bonding: science, technology and applications* (2nd ed.). Woodhead Publishing.
- Adams, R. D., & J Comyn. (2000). Joining using adhesives. *Assembly Automation*, 20(2), 109. <https://doi.org/10.1108/01445150010321724>
- Ainge, S. W., & Foley, C. M. (2012). *Repair and strengthening of bridge substructures*. ProQuest Dissertations and Theses; Marquette University.
- Albrecht, P., & Mecklenburg, M. F. (1996). Predicting cohesive strength of a bonded joint from properties of bulk adhesive. *First International Conference on Composites in Infrastructure* National Science Foundation National Science Foundation.
- Andrea, José Sena Cruz, & Vassilopoulos, A. P. (2020). Fabrication and curing conditions effects on the fatigue behavior of a structural adhesive. *International Journal of Fatigue*, 139. <https://doi.org/10.1016/j.ijfatigue.2020.105743>
- ASTM. (2018). *ASTM C1181/C1181M-17, Standard Test Methods for Compressive Creep of Chemical-Resistant Polymer Machinery Grouts*. American Society for Testing and Materials. doi: 10.1520/C1181_C1181M-17
- ASTM. (2021). *ASTM D618-21, Standard Practice for Conditioning Plastics for Testing*. American Society for Testing and Materials. doi: 10.1520/D0618-21
- ASTM. (2023). *ASTM D695-15, Standard Test Method for Compressive Properties of Rigid Plastics*. American Society for Testing and Materials. doi: 10.1520/D0695-15
- Banea, M. D., & Silva. (2009). Adhesively bonded joints in composite materials: An overview.

- Proceedings of the Institution of Mechanical Engineers, Part L: Journal of Materials: Design and Applications*, 223(1), 1–18. <https://doi.org/10.1243/14644207JMDA219>
- Cruz, R., Correia, L., Cabral-Fonseca, S., & José Sena-Cruz. (2021). Effects of the preparation, curing and hygrothermal conditions on the viscoelastic response of a structural epoxy adhesive. *International Journal of Adhesion and Adhesives*, 110. <https://doi.org/10.1016/j.ijadhadh.2021.102961>
- Duncan, B., & Croker, L. (2023). *Characterisation of flexible adhesives for design*. National Physical Laboratory. <https://doi.org/10.47120/npl.mgpg45>
- Emara, M., Torres, L., Baena, M., Barris, C., & Moawad, M. (2017). Effect of sustained loading and environmental conditions on the creep behavior of an epoxy adhesive for concrete structures strengthened with CFRP laminates. *Composites Part B: Engineering*, 129, 88–96. <https://doi.org/10.1016/j.compositesb.2017.07.026>
- Ghaffary, & Moustafa, M. A. (2020). Synthesis of repair materials and methods for reinforced concrete and prestressed bridge girders. *Materials*, 13(18). <https://doi.org/10.3390/ma13184079>
- Gresnigt, A. M., Sedlacek, G., & Paschen, M. (2000). INJECTION BOLTS TO REPAIR OLD BRIDGES . *Proc., Connections in Steel Structures IV*, 349–360.
- Higgins, A. (2000). Adhesive bonding of aircraft structures. *International Journal of Adhesion and Adhesives*, 20(5), 367–376. [https://doi.org/10.1016/S01437496\(00\)000063](https://doi.org/10.1016/S01437496(00)000063)
- Jahani, Y., Baena, M., Barris, C., Perera, R., & Torres, L. (2022). Influence of curing, postcuring and testing temperatures on mechanical properties of a structural adhesive. *Construction and Building Materials*, 324, 126698. <https://doi.org/10.1016/j.conbuildmat.2022.126698>

- Keller, T., Rothe, J., De, J., Osei-Antwi, M., & Asce, S. M. (2013). *GFRP-Balsa sandwich bridge deck: Concept, design, and experimental validation*.
[https://doi.org/10.1061/\(ASCE\)CC.1943-5614](https://doi.org/10.1061/(ASCE)CC.1943-5614)
- Loctite. (2022). *Technical Data Sheet, LOCTITE® EA 3471, Known as FIXMASTER STEEL PUTTY* . www.loctite.com
- Machalická, K., Vokáč, M., & Eliášová, M. (2017). *EFFECT OF LABORATORY AGEING ON STRUCTURAL ADHESIVE JOINTS WITH METAL SUBSTRATES* (pp. 11–15).
- Makevičius, L., Stranghöner, N., Kunde, C., & Thelen, S. (2021). *Duroplastic gap filling materials in preloaded bolted connections*. <https://doi.org/10.1002/cepa>
- Masoudi Jr, R. (2013). *Adhesion of epoxy coating to steel reinforcement under alkaline conditions* [Doctoral Dissertation].
- Miravalles, M., & Iip Dharmawan. (2007). *The creep behaviour of adhesives A numerical and experimental investigation*. CHALMERS UNIVERSITY OF TECHNOLOGY.
<https://odr.chalmers.se/server/api/core/bitstreams/734a5e6e-6bc6-4b62-9679-24cc7d538471/content>
- Morris, C. E. M. (1994). Strong durable adhesive bonding: Some aspects of surface preparation, joint design and adhesive selection. *MATERIALS FORUM-RUSHCUTTERS BAY*, vol. 17, pp. 211-211. CSIRO.
- Mouritz, A. P. (2012). *Introduction to aerospace materials*. Elsevier Science & Technology.
<http://ebookcentral.proquest.com/lib/uva/detail.action?docID=1584625>
- NIOSH. (2020, February 20). *Search the NIOSH Pocket Guide to Chemical Hazards | NIOSH | CDC*. [Www.cdc.gov](http://www.cdc.gov); Centers for Disease Control and Prevention.

<https://www.cdc.gov/niosh/npg/search.html>

Noury, P., Hayman, B., McGeorge, D., & J Weitzenböck. (2002). Lightweight construction for advanced shipbuilding-recent development. *Proceedings of the 37th WEGEMT Summer School, 11-15.*

OSHA. (2023). Personal protective equipment. In *www.osha.gov*.

<https://www.osha.gov/personal-protective-equipment>

Ozel, A., Betul Yazici, Salih Akpinar, Murat Demir Aydin, & Şemsettin Temiz. (2014). A study on the strength of adhesively bonded joints with different adherends. *Composites Part B: Engineering*, 62, 167–174. <https://doi.org/10.1016/j.compositesb.2014.03.001>

Panchuk, M., Ślaskowski, A., Panchuk, A., & Semianyk, I. (2021). New technologies for hull assemblies in shipbuilding. *NAŠE MORE: Znanstveni Časopis Za More I Pomorstvo*, 68(1), 48–57.

Panda, H. S., Samant, R., Mittal, K. L., & Panigrahi, S. K. (2020). Durability Aspects of Structural Adhesive Joints. In *Structural Adhesive Joints* (pp. 97–134).

<https://doi.org/10.1002/9781119737322.ch4>

Park, J. H., Choi, J. H., & Kweon, J. H. (2010). Evaluating the strengths of thick aluminum to aluminum joints with different adhesive lengths and thicknesses. *Fifteenth International Conference on Composite Structures*, 92(9), 2226–2235.

<https://doi.org/10.1016/j.compstruct.2009.08.037>

Perm Inc. (2016). *Wettability for multi-phase saturated rock / fundamentals of fluid flow in porous media*. Perminc.com. <https://perminc.com/resources/fundamentals-of-fluid-flow-in-porous-media/chapter-2-the-porous-medium/multi-phase-saturated-rock->

properties/wettab%E2%80%A61/4

Provines, J. T., & Abebe, H. (2020). *Slip coefficient testing of ASTM A709 grade 50CR steel and dissimilar metal slip-critical bolted connections*.

http://www.viriniadot.org/vtrc/main/online_reports/pdf/20-r12.pdf

RCSC Committee A.1. (2020). *Specification for Structural Joints Using High-Strength Bolts*. Research Council on Structural Connections. <https://www.aisc.org/publications/steel-standards/rcsc/>

Rollins, T., & Chajes, M. J. (2015). New and emerging methods of bridge strengthening and repair and development of a bridge rehabilitation website framework. In *ProQuest Dissertations and Theses* (No. 10014933, University of Delaware; p. 226). ProQuest Dissertations & Theses Global.

Rudawska, A. (2020). The effect of the salt water aging on the mechanical properties of epoxy adhesives compounds. *Polymers*, 12(4). <https://doi.org/10.3390/POLYM12040843>

Sahellie, S., & Pasternak, H. (2015). Expectancy of the lifetime of bonded steel joints due to long-term shear loading. *Archives of Civil and Mechanical Engineering*, 15(4), 1061–1069. <https://doi.org/10.1016/j.acme.2015.05.004>

Specker, L. (2023, June 16). *Austal USA lays keel for last LCS, the ship “that made the company.”* AL. <https://www.al.com/news/mobile/2023/06/austal-usa-lays-keel-for-last-littoral-combat-ship-the-vessel-that-made-the-company.html>

Sullivan, K., & Peterman, K. D. (2024). A review of adhesive steel-to-steel connections for use in heavy construction. *Journal of Constructional Steel Research*, 213, 108405. <https://doi.org/10.1016/j.jcsr.2023.108405>

- Thomas, S., Sinturel, C., Thomas, R., Sadek, E. A., Sahrim, A., Azlina, M., Yi, Y., Qin, Q., VázquezTorres, H., Boyard, N., Sobotka, V., Delaunay, D., Koshy, S., Sobotka, V., Delaunay, D., Boyard, N., Thomas, S., Vijayan P., Poornima, Pethrick, R. A., & Cicala, G. (2014). Life Cycle Assessment (LCA) of EpoxyBased Materials. In *Micro- and Nanostructured Epoxy/Rubber Blends*. <https://doi.org/10.1002/9783527666874.ch21>
- Wang, B., Bai, Y., Hu, X., & Lu, P. (2016). Enhanced epoxy adhesion between steel plates by surface treatment and CNT/short-fibre reinforcement. *Composites Science and Technology*, 127, 149–157. <https://doi.org/10.1016/j.compscitech.2016.03.008>
- Wang, W., Zhao, W., Zhang, J., & Zhou, J. (2021). Epoxy-based grouting materials with super-low viscosities and improved toughness. *Construction and Building Materials*, 267. <https://doi.org/10.1016/j.conbuildmat.2020.121104>
- Xu ,X. X, Crocombe ,A. D, & Smith ,P. A. (1996). Fatigue Crack Growth Rates in Adhesive Joints Tested at Different Frequencies. *The Journal of Adhesion*, 58(34), 191–204. <https://doi.org/10.1080/00218469608015200>
- Yamazaki, D., Mitsuyasu Iwanami, & Isa, M. (2020). Assessment of outdoor exposure effects on the long-term durability of epoxy resin adhesives used for steel-plate bonding. *Journal of Advanced Concrete Technology*, 18(8), 463–472. <https://doi.org/10.3151/jact.18.463>
- Yin, L., Gong, K., Pan, H., Qian, X., Shi, C., Qian, L., & Zhou, K. (2022). Novel design of MOFs-based hierarchical nanoarchitecture: Towards reducing fire hazards of epoxy resin. *Composites Part A: Applied Science and Manufacturing*, 158. <https://doi.org/10.1016/j.compositesa.2022.106957>
- Younes Jahani, Baena, M., Barris, C., Perera, R., & Torres, L. (2022). Influence of curing, post-

curing and testing temperatures on mechanical properties of a structural adhesive.

Construction and Building Materials, 324.

<https://doi.org/10.1016/j.conbuildmat.2022.126698>

Yu zhu Wang, Chun sheng Wang, & Duan, L. (2021). Bonding and bolting angle reinforcement for distortion-induced fatigue in steel girder bridges. *Thin-Walled Structures*, 166.

<https://doi.org/10.1016/j.tws.2021.108027>

Zhang, D., & Huang, Y. (2021). The bonding performances of carbon nanotube (CNT)-reinforced epoxy adhesively bonded joints on steel substrates. *Progress in Organic Coatings*, 159, 106407. <https://doi.org/10.1016/j.porgcoat.2021.106407>

Zuo, P., & Vassilopoulos, A. P. (2021). Review of fatigue of bulk structural adhesives and thick adhesive joints. *International Materials Reviews*, 66(5), 313–338.

<https://doi.org/10.1080/09506608.2020.1845110>